IMAGING OF STRESS IN ROCK SAMPLES USING NUMERICAL MODELING AND LABORATORY TOMOGRAPHY

By

Rudrajit Mitra

Dissertation submitted to the faculty of the Virginia Polytechnic Institute and State University in partial fulfillment of the requirements for the degree of

Doctor of Philosophy

In

Mining and Minerals Engineering

Committee Members:

Dr. Erik Westman, Chair

Dr. Thomas Novak Dr. Mario Karfakis

Dr. Marte S. Gutierrez Dr. Anthony T. Iannacchione

April 5, 2006

Blacksburg, VA

Keywords: Numerical Modeling, Tomography, Stress redistribution

IMAGING OF STRESS IN ROCK SAMPLES USING NUMERICAL MODELING AND LABORATORY TOMOGRAPHY

Rudrajit Mitra

(ABSTRACT)

Underground mining has one of the highest fatal injury rates among any of the industries in the United States, which is more than five times the national average of the other industries (MSHA). Many of these incidents take place due to stress redistribution resulting from mine workings. Thus it is very important to develop some tools to predict this failure in advance and prevent any fatalities arising from the failure.

The current study uses two tools – numerical modeling and laboratory tomography - to image the stress distribution in laboratory rock samples as they are uniaxially loaded. The discrete element code, PFC^{3D}, is used. The laboratory properties of the rock sample need to be converted to the micro-properties of the particles in the model. Currently no theory exists for this conversion. In the current study an equation has been developed for this process. Based on the users' input, the equation determines the micro-properties for the model. Further, various techniques to study the stress redistribution from these models at the particle level are discussed.

Tomography is a non-destructive technique through which the interior of a body can be imaged without penetrating the surface by any physical means. In the current study sensors were attached around the rock sample and tomograms were obtained at certain

intervals of the load. Initially, an indentation load was applied on a rectangular block to study the comparison between the stress and the velocity in two dimensions. In the last part of the study three-dimensional tomograms were obtained from the rock samples as they were loaded to failure.

ACKNOWLEDGEMENTS

In the very beginning I would like to thank my advisor and Committee Chair, Dr. Erik C. Westman. He has been of tremendous help and support to me during the last three years of my PhD program. He has not only been a great advisor to me but a person whom I have always looked forward to whenever I needed any help, be it in personal or in professional matters. I would also like to thank my Committee members, Dr. Tom Novak, Dr. Mario Karfakis, Dr. Marte Gutierrez and Dr. Anthony Iannacchione. I would like to specially thank Dr. Iannacchione for driving all the way from Pittsburgh, PA in spite of his busy schedule. I would like to thank the National Science Foundation for providing me the funding opportunity to carry on this study.

I would like to thank everyone in the Department of Mining and Minerals Engineering at Virginia Tech. In spite of being miles away from home, I have always felt being at home whenever I talked with Kathryn and Christine. I would also like to thank Wes Johnson, Kray Luxbacher, Michael Murphy, and Kwangmin Kim with whom I have spent the three years of my graduate life at Tech. I would also like to thank Brady Johnson, Heather Kraus and Crystal Seals for helping me with the laboratory experiments and Matt Delinger for developing the program, IPicker, for acquiring the arrival time data.

Finally, last but not the least, I would like to thank my family staying miles away but praying and wishing for my best. My parents have made me get through to where I am today with all their support and love. Thanks to all the sacrifice that they made

throughout their life for seeing me reach this day. I would like to thank my fiancé and her family for providing me with their constant support and encouragement.

TABLE OF CONTENTS

LIST OF FIGURES

LIST OF TABLES

CHAPTER 1: INTRODUCTION

1.1 BACKGROUND

Underground mining has one of the highest fatal injury rates among any of the industries in the United States which is more than five times the national average of the other industries (NIOSH). According to statistics obtained between 2001 to July 2005, approximately 33% of the fatalities have been due to geologic failure of the roof/back or face/rib/highwall (MSHA). Many of these incidents can take place because of a redistribution of stress resulting from mine workings. The ability to understand this stress redistribution within a mine will allow for greater extraction efficiency with reduced safety concerns.

One of the earliest methods for quantitative experimental determination of the internal state of stress in a body subjected to applied load was the photoelastic method (Brady and Brown 1993). With the growth of computing technology attention was focused on numerical computation of stress. Numerical analysis provides a useful tool to understand the behavior of rocks under stress (Hart 2003). The modeling methods in rock mechanics have changed dramatically during the past quarter of a century (Starfield and Cundall 1988). Earlier studies on rock mechanics focused on laboratory and field measurements while the mathematical or computational models were limited in their usage. Currently computer packages with capability of advanced failure mechanisms have provided the

rock engineer with various computational tools. The focus has now shifted to both measurement and computation, the later being used to understand the mechanism behind the process. The existing numerical codes replicate the failure of real structures.

Numerical methods can be broadly classified into four main classes.

- Finite Element Method
- Finite Difference Method
- Boundary Element Method
- Discrete Element Method

The first three methods are continuum methods while the discrete element method is a discontinuum method of modeling. Extensive studies have been conducted on stress distribution using the continuum methods. The discontinuum mechanics have attempted to solve the displacement, deformation and stability requirements for blocky systems such as rocks. The University of California at Berkeley has developed two important analytical tools for work primarily with engineering excavations and mines - block theory and discontinuous deformation analysis (DDA) (Shi 1988; Shi and Goodman 1988).

The interior of a body can be monitored without penetrating its surface by physical means with the help of tomography. Similar to medical CAT scanning, information can be obtained about the internal state of the rock mass (Young, Hutchins et al. 1989). It generates cross sectional images of the object by utilizing its response to the

nondestructive, probing energy of an external source (Lo and Inderwiesen 1994). Seismic tomography makes use of sources that generate seismic waves and are used to measure anomalous structures in the earth. Ultrasonic tomography, on the other hand, is used to detect changes in velocity for laboratory and mine-wide monitoring systems.

Rock is frequently treated as a linearly elastic, homogeneous and isotropic medium. However, this particular behavior provides only limited insight into the true character of stresses and deformations within a rock mass (Barla 1974). The presence of discontinuities in rocks causes them to behave differently than its true elastic behavior. Earlier work (Barla 1974; Amadei 1996) has shown the dependence of strength on the discontinuities.

1.2 PROPOSED SOLUTION

The goal of this research is to use both numerical modeling and laboratory tomograms to image the stress distribution in rocks as they are uniaxially loaded to failure. This will help in predicting the rock failure at the laboratory scale based on the redistribution of stress. With the application of stress, the elastic wave velocity traveling through the rock increases proportionately. This is known as the acousto-elastic effect in a rock. Velocity tomograms observed during this loading process will indicate the change in stress and also denote the presence of cracks developed during the loading of the sample. Sensors and receivers attached all around the sample will provide a three-dimensional image of the sample. The rocks were tested in the Rock Mechanics Laboratory, Department of Mining and Minerals Engineering, Virginia Tech. Uniaxial compression test were conducted on these laboratory samples having diameters of 2" (0.0508m) and 3" (0.0762m).

The results obtained from the laboratory were compared to the numerical models. The interaction and evolution of microstructures in rocks govern their mechanical response to loading (Plesha and Aifantis 1983). Because of this discontinuum nature of rocks, a distinct element code, PFC^{3D}, developed by Itasca Consulting Group, Inc. was used for this purpose. PFC^{3D} represents a model as an assemblage of spheres bonded together by either contact or parallel bonds. While stress has been studied previously with continuum-based models, a discontinuum model such as the PFC more accurately

represents rock behavior and thus such a model was used to study the stress redistribution in rock.

The first step in this type of numerical modeling is the calibration process in which the macro-properties of the rock are converted to the correct micro-properties for the particles in the model. Currently, there is no available procedure in this modeling code to do this conversion. The initial values for the micro-properties of the particles are obtained from the formula provided by the user's manual. The model is made to run to failure and the Young's modulus and uniaxial compressive strength of the rock are compared to those obtained from the model. If they match, the micro-properties are accepted; otherwise a trial and error process is used to obtain the correct properties. Figure 1.1 shows the flowchart for such a process. This entire process is time-consuming. The current research develops an equation that will provide the correct micro-properties based on the initial macro-properties of the rock.

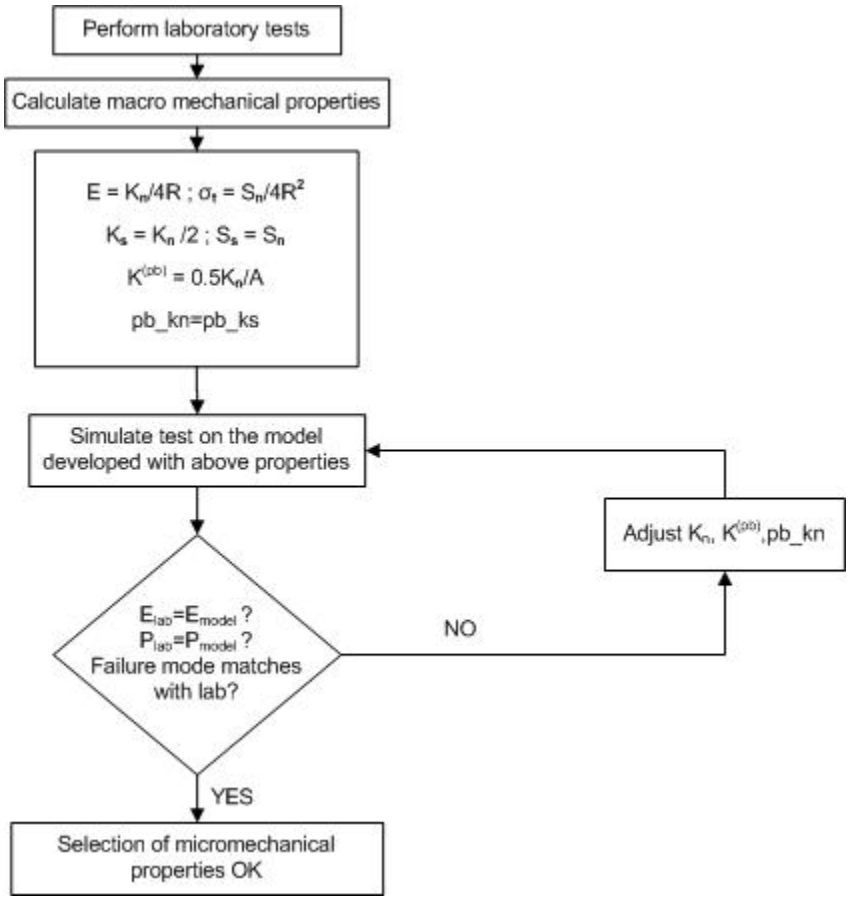

FIGURE 1.1 FLOWCHART FOR CONVERSION OF MACRO- TO MICRO-PROPERTIES

The following are the main tasks of the research:

- Perform uniaxial compression tests on cylindrical samples. The rocks will have sample diameters of 2" (0.0508m) and 3" (0.0762m). Velocity tomograms will be obtained during the loading process.
- Calibration of the results of the laboratory rock samples with the modeled samples.
- Generate a relationship between the macro-properties of the rock with the micro-parameters of the model.

- Image the stress redistribution as the rock is loaded to failure using both numerical modeling and laboratory tomograms.

1.3 SCOPE OF RESEARCH

The current study uses both numerical modeling and laboratory tomograms to image the stress redistribution in rocks as they are loaded to failure. Failure takes place when the stress exceeds the strength of the material. It is associated with the redistribution and concentration of stresses due to excavation, gravitational forces, inhomogeneities or crustal movement of the earth (Westman 2004). The ability to image this stress redistribution within laboratory samples coupled with the modeling techniques may allow for prediction of failure within laboratory samples.

A rockburst is believed to occur in response to either an over-stressed structure or the passing of a seismic wave (Friedel, Scott et al. 1995). Thus, applying these methods to the mine scale, if the stress ahead of a face can be monitored, rockbursts and falls from roof can be predicted in advance. Studies have been conducted to predict rock bursts from seismic imaging (Young 1993). Studies show that high stresses in the roof and floor have been responsible for bumps and rockbursts.

The new technologies that will benefit from this study are real time tomography, acoustic emission monitoring coupled with acoustic emission tomography, and calibrated modeling for crack propagation prediction.

1.4 DISSERTATION OUTLINE

This dissertation consists of seven chapters. The first chapter provides a brief overview of the study that has been undertaken and the purpose of this research. The second chapter describes the various works that have been done both using numerical modeling and instrumentation in the field and the laboratory.

The third chapter titled "Micro-mechanical modeling of Five Oaks Limestone" has been submitted to *Géotechnique* and is currently under review. Chapter four titled "Stress redistribution determination through coupled laboratory testing and numerical modeling" has been submitted to *Transactions of SME* and is also under review. Chapter five titled "Study on the effect of anisotropy in rocks on stress redistribution using numerical modeling" is also under review in *Rock Mechanics and Rock Engineering*. Chapter six titled "Investigation of the Stress Imaging in Rock Samples using Numerical Modeling and Laboratory Tomography" will be submitted to *International Journal of Rock Mechanics and Mining Sciences*.

Chapter seven includes the summary and conclusions obtained from the study and also some future recommendations.

REFERENCE

Amadei, B. (1996). "Importance of anisotropy when estimating and measuring in-situ stresses in rock." Int. J of R Mech., Min. Sc. & Geomech. Abstr. **33**(3): 293-325.

Barla, G. (1974). Rock Anisotropy: Theory & Laboratory Testing. Rock Mechanics. L. Muller, Udine, Italy**:** 131-169.

Brady, B. H. G. and E. T. Brown (1993). Rock Mechanics for underground mining, Chapman & Hall.

Friedel, M. J., D. F. Scott, et al. (1995). 3D tomographic imaging of mechanical conditions in a deep US gold mine. 2nd. International Conference on the Mechanics of Jointed and Faulted Rock, Vienna, Austria, Balkema, Rotterdam.

Hart, R. D. (2003). "Enhancing rock stress understanding through numerical modeling." Int. J of R Mech. & Min. Sc. **40**(7-8): 1089 - 1097.

Lo, T. and P. L. Inderwiesen (1994). Fundamentals of Seismic Tomography. L. R. Lines. **6:** 178.

Maxwell, S. C. and R. P. Young (1997). Assessing induced fracturing aroung underground excavations using velocity imaging and induced seismicity. 4th. International Symposium on Rockbursts and Seismicity in Mines, Kraków, Poland, A.A. Balkema.

MSHA Mine Safety and Health Administration, US Department of Labor, http://www.msha.gov.

NIOSH National Institute of Occupational Safety and Health, http://www.cdc.gov/niosh.

Plesha, M. E. and E. C. Aifantis (1983). On the modeling of rocks with microstructure. 24th. US Symposium on Rock Mechanics, **2**: 27 - 35.

Shi, G. (1988). Discontinuous deformation analyses - a new numerical model for the statics and dynamics of block systems, University of California, Berkeley. **PhD**.

Shi, G. and R. E. Goodman (1988). Discontinuous deformation analyses - a new method for computing stress, strain and sliding of block systems. Key questions in Rock Mechanics. P. A. Cundall, Balkema, Rotterdam: 381 - 383.

Starfield, A. M. and P. A. Cundall (1988). "Towards a methodology for rock mechanics modeling." Int. J. of R Mech., Min. Sc. & Geomech. Abstr. **25**(3): 99-106.

Westman, E. C. (2004). "Use of tomography for inference of stress redistribution in rock." IEEE Transactions on Industry Applications **40**(5): 1413 - 1417.

Young, R. P. (1993). "Seismic methods applied to Rock Mechanics." International Society for Rock Mechanics News Journal **1**: 4 -18.

Young, R. P., D. A. Hutchins, et al. (1989). "Geotomographic imaging in the study of mining induced seismicity." Reprint from Pure and Applied Geophysics - Seismicity in Mines **129**(3/4): 571 - 596.

CHAPTER 2: LITERATURE REVIEW

2.1 FAILURE IN ROCK MASSES

When load is applied to a rock mass, initially the microcracks normal to the direction of the load are closed. With further application of the load, cracks start to develop at an angle to the application of the load. Finally these microfractures coalesce into the failure plane. It has been observed that these cracks nucleate at around 90% of the peak stress to develop the fracture plane (Scholz 1968; Scholz 1968). The orientation of the failure plane is a function of several parameters, including size and shape of the sample, loading conditions, material properties, anisotropy, and jointing within the rock mass (Westman 2004).

Several failure criteria have been developed for predicting failure as a function of applied stress. The simplest and most important criterion was introduced by Coulomb (1773). According to his studies, the shear stress causing failure across a plane is resisted by the cohesion of the material and the normal stress across the plane. The criterion of shear failure in a plane is given by

$$| \tau | = S_0 + \mu\sigma \qquad (2.1)$$

where, σ and τ are the normal and shear stresses across the plane, S_o is a constant which may be regarded as the inherent shear strength of the material and μ is a constant called the coefficient of internal friction.

Mohr (1900) proposed that when shear failure takes place across a plane, the normal stress σ and shear stress τ across this plane are related by a functional relation characteristic of the material,

$$\tau = f(\sigma) \tag{2.2}$$

The Griffith criterion is based on the hypothesis enunciated by Griffith in 1921 that fracture is caused by stress concentrations at the tips of minute *Griffith cracks* which are supposed to pervade the material, and that fracture is initiated when the maximum stress near the tip of the most favorable oriented crack reaches a value characteristic to the material. They are scaled in terms of the uniaxial tensile strength T_o and state that, for principal stresses σ_1, σ_3 in two dimensions, failure takes place if

$$(\sigma_1 - \sigma_3)^2 = 8T_0, \qquad \text{if } \sigma_1 + 3\sigma_3 > 0 \tag{2.3}$$

$$\sigma_3 = -T_0, \quad \text{if } \sigma_1 + 3\sigma_3 < 0 \tag{2.4}$$

The original Hoek and Brown failure criterion was developed around 1980 (Hoek and Brown 1980). This criterion was required in order to provide information for designing underground excavations. The equation was neither new nor unique. However, the significant contribution to this criterion was that it linked the equation to geological observations, initially to Bieniawaski's Rock Mass Rating and later to the Geological Strength Index (Hoek and Brown 1997). Various other criteria have also been developed based on empirical data.

2.2 STRESS DETERMINATION IN ROCKS

Determination of the strength of the rock is the biggest concern in any engineering discipline using it for structural or supporting purposes (Karfakis 2003). The mechanical properties of a rock depend upon the physical properties of the rock and the presence of discontinuities (Jaeger and Cook 1979). Tests are conducted in the laboratory to determine the strength of the rock.

The current study was conducted with the uniaxial compression strength test. It is oldest and simplest test and continues to be one of the most convenient and useful ways to determine the properties of the rock (Jaeger and Cook 1979). It may be regarded as the largest stress that a rock specimen can carry when a unidirectional stress is applied to the ends of a specimen. In other words, the unconfined compressive strength represents the maximum load supported by the specimen during the test divided by the cross-sectional area of the specimen. Although the utility of the compressive strength value is limited, the unconfined compressive strength allows comparisons to be made between rocks and provides some indications of rock behavior under more complex stress systems (Tang, Liu et al. 2000). In the uniaxial compression test, right circular cylindrical rocks are compressed parallel to their longitudinal axis. The failure mode is dependent on the strength/stiffness of the platen with respect to that of the sample. The uniaxial compressive strength test is the basic test in numerous design methods (Pells 1993). Thus

it was decided to conduct this study using the most frequently used uniaxial compressive tests.

It is necessary to have an idea of the initial stress in a rock mass. If the initial stresses are high, the shape of the opening have to selected in such a way as to minimize the stress concentration. Further the layout of the opening can be arranged accordingly (Goodman 1980). Stresses in rocks have been studied for decades. One of the earlier methods to determine the stress state in a body due to application of load has been the photoelastic method. The principles of photoelasticity was first discovered by Brewster in 1816. Photoelastic models have been widely used for stress-strain analysis. The field applications of the photoelastic methods was started in the late 1940's by Coutinho (1948). In the 1960's cylindrical glass meters and light portable polariscope systems were developed for observing fringes (Robert, Hawkes et al. 1965). In this method, for two dimensions and for isotropic elasticity, the stress distribution is independent of the elastic properties of the material and is the same for plane stress and plane strain. In all photoelastic methods, the determination of stress or strain is achieved by measuring the interference patterns produced within the stressed photoelastic materials as a direct result of their effect on the transmission of polarized light (Dhir, Moore et al. 1978). A brief description of this method can be found in Brady and Brown (1993). Since then, innumerable studies have been conducted to monitor the stress distribution using both analytical and numerical models.

In engineering analyses, rock is frequently treated as a linearly elastic, homogeneous and isotropic medium. However, rock is never isotropic in nature. This particular assumption provides only limited insight into the true character of the stresses and deformations within a rock mass. By assuming anisotropic rocks to be isotropic, significant errors can be introduced in the analyses of stress and deformation (Barla 1974). Rocks need to be considered as an anisotropic material to get more accurate information about stress redistribution. Barla (1974) conducted extensive laboratory experiments on anisotropic behavior of rocks. Amadei (1996) and Tonon and Amadei (2003) also conducted laboratory and field experiments on anisotropic rock behavior. Figure 2.1 shows the relationship between the strength of the rock and the angle of the bedding planes (Amadei 1996).

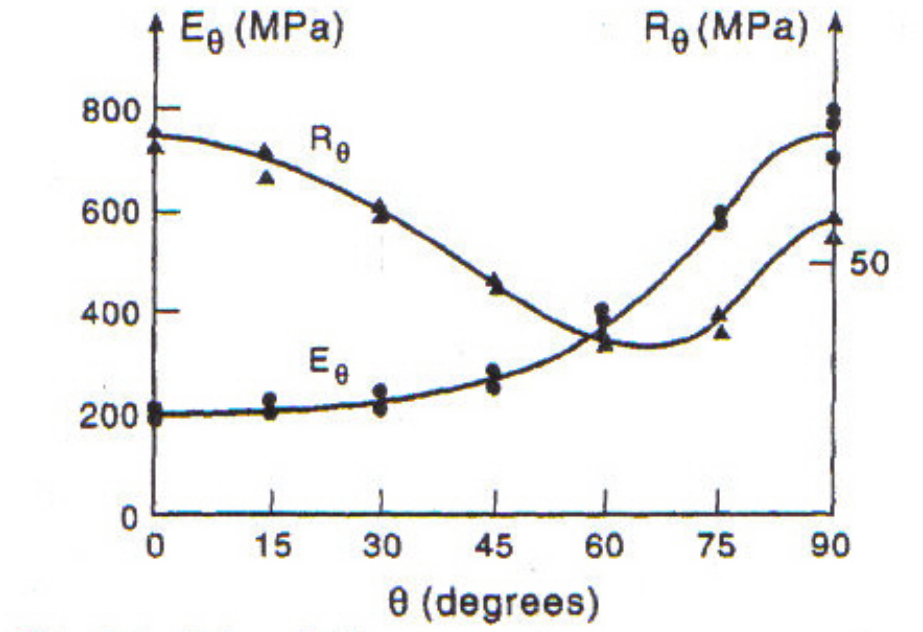

FIGURE 2.1 VARIATION OF ULTIMATE STRENGTH R_Θ AND APPARENT YOUNG'S MODULUS E_Θ, FOR A DIATOMITE TESTED UNDER UNIAXIAL COMPRESSION (AMADEI 1996) [1]

[1] Reprinted from Int. J of R Mech., Min. Sc. & Geomech. Abstr., 33(3), Amadei, B., Importance of anisotropy when estimating and measuring in-situ stresses in rock, 293-325, Copyright (1996) with permission from Elsevier

2.3 NUMERICAL METHODS IN ROCK MECHANICS

Numerous numerical methods of analysis have been developed over the past three decades (Pande, Beer et al. 1990). Their popularity has risen due to the increasing trend in computer technology and its availability to engineers. Rock structures are designed largely based on the designer's experience. Today's engineers are often faced with problems for which no past experience is available. Civil or mining engineering construction is usually a "one off" situation every time. The increased consciousness amongst the public regarding safety and economy has led engineers to seek more rational solutions to the problems in rock mechanics related to civil and mining engineering. Numerical methods provide a solution to this problem. With the help of this method, various solutions can be simulated and the best option can be used in practice.

Numerical methods for the stress analysis problems in rock mechanics can be divided into two classes (Hoek 2000):

- *Boundary methods*, in which the boundary of the model is divided into elements and the interior of the rock mass is represented mathematically as an infinite continuum.
- *Domain methods*, in which the interior of the rock mass is divided into simple geometrical elements each with assumed properties.

There are four main numerical methods which have been used in this area.

- Finite Element Method (FEM),
- Finite Difference Method (FDM)
- Boundary Element Method (BEM), and
- Discrete Element Method (DEM).

The next few paragraphs will discuss about the various attributes of each of these methods.

2.3.1 FINITE ELEMENT METHOD

This is the most popular method in engineering sciences. It was first applied to aircraft structure in the 1940s. It is a domain method in which the fundamental idea is the replacement of continuous functions by piecewise approximations, usually polynomials (Davies 1980). It has been applied since then to a large number of problems in widely different fields. The well-known 'Goodman joint element' in rock mechanics literature has been widely implemented in finite element modeling codes and applied to many practical rock engineering problems (Jing and Hudson 2002). The method involves dividing the structure under consideration to smaller zones, known as elements. Each element can have different material properties connected to each other at corners called nodes. It is at these nodes that the displacement is computed. The strains can be calculated from the displacement field within the element, and then using the stress-strain relation the stresses are computed. The major disadvantage of this method is that

considerable effort is required in preparing data for a problem. This is particularly crucial in three-dimensional problem and has led to 'mesh generation' programs. The method is also expensive in computer time.

Numerous studies have been conducted in the field of mining engineering using this modeling method. Only a few of them are mentioned here. Peng and Dutta (1992) simulated the interaction of roof, pillar and floor at the Smoot Mine located in Bolair, West Virginia using MSC/NASTRAN, a large-scale finite element program which is used to solve a wide variety of engineering problems. Hasenfus and Su (1992) performed a finite element study at an Appalachian longwall mine using MSC/NASTRAN too. Su and Hasenfus (1996; 1999) also conducted studies to show that finite-element modeling can be used to predict in situ coal pillar strength, especially under non-ideal conditions where interface friction and roof and floor deformation are the primary controlling factors. Pariseau conducted numerous studies using finite element modeling in various aspects of mining (Pariseau 1995; Pariseau, Johnson et al. 1995; Pariseau, Schmelter et al. 1997).

Peng, Tsang et al. (1989) used a 2-D finite element model to study the design of yield pillars in order to improve the floor and roof conditions. Moes and Belytschko (2002) studied the crack growth phenomenon using the finite element method. Dhawan, Singh et al. (2002; 2004) used finite element modeling for studying underground openings. Yufin,

Lamonina et al. (2005) studied the joint rock masses using the existing finite element models.

Progressive failure of rock has been modeled using the Rock Failure Process Analysis in two-dimensions ($RFPA^{2D}$) (Tang 1997; Tang, Yang et al. 1998). $RFPA^{2D}$ is a two-dimensional rock failure analysis package based on the linear finite element method. The program allows simulation of the progressive failure of rock leading to collapse via a simple approximation, eliminating the numerical complexities of non-linear, discontinuum codes. The program allows modeling of the observed evolution of damage and associated seismic events due to progressive failure leading to collapse in brittle rock. Liang, Tang et al. ( ) simulated the rock failure process in heterogeneous rocks using $RFPA^{3D}$. However, further studies need to be conducted using this software and also it is not available for commercial use. $PHASE^2$ is another two-dimensional finite element model developed by the Rock Engineering Group in the Department of Civil Engineering at the University of Toronto.

2.3.2 FINITE DIFFERENCE METHOD

The finite difference method is perhaps the oldest numerical method used for the solution of sets of differential equations, given initial values and/or boundary values (Itasca Consulting Group Inc.). In this method, every derivative in the set of governing equations is replaced directly by an algebraic expression written in terms of the field variables (e.g., stress or displacement) at discrete points in space; these variables are undefined within

elements. Although both the finite element and the finite difference methods derive equations in different ways, the results are identical (Itasca Consulting Group Inc.). One of the most commercially available software which has been used in both soil and rock mechanics is FLAC (Itasca Consulting Group Inc.) in both two- and three-dimensions. Some of the studies using this method of modeling include works by Iannachhione (1989), Iannacchione and Vallejo (1991), Burke (2003), MSHA (1996), Zipf Jr. (1999; 2001), Esterhuizen and Iannacchione (2005), Esterhuizen and Karacan (2005), etc.

2.3.3 BOUNDARY ELEMENT METHOD

The Boundary Element Method derives its name from its basic idea that only the boundary of the problem geometry is divided into elements (Hoek 2000). This method is becoming increasingly popular. It lacks the generality and flexibility of the finite element method. It is a complicated method and requires a higher level of understanding of mathematical complexities. In this method only the surface of the rock mass to be analyzed needs to be divided into smaller particles, thereby reducing the computation time. For two-dimensional situations, line elements at the boundary represent the problem, while for fully three-dimensional problems, surface elements are required.

MULSIM/NL (Zipf Jr. 1992) is a boundary element program that was developed by US Bureau of Mines to calculate stresses and displacements (i.e. convergence) in coal mines or thin, tabular metalliferous veins. The program is based on its predecessors MULSIM/BM (Beckett and Madrid 1988) and MULSIM (Sinha 1979). It analyzes one to

four parallel seams that have any orientation with respect to the Earth's surface. LaModel is another boundary element program developed by NIOSH (Heasley and Akinkugbe 2005) for modeling stress in coal mines. It calculates stresses and displacements in multiple seam situations. Some of the other works in the area of rock and soil mechanics include those by Seghatchian, Cerrolaza et al. (1997), Banerjee and Butterfiled (1975), Eberhardt (1994), Wardle (1980; 1982), Peirce and Ryder (1983), von Estorff and Schmidt (1984), etc.

2.3.4 DISCRETE ELEMENT METHOD

Most of the computer programs based on the earlier methods can simulate variation in material types and non-linear constitutive behavior of a rock mass. The presence of discontinuities is limited in these methods in which interfaces are made to represent the joints, fractures or faults. However, the location of these interfaces has to be specified in advance. The following are the some of the disadvantages of using these methods (Itasca Consulting Group):

- The logic may break down when many intersecting interfaces are used,
- There are no automatic schemes for recognizing new contacts, and
- Displacements or rotations are large.

Thus the continuum codes are restricted in their usage in jointed rock mass. All rock masses are jointed. These codes are limited to modeling only the major discontinuities.

The discrete element method is based on treating the rock as a discontinuum rather than continuum (Pande, Beer et al. 1990). When loads are applied, the changes in contact forces are traced with time. It has the capability to maintain a data structure and memory allocation scheme that can handle many hundreds or thousands of discontinuities (Itasca Consulting Group). The equations of dynamic equilibrium for each element are repeatedly solved till the laws of contacts and boundary conditions are satisfied. This method has the capability to model the mechanical behavior of the rock at the grain-scale (Holt, Kjølaas et al. In press).

Cundall and Hart (1985) provide the following definition of a discrete element method: The name "discrete element" applies to a computer program *only* if it:

- allows finite displacement and rotations of discrete bodies, including complete detachment, and
- recognizes new contacts automatically as the calculation progresses.

They further define four basic classes of discrete element methods:

- Distinct element methods (Cundall 1971; Cundall and Strack 1979)
- Modal methods (Williams and Mustoe 1987)
- Discontinuous deformation analysis (Shi 1988; Shi and Goodman 1988)
- Momentum exchange methods (Hahn 1988)

These methods have been explained in detail in the UDEC Users Manual (Itasca Consulting Group).

2.4 SELECTION OF NUMERICAL METHOD

The major objective of this research is to first simulate the behavior of the rock using numerical modeling and then to image the stress redistribution as the rock is loaded to failure using both laboratory studies and numerical modeling. With rock being a discontinuum mass, its behavior can best be represented by a discontinuum code. Currently, the two most commercially available discrete element modeling software codes are UDEC (Itasca Consulting Group) and PFC (Itasca Consulting Group 2003), both developed by Itasca Consulting Group, Inc.

The Universal Distinct Element Code (Itasca Consulting Group) simulates the response of discontinuous media (such as a jointed rock mass) subjected to either static or dynamic loading. The discontinuous medium is represented as an assemblage of discrete blocks. Individual blocks behave as either rigid or deformable material. Deformable blocks are subdivided into a mesh of finite-difference elements, and each element responds according to a prescribed linear or non-linear stress-strain law. The relative motion of the discontinuities is also governed by linear or non-linear force-displacement relations for movement in both the normal and shear directions. It is suitable for modeling jointed rock mass.

The Particle Flow Code (PFC) is represented as an assemblage of circles or spheres. PFC is designed to be an efficient tool to model complicated problems in solid mechanics and

granular flow. According to Potyondy (2002), PFC modeling has the following advantages when compared to continuum modeling:

- Damage and its growth are explicitly represented in the model - no empirical relations are needed to define damage or quantify its effect upon material behavior.
- Microcracks form and coalesce of its own without the need to reformulate the grid.
- Complex non-linear behaviors arise as emergent features, given the simple behavior at the particle level.
- Secondary phenomena, such as acoustic emission, occur in the model without additional assumptions.

The current study develops models to simulate the laboratory rock samples as they are loaded to failure. Since rock is made up of granular materials, it was decided to use PFC for the current study. The three-dimension version of the code was used to get an overview of the rock in all dimensions.

2.5 APPLICATIONS OF MICRO-MECHANICAL MODELING TO ROCK MECHANICS PROBLEMS

The mechanical behavior of rock has been successfully modeled using both two- and three-dimensional continuum modeling techniques. The success of this approach is because the smallest element in the model has a length scale much smaller than those of the objects of interest (e.g. dams, bridge decks). However it is often rewarding to model such 'continua' as discontinua, because new knowledge about their macroscopic behavior can be obtained after their microscopic mechanisms are understood (Cundall and Hart 1993). The new trend in this area is the use of the two- and three-dimensional discontinuum modeling codes. The advantage of using these micro-mechanical modeling techniques is that no assumptions have to be made about the location and type of fracture and failure – cracking takes place spontaneously and can exhibit a variety of mechanisms when certain local stress conditions are exceeded. According to Hazzard and Young (2002), interesting insights about the micro-mechanics of deformation and failure will be obtained under different stress conditions if the failure mechanisms produced by the models are quantified and studied.

Particle Flow Code in two-dimensions, PFC^{2D} (Itasca Consulting Group) have been used with much success in various fields. It is well-documented and commercially available software developed by Itasca Consulting Group, Inc. A two dimensional bonded-particle model was used by Hazzard, Collins et al. (2002) to simulate the shear-type micro-

seismic events induced by tunnel excavation in granite. The results were compared with actual results obtained from seismic monitoring around an underground excavation. According to the authors, the combination of monitoring the same rock mass using both micro-seismic and ultrasonic techniques affords the unique ability to investigate fracturing over different magnitude scales. Hazzard and Young (2002) present a numerical modeling approach using PFC^{2D} that simulates cracking and failure in rock and the associated seismicity. A technique is also described for quantifying the seismic source mechanisms of the modeled events. A new geomechanical modeling technique was developed using PFC^{2D} by Hazzard and Young (2001) in which the models can generate seismicity from induced cracks and fractures. Hazzard and Young (2000) also simulated acoustic emissions in Lac du Bonnet granite using PFC^{2D}.

PFC^{2D} has also been used to simulate a loading-type failure around an underground excavation in brittle rock by Fakhimi, Carvalho et al. (2002). The results from the modeling were in good agreement with the experimental test. It was concluded that by simulating the rock as an assemblage of cylindrical particles, surface spalling and crack propagation can be easily modeled. Wang, Tannant et al. (2003) studied the stability of heavily jointed rock slopes using PFC^{2D}. The modeling methods and procedures presented in the study demonstrate a new approach to the simulation of a rock mass and the stability analysis of excavations in a rock mass. With this new approach, study of the stability of excavations can be carried out in such a way that the development and movement of the rock mass and failure surface can be visualized in two dimensions.

Park, Martin et al. (2004) simulated the mechanical behavior of discontinuous rock masses using UDEC and PFC^{2D}. The study reviews the methodology developed in Sweden for the Rock Mechanical Descriptive Model. The results from the UDEC Rock Mechanical Descriptive Model are compared to results from the discrete element software PFC^{2D}. The post-peak response of the PFC model was not determined by a user-specified model, while the UDEC results were determined by the constitutive model applied to the joints. Park, Choi et al. (2005) also studied the effect of the various components of a ground subsidence process on each other using PFC^{2D}.

All the studies mentioned above were done using the two dimensional micro-mechanical models. The models were able to develop fracture and failure on their own and there was no need to specify any constitutive models for them. However due to the two dimensional nature of these models, only a section of the model could be analyzed. Analysis of the model in its entirety can be made using the three dimensional version of this code. The Particle Flow Code in 3-dimensions (Itasca Consulting Group) is the three dimensional version of PFC^{2D}. In this code, the model is represented by a collection of spheres. Hazzard and Young (2002) extended their earlier study on acoustic emission using PFC^{3D}. Kulatilake, Malama et al. (2001) investigated the effect of joint geometry parameters on the uniaxial compressive strength of jointed blocks, and the results of the laboratory experiments and numerical simulations were compared. It was concluded from the study that there is a great dependence of the block strength of a jointed rock on the joint geometry configuration. The joint geometry configuration was also found to control

the mode of failure of a jointed block of rock under uniaxial loading. Wanne (2002) studied the effect of anisotropy of the rock on strength and deformation properties by simulating a standard unconfined compression test with PFC^{3D}. Quantitative results for peak strength and Young's modulus obtained from the simulations were similar to those obtained from the laboratory. Wanne, Johansson et al. (2004) have also studied the pillar stability in the Aspö Hard Rock Laboratory using PFC coupled with FLAC.

Holt (2001) uses both the two- and three-dimensional version of PFC to describe the virgin compaction behavior, and to illustrate the main effects of stress release induced core damage. Measurement circles were employed in this study to measure the stresses and strains. Gill, Roegiers et al. (2005) used PFC^{3D} to model the mechanical properties of the Antler sandstone, a poorly-consolidated rock outcropping near Ardmore, Oklahoma. The results of the model were compared to triaxial laboratory results. The micro properties of the model were obtained from a mineralogical analysis of the rock modeled. Holt, Kjølaas et al. (In press) uses PFC^{3D} in the petroleum applications of rock mechanics. A strategy for calibration is outlined in the study and the results are compared with artificial rock-like materials consisting of spherical grains (glass beads). According to the authors, they have been able to demonstrate that this type of modeling is becoming popular to understand rock mechanics from the pore to core and finally to the reservoir scale.

2.6 TOMOGRAPHY

Tomography is derived from the Greek word *tomos*, meaning section. It is a nondestructive testing method to view the interior of a body without penetrating its surface by physical means. It is based on the mathematical procedure called tomographic reconstruction. Tomography has been defined by Lo and Inderwiesen (1994) as an "imaging technique which generates a cross-sectional picture (a tomogram) of an object by utilizing the object's response to the nondestructive, probing energy of an external source". This technology was first described by Radon (1917), who said that the interior of the body can be imaged by analyzing energy which passed from one boundary to another. It has been widely used in the medical field, where x-ray is used to create the images. Dines and Lytle (1979) used the idea of tomography in geophysical applications. When load is applied to a rock, the microcracks are initially closed. This makes the elastic waves travel at a higher velocity through the rock. According to Westman (2004), the best way to monitor the changes in a rock mass is to perform high-resolution imaging as it is loaded.

Ultrasonic waves are used for laboratory tomographic studies while seismic waves are employed in the field studies. The resulting image will accurately portray the actual condition in the body if more sensors surround the body, as can be seen in Figure 2.2 (Westman 2004).

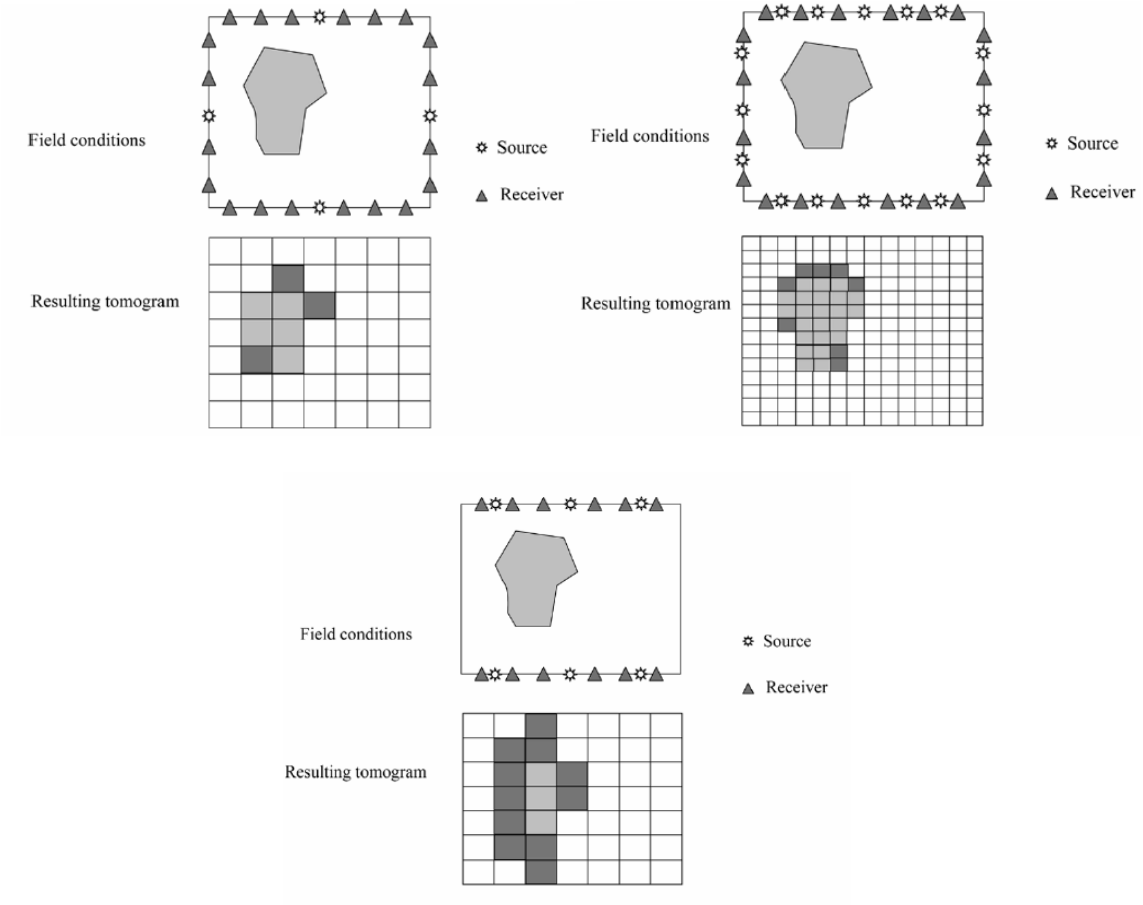

FIGURE 2.2 ILLUSTRATION OF THE TOMOGRAPHIC LAYOUT BASED ON THE POSITION OF THE SENSORS (WESTMAN 2004) (© 2006 IEEE)

The difference between the seismic and the ultrasonic tomographic imaging is in the frequency ranges used. Seismic tomography utilizes low frequency waves to measure anomalies like fracture or high stressed zones within the earth. The low frequencies correspond to long wavelengths capable of traveling long distances. In ultrasonic tomography, the waves have smaller wavelengths which can resolve small structures; however these waves attenuate quickly and can therefore only be transmitted over short

distances. Ultrasonic tomography can be used to measure the slowness of the P or S wave across the sample as well as amplitude variations across the sample (Johnson 2005).

Rocks behave elastically and when load is applied to a rock, the velocity of the elastic wave through the rock will increase proportionately due to the closing of the microfractures. This effect is known as the acousto-elastic effect. Tomograms taken at various stages of loading will show this change in velocity which is directly proportional to the stress change.

2.7 APPLICATIONS OF TOMOGRAPHY

Tomography has been applied in various fields including volcanic imaging, earthquake tomography, geologic hazard detection and stress identification. Computerized tomography was adapted and applied to geophysical exploration using data collected by cross-borehole electromagnetic probing (Dines and Lytle 1979). Various studies have been conducted on both seismic and ultrasonic tomography, since then. Seismic tomography is used on large scale as the waves used in this method have a large wavelength and therefore can travel larger distances. Gustavsson, Ivansson et al. (1986) used seismic tomography for mapping magnetite ore body in the Kiruna Research Mine, Sweden. Cross-hole seismic tomography has been used by Leung, Downey et al. (1988) to search for lead and zinc sulfide deposits in Western Australia. It has also been used by Goulty, Thatcher et al. (1990) to detect presence of coal in the UK. Seismic tomography has also been applied in other areas. Romanowicz (2003) studied the structure of the Earth's lower mantle using seismic tomography. Terada and Yanagidani (1986) mapped the distribution of the P-wave velocity within a sliced sample to observe how the microcracks localizes before faulting under uniaxial compression.

Tomography has been used in mines to monitor roof or pillar failure, identify regions of relatively higher stress, and strata identification. Peterson, Paulsson et al. (1985) carried out experiments at the Retsoff salt mine in New York and at the underground radioactive waste study site at the Stripa mine facility in Sweden. The study imaged a collapse zone

due to dissolution of overlying carbonates by groundwater from an old shaft which was a hazard to the mine. A high proportion of faces in coal mines run into underground faults thereby reducing the output. These faults cannot be mapped from surface surveys. Mason (1981) conducted underground seismic survey to map these faults at the High Hazles seam of Thoresby Colliery in the Nottingham Coalfield, UK. (Itakura, Sato et al. 1991) combined acoustic emission and seismic tomography to investigate the microcracking activity on an experimental scale. The authors traced the microcracking cluster by means of both the AE method and seismic tomography techniques in order to investigate the relationship between the AE cluster and velocity image. Westman, Haramy et al. (1996) used seismic tomography to analyze the stress on a longwall face using the longwall shearer as a source.

Ultrasonic tomography is used mostly for laboratory purposes because of the low wavelengths of the ultrasonic waves. They can also be used in mines to get an idea of what lies ahead of the face to prevent rock bursts and falls from the roof. Falls, Young et al. (1992) monitored acoustic emissions and performed tomographic velocity imaging during the hydraulic fracturing tests on two large, unconfined Lac du Bonnet grey granite cylinders. The purpose of these tests was to investigate granite's micromechanical response to the stress field generated by hydraulic fracturing and to investigate fluid penetrations effects. The capabilities of ultrasonic tomography on identifying inhomogeneity and fractures inside the rock were investigated by Li, Zhang et al. (2005). Scott, Ma et al. (1993) conducted indentation loading tests on a Berea sandstone sample.

Tomograms constructed of the cross-section of the sample showed that the density underneath the load increases with the application of the load.

Johnson (2005) designed a new instrumentation system to allow rapid data collection through varying sample geometries and rock types with a low initial investment. The system is composed of sensors, an ultrasonic pulser, a source switchbox, and analog to digital converters; it is tied together using LabVIEW. The system was initially calibrated and then applied to obtain two-dimensional tomograms on samples of Berea sandstone and Five Oaks limestone.

2.8 CONCLUSIONS

As can be seen, numerous studies have been conducted using the discrete element method of modeling. It can be observed that the program has been very successful in predicting fracture without the use of any interfaces. However, attempts have not been made to study the stress redistribution at the micro scale using this modeling method. One of the objectives of this study is to observe the stress distribution for the models developed along with the fracture development as they are loaded to failure. Observing this change in stress on a mine scale will help to detect the fracture in advance and thereby prevent problems in the mine arising due to this high stress.

Studies have been done in the past with the ultrasonic imaging of rocks in two-dimensions. The current study will develop velocity tomograms in three-dimensions. The objective is to detect the presence of the failure plane in rock samples in advance. This study can be extended to the mine site and further studies can be conducted to monitor the increase in the stress field using coupled numerical modeling and tomographic imaging. An ultrasonic data acquisition system developed by Johnson (2005) was used for the current study. Sensors and receivers attached all around the rock will produce this three-dimensional image as they are loaded to failure.

REFERENCE

Amadei, B. (1996). "Importance of anisotropy when estimating and measuring in-situ stresses in rock." Int. J of R Mech., Min. Sc. & Geomech. Abstr. **33**(3): 293-325.

Banerjee, P. K. and R. Butterfield (1975). Boundary element methods in geomechanics. Finite elements in geomechanics Karlsruhe, Federal Republic of Germany, John Wiley & Sons, London, United Kingdom (GBR): 529 – 570.

Barla, G. (1974). Rock Anisotropy: Theory & Laboratory Testing. Rock Mechanics. L. Muller, Udine, Italy: 131-169.

Beckett, L. A. and R. S. Madrid (1988). MULSIM/BM - A structural analysis computer program for mine design. Bureau of Mines IC 9168**:** 302.

Brady, B. H. G. and E. T. Brown (1993). Rock Mechanics for underground mining, Chapman & Hall.

Brewster, D. (1816). "On the communication of the structure of doubly refracting crystals to glass and other substances by mechanical compression and dilatation." Trans. of Royal Society: 156 - 178.

Burke, L. M. (2003). Numerical modeling for increased understanding of the behavior and performance of coal mine stoppings. Mining and Minerals Engineering. Blacksburg, Virginia Tech. **M.S.:** 114 pp.

Coulomb, C. A. (1773). "Sur une application des règles de Maximis et Minimis a quelques problèmes de stratique relatifis à l'Architecture " Acad. Roy. des Sciences Memoires de math. et de physique par divers savans **7**: 343 - 382.

Coutinho, A. (1948). "Determination of stresses in concrete by photoelastic tensometer method." Annales d'Inst. Tech. Bat. Travail Publique, Series on Test and Measurements **4**: 20.

Cundall, P. A. (1971). A computer model for simulating progressive large scale movements in blocky rock systems. Symposium of the International Society of Rock Mechanics Nancy, France: Vol. 1, Paper # II-8.

Cundall, P. A. and R. Hart (1985). Development of generalized 2D and 3D distinct element programs for modeling jointed rock. Itasca Consulting Group; US Army Corps of Engineers, Misc. Paper SL-85-1.

Cundall, P. A. and R. D. Hart (1993). Comprehensive Rock Engineering, Vol. 2: Analysis and Design Methods - Numerical modeling of discontinua., Pergamon Press.

Cundall, P. A. and O. D. L. Strack (1979). "A discrete element model for granular assemblies." Geotechnique **29**(1): 47 - 65.

Davies, A. J. (1980). The Finite Element Method - A first approach, Oxford University Press.

Dhawan, K. R., D. N. Singh, et al. (2002). "2D and 3D finite element analysis of underground openings in an inhomogeneous rock mass." Int. J. of Rock Mech. and Min. Sc. **39**(2): 217 - 227.

Dhawan, K. R., D. N. Singh, et al. (2004). "Three-dimensional finite element analysis of underground caverns." Int. J. Geomech. **4**(3): 224 - 228.

Dhir, R. K., D. R. Moore, et al. (1978). Photoelastic methods for rock stress measurement. GEOCON - India, Conference on Geotechnical Engineering, New Delhi, India: 266 – 271.

Dines, K. A. and R. J. Lytle (1979). "Computerized geophysical tomography." Proceedings of the IEEE **67**(7): 1065-1073.

Eberhardt, E. (1994). Tabular excavations in foliated rock; an integrated numerical modelling study. Saskatoon, Canada, University of Saskatchewan, **Masters:** 203.

Esterhuizen, G. S. and A. T. Iannacchione (2005). Effect of the dip and excavation orientation on roof stability on moderately dipping stone mine workings. Alaska Rocks 2005 - Rock Mechanics for Energy, Mineral and Infrastructure Development in the Northern Regions. Ed. S. H. G. Chen, W. Zhou, J. Tinucci. Anchorage, AL**:** Preprint # ARMA/USRMS 05-743.

Esterhuizen, G. S. and C. O. Karacan (2005). Development of numerical models to investigate permeability changes and gas emission around Longwall mining panel. Alaska Rocks 2005 - Rock Mechanics for Energy, Mineral and Infrastructure Development in the Northern Regions. Ed. S. H. G. Chen, W. Zhou, J. Tinucci. Anchorage, AL**:** Preprint # ARMA/USRMS 05-744.

Fakhimi, A., F. Carvalho, et al. (2002). "Simulation of Failure around a circular opening in rock." Int. J of R Mech. & Min. Sc. **39**(4): 507 - 515.

Falls, S. D., R. P. Young, et al. (1992). "Ultrasonic tomography and acoustic emission in hydraulically fractured Lac du Bonnet grey granite." Journal of Geophysical Research **97**(B5): 6867 - 6884.

Gil, I., J. C. Roegiers, et al. (2005). Modeling the mechanical properties of Antler Sandstone using a Discrete Element Model. Alaska Rocks 2005 - Rock Mechanics for Energy, Mineral and Infrastructure Development in the Northern Regions. S. H. G. Chen, W. Zhou, J. Tinucci. Anchorage, AL: Preprint # ARMA/USRMS 05-717.

Goodman, R. E. (1980). Introduction to Rock Mechanics, John Wiley and Sons.

Goulty, N. R., J. S. Thatcher, et al. (1990). "Experimental investigation of crosshole seismic techniques for shallow coal exploration." Quar. J. Eng. Geol. **23**: 217 - 228.

Gustavsson, M., S. Ivansson, et al. (1986). "Seismic borehole tomography - measurement system and field studies." Proc. IEEE **74**(2): 339 - 346.

Hahn, J. K. (1988). "Realistic animation of rigid bodies." Comp. Graph **22**: 299 - 308.

Hasenfus, G. J. and D. W. H. Su (1992). A comprehensive integrated approach for longwall development design. Proceedings of the Workshop on Coal Pillar Mechanics and Design, Bureau of Mines, USA.: 225 – 237.

Hazzard, J. F., D. S. Collins, et al. (2002). "Simulation of unstable fault slip in granite using a bonded-particle model." Pure & Applied Geophysics **159**: 221 - 245.

Hazzard, J. F. and R. P. Young (2000). "Simulating Acoustic Emissions in Bonded-Particle Models of Rock." Int. J. of R. Mech. & Min. Sc. **37**(5): 867-872.

Hazzard, J. F. and R. P. Young (2001). Seismic validation of micromechanical models. 38th. US Rock Mech. Sym., DC Rocks 2001, Washington DC, A.A.Balkema: 1327 – 1333.

Hazzard, J. F. and R. P. Young (2002). 3D numerical modeling of acoustic emission. 5th. Int. Workshop on the Appl. Of Geophysics in Rock Engg., Toronto,Canada: 40 – 47.

Hazzard, J. F. and R. P. Young (2002). "Moment Tensors and Micromechanical Models." Tectonophysics **356**(1 - 3): 181 - 197.

Heasley, K. A. and O. O. Akinkugbe (2005). A simplified two-dimensional boundary element program for estimating multiple-seam interactions. Alaska Rocks 2005 -

Rock Mechanics for Energy, Mineral and Infrastructure Development in the Northern Regions. Ed. S. H. G. Chen, W. Zhou, J. Tinucci. Anchorage, AL**:** Preprint # ARMA/USRMS 05-707..

Hoek, E. (2000). Practical Rock Engineering, Rocscience - http://www.rocscience.com/roc/Hoek/Hoeknotes2000.htm.

Hoek, E. and E. T. Brown (1980). "Empirical strength criterion for rock masses." Journal of the Geotechnical Engineering Division **106**(GT9): 1013 - 1035.

Hoek, E. and E. T. Brown (1997). "Practical estimates of rock mass strength." Int. J. of Rock Mech. and Min. Sc. **34**(8): 1165 - 1186.

Holt, R. M. (2001). "Particle vs. laboratory modeling of in situ compaction." Phys. Chem. Earth (A) **26**(1 - 2): 89 - 93.

Holt, R. M., J. Kjølaas, et al. (In press). "Comparison between controlled laboratory experiments and discrete particle simulations of the mechanical behaviour of rock." Int. J. of Rock Mech. and Min. Sc.

Iannacchione, A. T. (1989). Numerical simulation of coal pillar loading with the aid of a strain-softening finite difference model. Proceedings 30th. U.S. Symposium on Rock Mechanics, West Virginia University, Morgantown, Balkema, Rotterdam: 775 – 778.

Iannacchione, A. T. and L. E. Vallejo (1991). Stress and Behavior of Material Under Direct Shear. Rock Mechanics as a Multidisciplinary Science, Balkema, Rotterdam**:** 549 - 558.

Itakura, K., K. Sato, et al. (1991). Monitoring of AE Clustering Activity prior to Main Faulting of Stressed Rock by Acoustic Tomography Technique. Fifth Conference on Acoustic Emission/Microseismic Activity in Geologic Structures and Materials, Trans Tech Pubn., Clausthal-Zellerfiled, Germany: 3 – 17.

Itasca Consulting Group, Inc., PFC^{2D}. Minneapolis, MN.

Itasca Consulting Group, Inc., PFC^{3D} (2003). Minneapolis, MN.

Itasca Consulting Group, Inc., UDEC. Minneapolis, MN.

Itasca Consulting Group Inc., FLAC^{2D}. Minneapolis, MN.

Jaeger, J. C. and N. G. W. Cook (1979). Fundamentals of Rock Mechanics, Chapman and Hall.

Jing, L. and J. A. Hudson (2002). "Numerical methods in rock mechanics." Int. J. of Rock Mech. and Min. Sc. **39**(4): 409 - 427.

Johnson, W. B. (2005). Design and testing of a laboratory ultrasonic data acquisition system for tomography. Mining & Minerals Engineering. Blacksburg, Virginia Tech. **M.S.**: 108.

Karfakis, M. G. (2003). Rock Mechanics Notes.

Kulatilake, P. H. S. W., B. Malama, et al. (2001). "Physical and particle flow modeling of jointed rock block behavior under uniaxial loading." Int. J. of R. Mech. & Min. Sc. **38**: 641 - 657.

Leung, L., M. Downey, et al. (1988). Cross-hole seismic tomography for mineral exploration and mine planning. Expanded Abstracts, 58th. SEG Annual Meeting, Anaheim, CA: 328 – 330.

Li, H., T. G. Zhang, et al. (2005). Laboratory experiment and computer simulation of ultrasonic wave propagation in fractured and imhomogeneous rock. Alaska Rocks 2005 - Rock Mechanics for Energy, Mineral and Infrastructure Development in the Northern Regions. Ed. S. H. G. Chen, W. Zhou, J. Tinucci. Anchorage, AL**:** Preprint # ARMA/USRMS 05-861.

Liang, Z. Z., C. A. Tang, et al. (____). "Numerical simulation of 3D failure process in heterogeneous rocks." from http://www.fegensoft.com/DOWN/Z.Z.pdf.

Lo, T. and P. L. Inderwiesen (1994). Fundamentals of Seismic Tomography. L. R. Lines. **6:** 178.

Mason, I. M. (1981). "Algebraic reconstruction of a two-dimensional velocity inhomogeneity in the High Hazles seam of Thoresby Colliery." Geophysics **46**(3): 298 - 308.

Moes, N. and T. Belytschko (2002). "Extended finite element method for cohesive crack growth." Engineering Fracture Mechanics **69**(7): 813 - 833.

Mohr, O. (1900). "Welche Umstände bedingen die Elastizitätsgrenze und den Bruch eines Materials?" Z. Ver. dt. Ing. **44**: 1524 - 1530; 1572 - 1577.

MSHA (1996). Report of technical investigation, Underground non-metal mine, Mine collapse accident, Solvay Mine, Solvay Minerals Inc., Green River, Sweetwater County, Wyoming.

Pande, G. N., G. Beer, et al. (1990). Numerical Methods in Rock Mechanics, John Wiley & Sons Ltd.

Pariseau, W. G. (1995). Coupled three-dimensional finite element modeling of mining in wet ground. 3rd. Canadian Conference on Computer Application in Mineral Industry (CAMI '95): 283 – 292.

Pariseau, W. G., J. C. Johnson, et al. (1995). Finite element simulation of central pillar mining at the Homestake Mine. 3rd. Canadian Conference on Computer Application in Mineral Industry (CAMI '95) 456 – 463.

Pariseau, W. G., S. C. Schmelter, et al. (1997). "Mine slope stability by coupled finite element analysis." Int. J. of Rock Mech. and Min. Sc. **34**(3/4): 520 - 520.

Park, E., S. Choi, et al. (2005). Simulation of the ground subsidence mechanism using a PFC2D. Alaska Rocks 2005 - Rock Mechanics for Energy, Mineral and Infrastructure Development in the Northern Regions. Ed. S. H. G. Chen, W. Zhou, J. Tinucci. Anchorage, AL**:** Preprint # ARMA/USRMS 05-735.

Park, E., C. D. Martin, et al. (2004). Simulation of the mechanical behavior of discontionous rock masses using a bonded-particle model. Gulf Rocks 2004 - 6th. North American North American Rock Mechanics Association. Houston ,Texas. Preprint No. ARMA/NARMS 04/480.

Peirce, A. P. and J. A. Ryder (1983). Extended boundary element methods in the modelling of brittle rock behaviour. Fifth international congress on rock mechanics, Melbourne, Victoria, Australia, A. A. Balkema, Rotterdam, Netherlands.

Pells, P. J. N. (1993). Uniaxial strength testing. Comprehensive Rock Engineering - Principles, Practice & Projects. J. A. Hudson, Pergamon Press. **3:** 67 - 85.

Peng, S. S. and D. Dutta (1992). Evaluation of various pillar design methods: A case study. Proceedings of the Workshop on Coal Pillar Mechanics and Design, Bureau of Mines, USA: 269 – 276.

Peng, S. S., P. Tsang, et al. (1989). Yield pillar applications under strong roof and strong floor condition - A case study. Rock Mechanics as a Guide for Efficient Utilization of Natural Resources, Balkema, Rotterdam, Netherlands.

Peterson, J. E., B. N. P. Paulsson, et al. (1985). "Application of algebraic reconstruction techniques to crosshole seismic data." Geophysics **50**(10): 1566 - 1580.

Potyondy, D. (2002). Modeling solids via bonding, Particle Flow Code (PFC2D/3D) Training Course, First International PFC Symposium, Gelsenkirchen, Germany, November 6, 2002.

Radon, J. (1917). "Uber die bestimmung von functionen durch ihre integralwere lange gewisser mannigfaltigkeiten." Ber. Verh. Saechs. Akad. Wiss. **69**: 262 - 267.

Robert, A., I. Hawkes, et al. (1965). "Some field applications of the photoelastic stressmeter." Int. J. of Rock Mech. and Min. Sc. **2**: 93 - 103.

Romanowicz, B. (2003). "3D structure of the Earth's lower mantle." Comptes Rendus - Academie des sciences. Geoscience **335**(1): 23 - 35.

Scholz, C. H. (1968a). "Experimental study of the fracturing process in brittle rock." J. Geophy. Res. **73**(4): 1447 - 1454.

Scholz, C. H. (1968b). "Microfracturing and the inelastic deformation of rock in compression." J. Geophy. Res. **73**(4): 1417 - 1432.

Scott, T. E., Q. Ma, et al. (1993). "Tomographic acoustic velocity changes induced during indentation of Berea sandstone." EOS, Trans. Amer. Geophys. Union **74**(43): 408.

Seghatchian, J., M. Cerrolaza, et al. (1997). "Boundary elements and damage mechanics to analyze excavations in rock mass." Engineering Analysis with Boundary Elements **20**(1): 1 - 16.

Shi, G. (1988). Discontinuous deformation analyses - a new numerical model for the statics and dynamics of block systems, University of California, Berkeley. **PhD**.

Shi, G. and R. E. Goodman (1988). Discontinuous deformation analyses - a new method for computing stress, strain and sliding of block systems. Key questions in Rock Mechanics. P. A. Cundall, Balkema, Rotterdam**:** 381 - 383.

Sinha, K. P. (1979). Displacement discontinuity technique for analyzing stresses and displacements due to mining in seam deposits, University of Minnesota. **Ph.D.:** 311.

Su, D. W. H. and G. J. Hasenfus (1996). Practical coal pillar design considerations based on numerical modeling. 15th. International Conference on Ground Control in Mining, Golden, CO.

Su, D. W. H. and G. J. Hasenfus (1999). Coal pillar strength and practical coal pillar design considerations. 2nd. International Workshop on Coal Pillar Mechanics and Design, Vail, CO: 155 – 162.

Tang, C. (1997). "Numerical simulation of progressive rock failure and associated seismicity." Int J of R Mech. & Min. Sc. **34**(2): 249 - 261.

Tang, C. A., H. Liu, et al. (2000). "Numerical studies of the influence of microstructure on rock failure in uniaxial compression - Part I: effect of heterogeneity." Int. J. of Rock Mech. and Min. Sc. **37**: 555 - 569.

Tang, C. A., W. T. Yang, et al. (1998). "A new approach to numerical method of modelling geological processes and rock engineering problems--continuum to discontinuum and linearity to nonlinearity." Engineering Geology **49**(3): 207 - 214.

Terada, M. and T. Yanagidani (1986). Application of Ultrasonic Computer Tomography to Rock Mechanics. Ultrasonic spectroscopy and its applications to material science**:** 205 - 210.

Tonon, F. and B. Amadei (2003). "Stresses in anisotropic rock masses: an engineering perspective building on geological knowledge." Int. J of R Mech. & Min. Sc. **40**(7-8): 1099 - 1120.

von Estorff, O. and G. Schmid (1984). Application of the boundary element method to the analysis of the vibration behavior of strip foundations on a soil layer. International symposium on dynamic soil-structure interaction, Minneapolis, MN, A.A. Balkema, Rotterdam, Netherlands: 11-17.

Wang, C., D. D. Tannant, et al. (2003). "Numerical analysis of the stability of heavily jointed rock slopes using PFC2D." Int J of R Mech. & Min. Sc. **40**: 415-424.

Wanne, T. (2002). PFC3D simulation procedure for compressive strength testing of anisotropic hard rock. 1st. Intl. PFC Symposium, Numerical Modeling in Mocromechanics via Particle Methods, Germany, A.A. Balkema Publishers: 241 – 249.

Wanne, T., E. Johansson, et al. (2004). Report on "Äspö Pillar Stability Experiment"**:** 38.

Wardle, L. J. (1980). Boundary element methods for solution of stress analysis problems in mining Technical Report - Division of Applied Geomechanics, CSIRO, Vol 102. **102:** 19.

Wardle, L. J. (1982). Fundamental solutions and boundary integral formulation for tabular excavations in a non-homogeneous rock mass. Technical Report - Division of Applied Geomechanics, CSIRO, Vol.133**:** 18.

Westman, E. C. (2004). "Use of tomography for inference of stress redistribution in rock." IEEE Transactions on Industry Applications **40**(5): 1413 - 1417.

Westman, E. C., K. Y. Haramy, et al. (1996). Seismic tomography for longwall stress analysis. 2nd. North American Rock Mechanics Symposium: NARMS '96, Montreal, Quebec, Canada, A.A.Balkema, Rotterdam, Brookfield: 397 – 401.

Williams, J. R. and G. G. W. Mustoe (1987). "Modal methods for the analysis of discrete systems." Comp. Geotechnics **4**: 1 - 19.

Yufin, S. A., E. V. Lamonina, et al. (2005). Numerical Modeling of Jointed Rock Masses Using Existing Models of Continua. Alaska Rocks 2005 - Rock Mechanics for Energy, Mineral and Infrastructure Development in the Northern Regions. Ed. S. H. G. Chen, W. Zhou, J. Tinucci. Anchorage, AL**:** Preprint # ARMA/USRMS 05-760.

Zipf Jr., R. K. (1992). MULSIM/NL Application and Practitioner's Manual. Bureau of Mines, Information Circular (IC 9322)**:** 54.

Zipf Jr., R. K. (1999). Using a postfailure stability criterion in pillar design. Second International Workshop on Coal Pillar Mechanics and Design, Vail, CO: 181 – 192.

Zipf Jr., R. K. (2001). Pillar design to prevent collapse of room-and-pillar mines. Underground Mining Methods: Engineering Fundamentals and International Case Studies. W. A. H. a. R. L. Bullock. Littleton, CO.

CHAPTER 3: MICRO-MECHANICAL MODELING OF FIVE OAKS LIMESTONE

ABSTRACT

A study was conducted to simulate the results of uniaxial compressive tests using micro-mechanical models on Five Oaks Limestone samples obtained from a mine in southwest Virginia. The modeling was done using the distinct element code PFC^{3D}. The advantage of using a micro-mechanical model is that no assumptions regarding the location and type of failure have to be made. In the initial part of the study, an attempt was made to find the relationship between the particle size used in the model with the peak load and the Young's modulus. The second half of the study simulated the results of the model to that of the laboratory tests. The model was made to run to failure and the Young's modulus, peak load and the fracture mode was made to match with those in the laboratory. The current study will help future research in this area in the calibration process for micro mechanical models and for other studies based on this model.

3.1 INTRODUCTION

The mechanical behavior of rock has been successfully modeled using two- and three-dimensional continuum modeling techniques. This approach has been successful because the smallest element in the model has a length scale much smaller than those of the objects of interest (e.g. dams, bridge decks). However it is often rewarding to model such 'continua' as discontinua, because new knowledge about their macroscopic behavior can be obtained after their microscopic mechanisms are understood (Cundall and Hart 1993). The new trend in this area is the use of the two- and three-dimensional discontinuum modeling codes. The advantage of using these micro-mechanical modeling techniques is that no assumptions have to be made about the location and type of fracture and failure –

cracking takes place spontaneously and can exhibit a variety of mechanisms when certain local stress conditions are exceeded. According to Hazzard and Young (2002), interesting insights about the micro-mechanics of deformation and failure will be obtained under different stress conditions if the failure mechanisms produced by the models are quantified and studied.

Discontinuum models like PFC^{2D} (Itasca Consulting Group) have been used with much success in various fields. A two dimensional bonded-particle model was used by Hazzard, Collins et el. (2002) to simulate shear-type micro-seismic events induced by tunnel excavation in granite. A plane of weakness was included in the model and subjected to increasing shear load while the normal load across the plane was held constant. The results were compared with actual results obtained from seismic monitoring around an underground excavation. According to the authors, the combination of monitoring the same rock mass using both micro-seismic and ultrasonic techniques affords the unique ability to investigate fracturing over different magnitude scales. Hazzard and Young (2002) presents a numerical modeling approach using PFC^{2D} that simulates cracking and failure in rock and the associated seismicity. A technique is also described for quantifying the seismic source mechanisms of the modeled events. The procedure describes how moment tensors and moment magnitudes can be calculated for these simulated seismic events. A new geomechanical modeling technique was developed using PFC^{2D} by Hazzard and Young (2001) in which the models can generate seismicity

from induced cracks and fractures. Hazzard and Young (2000) also simulated acoustic emissions in Lac du Bonnet granite using PFC^{2D}.

PFC^{2D} has also been used to simulate a loading-type failure around an underground excavation in brittle rock by Fakhimi, Carvalho et al. (2002). The authors performed a plane strain (biaxial) test on a rectangular prism of Berea sandstone with a circular opening to observe the damaged zone around the opening. The results from the modeling were in good agreement with the experimental test. It was concluded that by simulating the rock as an assemblage of cylindrical particles, surface spalling and crack propagation can be easily modeled. Wang, Tannant et al. (2003) studied the stability of heavily jointed rock slopes using PFC^{2D}. The modeling methods and procedures presented in the study demonstrated a new approach to the simulation of a rock mass and the stability analysis of excavations in a rock mass. With this new approach, study of the stability of excavations was carried out in such a way that the development and movement of the rock mass and failure surface can be visualized in two dimensions. Park, Martin et al. (2004) simulated the mechanical behavior of discontinuous rock masses using UDEC (Itasca Consulting Group) and PFC^{2D}. The paper reviews the methodology developed in Sweden for the Rock Mechanical Descriptive Model. The results from the UDEC Rock Mechanical Descriptive Model are compared to results from the discrete element software, PFC^{2D}. The post-peak response of the PFC model was not determined by a user-specified model, while the UDEC results were determined by the constitutive model applied to the joints.

All the studies mentioned above were done using the two dimensional micro-mechanical models. The models were able to develop fracture and failure on their own and there was no need to specify any constitutive models for them. However due to the two dimensional nature of these models, only a section of the model could be analyzed. Analysis of the model in its entirety can be made using the three dimensional version of this code. The Particle Flow Code in 3-dimensions (PFC^{3D}) (Itasca Consulting Group 2003) is a discrete element code and is a well-documented and commercially available tool developed by Itasca Consulting Group, Inc. Hazzard and Young (2002) extended their earlier study on acoustic emission using PFC^{3D}. Kulatilake, Malama et al (2001) investigated the effect of joint geometry parameters on the uniaxial compressive strength of jointed blocks and the results of the laboratory experiments and numerical simulations were compared. It was concluded from the study that there is a great dependence of the block strength of a jointed rock on the joint geometry configuration. The joint geometry configuration was also found to control the mode of failure of a jointed block of rock under uniaxial loading. Wanne (2002) studied the effect of anisotropy of the rock on strength and deformation properties by simulating a standard unconfined compression test with PFC^{3D}. Quantitative results for peak strength and Young's modulus obtained from the simulations were similar to that obtained from laboratory.

The current study has been done with the use of the Particle Flow Code in 3-dimensions (PFC^{3D}). The first part of the study analyzed the effect of the particle size on the macro-properties of the sample. The second part of the study was conducted to simulate the

properties of the Five Oaks Limestone using the micro-mechanical modeling. The current study will help future studies in the calibration stage of the numerical model. The Young's modulus, peak load and the fracture mode were matched to that obtained in the laboratory using the micro-mechanical modeling.

3.2 MICRO-MECHANICAL MODEL

PFC^{3D} simulates a rock as an assemblage of spheres of specified stiffness bonded together with bonds of specified strength using the distinct element method. Cundall (1971) introduced the distinct element method (DEM) for analyzing rock mechanics problems and later Cundall and Strack (1979) applied it to soils. The interaction of the particles in the distinct element method is viewed as a transient problem with equilibrium state developing whenever the internal forces balance each other (Cundall and Strack 1979).

The calculation cycle in PFC^{3D} is a time stepping algorithm that requires the repeated application of the law of motion to each particle, a force-displacement law to each contact and a constant updating of wall positions. Contacts, which may exist between two balls or walls, are formed and broken automatically during the course of a simulation (Itasca Consulting Group 2003). The micro-stiffnesses (normal and shear) and micro-strengths (normal and shear) can be adjusted in the model to produce realistic macro rock behavior.

3.3 METHODS

3.3.1 LABORATORY EXPERIMENTS

Limestone samples were obtained from the Five Oaks limestone bed in southwest Virginia. Cylindrical cores were prepared at the Rock Mechanics Laboratory, Department of Mining and Minerals Engineering, Virginia Tech. Uniaxial compressive tests were conducted on cylindrical limestone samples. Each of the samples had a height of 0.102 m (4 in) and width of 0.05 m (2 in). The loading rate for the tests was 0.003 mm/sec. The samples were made to fail and the Young's modulus and the compressive strength were calculated from these tests along with other properties of the rock. Figure 3.1 shows the sample just before it was loaded while Figure 3.2 is a picture of the sample after it failed under the uniaxial compressive tests.

FIGURE 3.1 SAMPLE IN THE UNIAXIAL COMPRESSIVE TESTING MACHINE.

FIGURE 3.2 SAMPLE AFTER BEING CRUSHED IN THE UNIAXIAL COMPRESSIVE TESTING MACHINE.

3.3.2 NUMERICAL MODELING

PFC^{3D} Version 3.00 was used to simulate these tests in the computer. The first part of the study was conducted to see the effect of the particle size on the peak load and the Young's modulus of the model. The purpose of the second part of the study was to convert the macro-properties of the sample in the laboratory to micro-properties for the model.

In the first part of the study cylindrical samples were developed using PFC^{3D} having a height-to-width ratio of 2:1. Figure 3.3 shows the cylindrical model that was developed for the study in PFC^{3D}. Table 3.1 shows the range of particle radii chosen for this study along with the average particle radii.

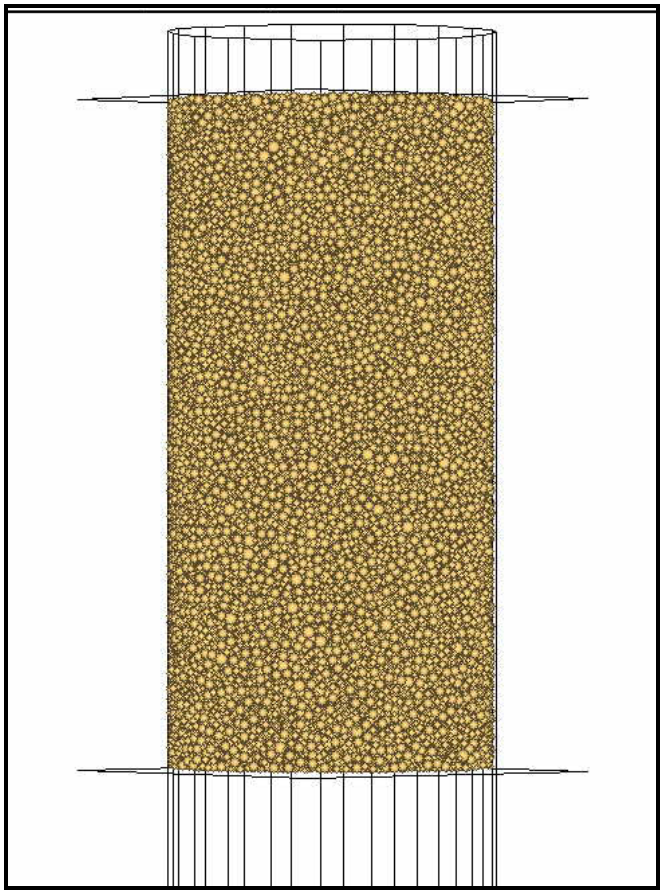

FIGURE 3.3 INITIAL MODEL DEVELOPMENT IN PFC^{3D} ALONG WITH THE PLATENS.

TABLE 3.1 RANGE OF PARTICLE RADII CHOSEN FOR THE STUDY.

Radius (m)		
R_{min}	R_{max}	R_{ave}
0.00045	0.0012	0.000825
0.00055	0.0013	0.000925
0.00065	0.0014	0.001025
0.00075	0.0015	0.001125
0.00085	0.0016	0.001225
0.00095	0.0017	0.001325
0.00105	0.0018	0.001425
0.00115	0.0019	0.001525
0.00125	0.002	0.001625
0.00135	0.0021	0.001725
0.00145	0.0022	0.001825
0.00155	0.0023	0.001925
0.00165	0.0024	0.002025

The density for the particles in the model was calculated on the basis of an earlier study by Hazzard (1988).

A porosity of 40% was chosen for the model. Attempts were made to reduce the porosity below the chosen value. The machine used for the validation study had 512 MB of processor speed of and it was not possible to reduce the porosity beyond the chosen value in the machine. Also, there are limits to the porosity that can be achieved. It is not possible to pack particles to an arbitrarily low porosity value (Itasca Consulting Group 2003). Hence, for further studies, a porosity of 40% was used.

The initial particle stiffness and strengths are calculated using equations 3.1 – 3.4, obtained from the PFC^{3D} manual (Itasca Consulting Group 2003).

$$\overline{E} = \frac{K_n}{4R} \tag{3.1}$$

$$\sigma_t = \frac{S_n}{4R^2} \tag{3.2}$$

$$K_s = \frac{K_n}{2} \tag{3.3}$$

$$S_s = S_n \tag{3.4}$$

where, $\overline{E}$ = apparent Young's modulus of the rock of a cubic array of spheres, assuming that the principal axes coincide with the axes of symmetry of the particle array.

σ_t = tensile strength of the of the cubic array, as discussed in $\overline{E}$.

K_n / K_s = Normal / shear stiffnesses of the particle

S_n / S_s = Normal / shear bond strength

The normal particle stiffness was set to two times the shear stiffness based on an earlier study by Hazzard (1988). Parallel bonds were used in the model so as to get a better compaction in the model, with a porosity of 40%. The final parallel bond strength was chosen as 1.25×10^9 N/m. The initial parallel bond stiffnesses were calculated using equation 3.5.

$$k^{(pb)} = \frac{0.5\,K_n}{A} \tag{3.5}$$

where, $k^{(pb)}$ = Parallel bond stiffness

A = Cross-sectional area of the parallel-bond material.

The initial properties used for the model were derived from the equations mentioned earlier. The initial values of the stiffnesses and strengths were obtained by using the values obtained from the laboratory in the equation for the apparent Young's modulus and tensile strength. The model was made to run until failure. The values of the Young's modulus and the peak load and the mode of failure were compared with those obtained in the laboratory. If the results were within a range of ±10%, it was accepted, otherwise the values were changed and the entire program was made to run again. Once the results were within the acceptable range the micro-properties of the model was accepted.

3.4 MODELING RESULTS

The first part of the study was aimed at finding if there is any correlation between the particle size and the Young's modulus and the peak load of the model. The peak stress was noted from each of these models along with the Young's modulus. Figure 3.4 shows the variation of the peak stress and the Young's modulus for varying particle radii for the model having a height of 0.102 m (4 in) and width of 0.05 m (2 in). Similar tests were run for another cylindrical model having the same height-to-width ratio of 2:1 and a similar trend was observed.

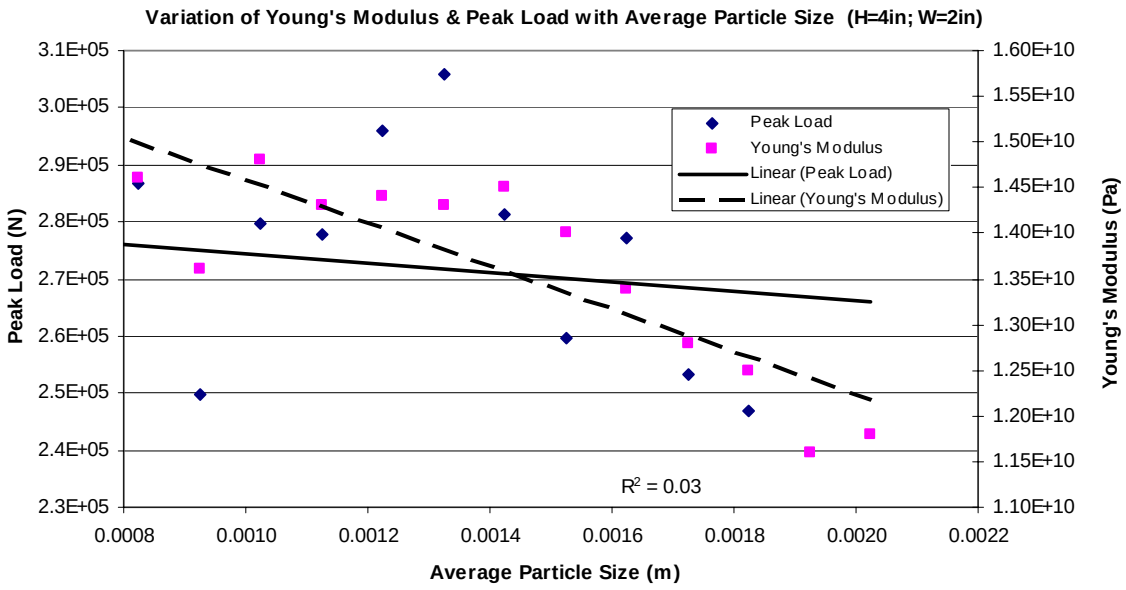

FIGURE 3.4 VARIATION OF PEAK LOAD AND YOUNG'S MODULUS WITH AVERAGE PARTICLE RADII ALONG WITH THE TRENDLINE (H=4IN; W=2IN)

In the second half of the study, the macro-properties of the sample in the laboratory were converted to the micro-properties for the model. Also the fracture mode was matched with that in the laboratory. Calibration is the term used to describe the iterative process of determining and modifying the micro-properties for a PFC^{3D} model. In this process, the responses of the model are compared to that in the laboratory and the micro properties of the model are modified in an iterative way to achieve good agreement (Wanne 2002). An inverse modeling method is used to determine the correct micro-mechanical properties of the numerical models from the macro-mechanical properties of the rock obtained during laboratory testing. This is a trial and error approach as no theory exists in order to obtain the correct relationship between the two properties. Figure 3.5 shows the simple flowchart that was developed in order to transform the macro properties of the rock to the micro properties of the sample.

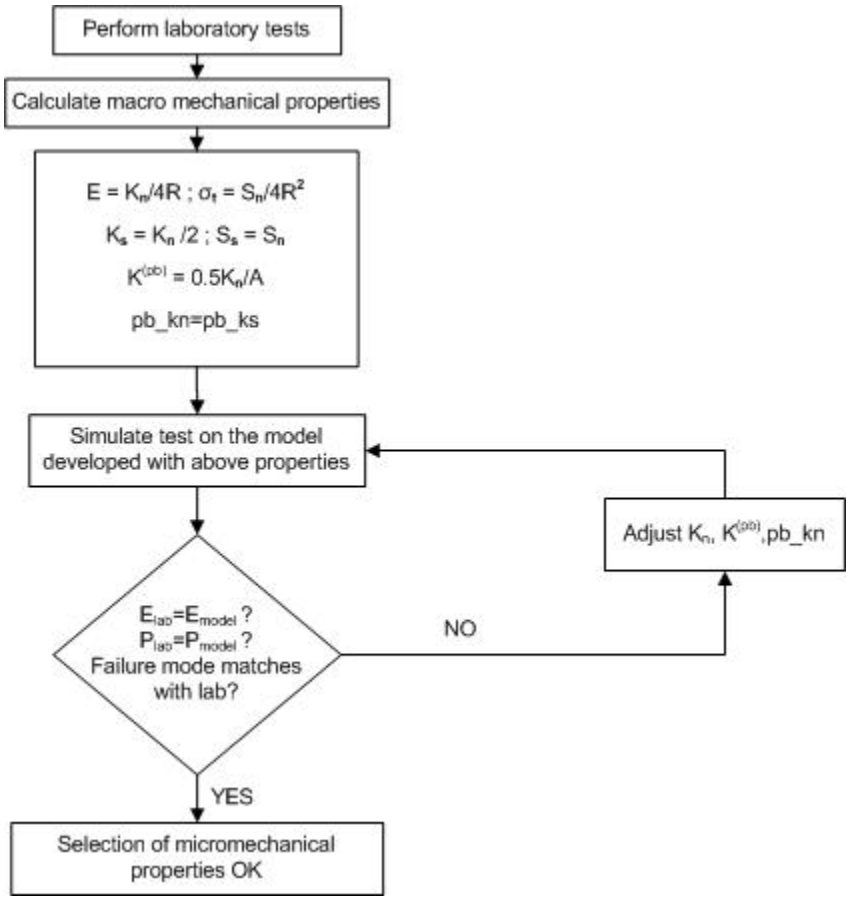

FIGURE 3.5 FLOWCHART FOR CONVERSION OF MACRO TO MICRO PROPERTIES.

The Young's modulus obtained from the model was matched with that from the laboratory. The values were accordingly adjusted in order to match these two properties. The values of the initial properties were decided on the basis of equations 3.1 – 3.5. The model was then made to run to failure. The peak load and the Young's modulus were calculated. The results were compared to that obtained in the laboratory. If the results were within ±10%, then the values were accepted, else the micro-parameters were changed and the model was made to run again. First, the Young's modulus was compared to that in the laboratory and then comparison was made for the peak load and the mode of

failure. Earlier studies compared the Young's modulus and the uniaxial compressive strength of the rock with that of the model. However, the authors feel that it is also important to match the fracture mode of the rock sample to that obtained from the model. Thus the Young's modulus, peak load and the fracture mode of the rock was matched with that of the model.

Figure 3.6 shows the PFC model just after it reaches its peak load. A FISH program was used in PFC^{3D}, in which cracks are formed whenever the applied load exceeds the strength of the bonds. The varying colored polygons show the formation of the cracks with time. The light colors indicate initial failures while the dark ones denote recent failures. The stress versus strain curve is also plotted along with the cracks. Figure 3.7 shows the same model with the tensile and shear failures. Figure 3.8 shows the model in post failure region.

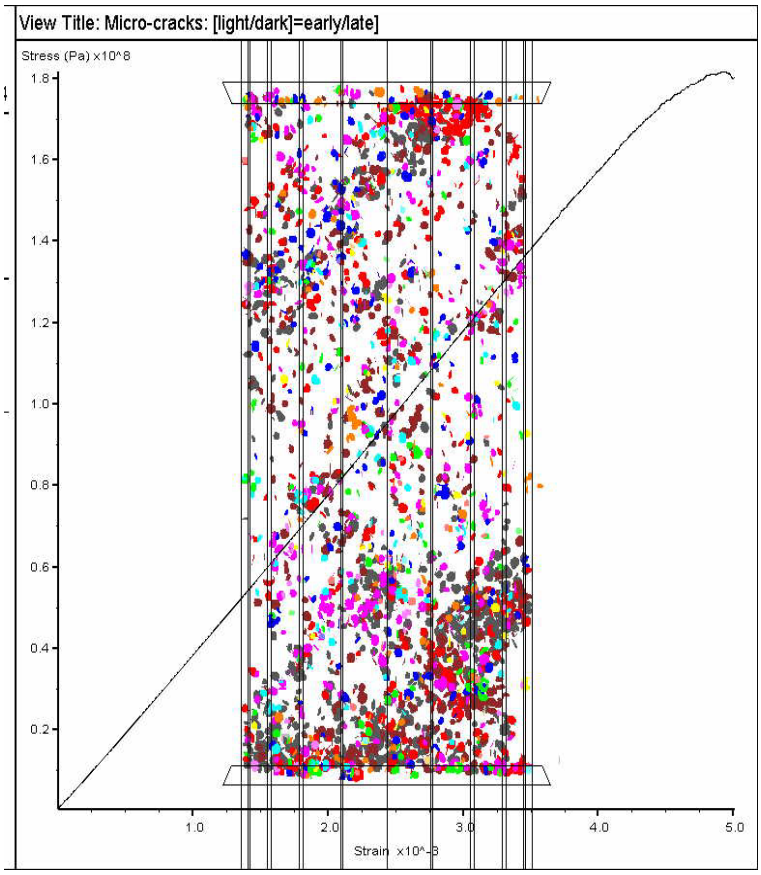

FIGURE 3.6 PFC MODEL JUST AFTER IT REACHES PEAK LOAD. VARYING COLORED CRACKS INDICATE CRACK FORMATION AT VARYING TIMES. LIGHT COLORS INDICATE EARLY FORMATION, WHILE DARK COLORS DENOTE RECENT FORMATION.

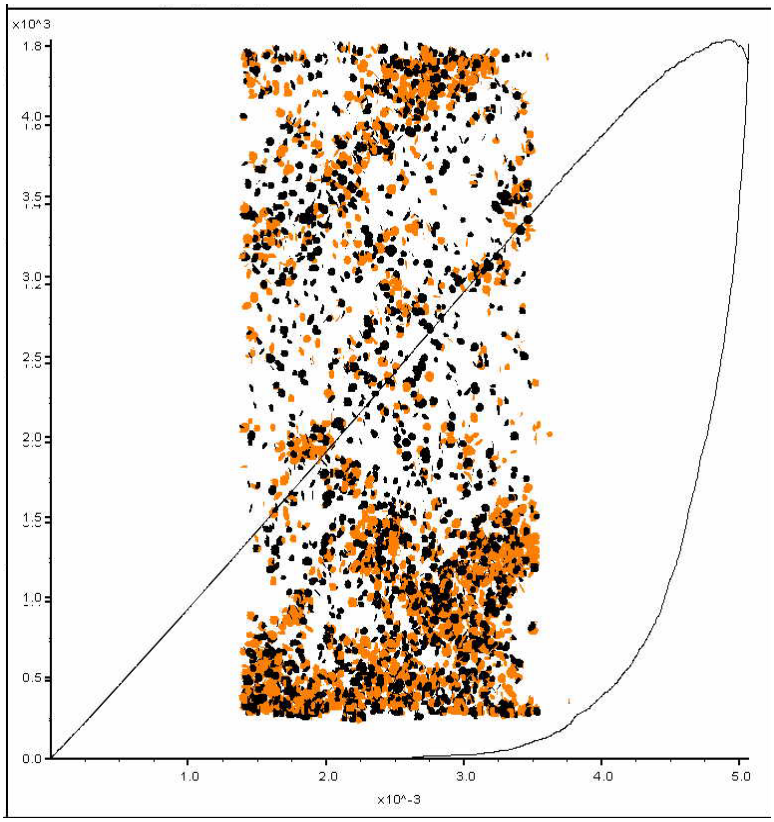

FIGURE 3.7 PFC MODEL JUST AFTER IT REACHES PEAK LOAD. ORANGE COLORED POLYGONS SHOW TENSILE FAILURE WHILE BLACK POLYGONS SHOW SHEAR FAILURE.

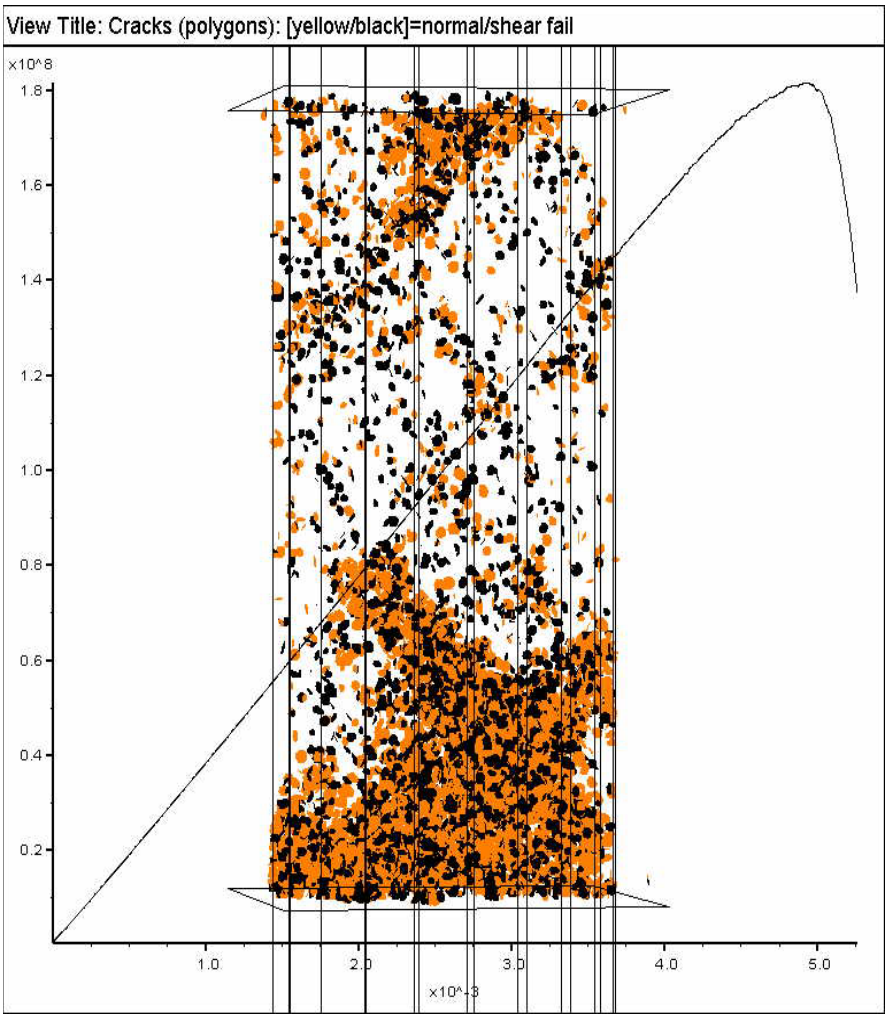

FIGURE 3.8 PFC MODEL IN THE POST FAILURE REGION.

3.5 ANALYSIS OF RESULTS

From Figure 3.4 it can be observed that neglecting a few outliers, there is an increasing trend in the Young's modulus as the size of the particle decreased. The R^2 value obtained from the Young's modulus data was approximately 75%. The peak load also changes with the increase in the number of particles. However, it was observed that as the radii of particles decreased, the model showed a better fracture mode. As the number of particles increases, the resolution, which is defined as the number of particles across the model diameter will be greater (Wanne 2002). Thus, greater the number of particles, the better the resolution and hence better results are expected to be obtained. However, with the increase in the number of particles, there was an increase in the computation time.

A time study was done by running the same model on various machines. The time of computation was observed for the study as shown below in Table 3.2. Based on this study, the later experiments will be done in a dual processor machine with 2.80 GHz and 2.00 GB of RAM. It was observed that though there is a slight increase in time for the dual processor, the advantage of using this machine was that more than one program could be run efficiently at the same time. Hence the later studies were conducted on the dual processor machine. A statistical package SAS® was used to do all the statistical calculations.

TABLE 3.2 TIME FOR RUNNING SIMILAR PROGRAM IN VARIOUS COMPUTERS

Speed (MHz)	RAM (MB)	Time (min)
24000	512	135
24000	1000	100
32000	1000	90
28000	2000	112
597	240	281

It was observed that the computer memory did not play a role in the processing time for the program. The computing time was observed to be dependent on the processor speed. On the basis of the study and also considering the resolution and the computing time, the final radii selected for the second half of the study was 0.00035 – 0.0011 m. This range of radii selected produced approximately 75,000 particles for a model with height 0.102 m (4 in) and width of 0.05 m (2 in).

It was observed that the normal and shear stiffness of the particles had a major impact on the Young's modulus while having a minor effect on the peak load. In other words, changing the normal and shear stiffness changed the Young's modulus more than the peak load. Similarly, the normal and shear strength of the parallel bonds produced a major change on the peak load and a minor change on the Young's modulus. Thus, in general, the particle stiffnesses and strength determines the Young's modulus while the parallel bond strength determines the strength or the peak load of the model. Similar observations were made in an earlier study by Hazzard (1998).

Table 3.3 shows the results from the laboratory and those that were obtained with the micro-properties of the model.

TABLE 3.3 COMPARISON OF LABORATORY AND NUMERICAL MODEL

	LABORATORY	PFC^{3D} MODEL	DIFF. IN LAB AND PFC^{3D} MODEL(%)
PEAK LOAD (N)	3.68E+05	3.57E+05	-2.79
COMPR. STR. (N/M^2)	1.86E+08	1.82E+08	-2.03
YOUNG'S MODULUS (N/M^2)	3.50E+10	3.90E+10	11.43

It was found that cracks formed in the rock are randomly located until the applied stress reaches 90 – 95% of the rock's peak strength. From Figure 3.7, it is clear that above this stress, the event locations exhibit clustering on the eventual failure plane. The observation matched with the earlier study by Hazzard (1998). Also it can be observed that the majority of the cracking takes place above 90 – 95% of the peak stress.

3.6 CONCLUSIONS AND RECOMMENDATIONS

The current study was conducted in PFC^{3D}. One of the biggest advantages of this model is that no initial assumption needs to be made regarding the position and type of failure. On loading the sample, fractures are developed with the breaking of bonds. Thus PFC^{3D} is best suited to model rock samples and conduct tests on them.

The first half of the study was conducted to see the effect of particle size on the peak load and the Young's modulus of the model developed. It was observed that both the Young's modulus and the peak load changes with the change in the particle size. It was also observed that as the number of particles increased, a better fracture mode was observed due to a smaller size of the particles. However, with the increase in the number of particles, there was an increase in the computing time. Keeping both factors in mind, the second half of the study was conducted with the particle radii ranging from 0.00035 – 0.0011 m. Thus for future studies, the particle size should be kept small depending on the computing capability of the machine in which the study is being done.

The second part of experiment was aimed to convert the macro-properties to the micro-properties of the model and also to simulate the fracture mode to that obtained in the laboratory. The results of the Young's modulus, peak load and also the failure mode obtained in the model were compared to that in the laboratory. A flowchart was developed on the basis of an earlier study in order to simulate these properties. However,

the earlier studies made a comparison of the Young's modulus and the uniaxial compressive strength of the rock to that in the model. The authors felt that it is also necessary to match the fracture mode. Thus the current study matches the Young's modulus, peak load and also the fracture mode obtained in the laboratory to that from the model. The peak load obtained from the model was approximately 3% less than the value obtained from the model, while the value of the Young's modulus was approximately 11% more than that obtained from the laboratory. Considering the variation of the values that are obtained in the laboratory during testing, the values obtained from the model can be accepted.

Studies have being undertaken to study the stress redistribution during an unconfined compressive test using PFC^{3D} and compare the results to that obtained in the laboratory using computer tomograms. Various other tests have been performed using this micro-mechanical model to see its capability in other areas. Studies have also been conducted to find a correlation between the micro-properties of the model and the macro-properties of the sample.

ACKNOWLEDGEMENT

We would like to acknowledge the support provided by the National Science Foundation (CMS-0134034).

REFERENCES

Cundall, P. A. (1971). A computer model for simulating progressive large scale movements in blocky rock systems. Symposium of the International Society of Rock Mechanics Nancy, France.

Cundall, P. A. and R. D. Hart (1993). Comprehensive Rock Engineering, Vol. 2: Analysis and Design Methods - Numerical modeling of discontinua., Pergamon Press.

Cundall, P. A. and O. D. L. Strack (1979). "A discrete element model for granular assemblies." Geotechnique **29**(1): 47 - 65.

Fakhimi, A., F. Carvalho, et al. (2002). "Simulation of Failure around a circular opening in rock." Int. J of R Mech. & Min. Sc. **39**(4): 507 - 515.

Hazzard, J. F. (1998). Numerical modeling of acoustic emissions and dynamic rock behavior. Dept. of Earth Sciences, Keele University. **Ph.D.**: 231.

Hazzard, J. F., D. S. Collins, et al. (2002). "Simulation of unstable fault slip in granite using a bonded-particle model." Pure & Applied Geophysics **159**: 221 - 245.

Hazzard, J. F. and R. P. Young (2000). "Simulating Acoustic Emissions in Bonded-Particle Models of Rock." Int. J. of R. Mech. & Min. Sc. **37**(5): 867-872.

Hazzard, J. F. and R. P. Young (2001). Seismic validation of micromechanical models. 38th. US Rock Mech. Sym., DC Rocks 2001, Washington DC, A.A.Balkema.

Hazzard, J. F. and R. P. Young (2002). 3D numerical modeling of acoustic emission. 5th. Int. Workshop on the Appl. Of Geophysics in Rock Engg., Toronto,Canada.

Hazzard, J. F. and R. P. Young (2002). "Moment Tensors and Micromechanical Models." Tectonophysics **356**(1 - 3): 181 - 197.

Itasca Consulting Group, Inc., PFC^{2D}. Minneapolis, MN.

Itasca Consulting Group, Inc., PFC^{3D} (2003). PFC^{3D}. Minneapolis, MN.

Itasca Consulting Group, Inc., UDEC. Minneapolis, MN.

Kulatilake, P. H. S. W., B. Malama, et al. (2001). "Physical and particle flow modeling of jointed rock block behavior under uniaxial loading." Int. J. of R. Mech. & Min. Sc. **38**: 641 - 657.

Park, E., C. D. Martin, et al. (2004). Simulation of the mechanical behavior of discontionous rock masses using a bonded-particle model. Gulf Rocks 2004 - 6th. North American North American Rock Mechanics Association. Houston ,Texas. Preprint No. ARMA/NARMS 04/480.

Wang, C., D. D. Tannant, et al. (2003). "Numerical analysis of the stability of heavily jointed rock slopes using PFC2D." Int J of R Mech. & Min. Sc. **40**: 415-424.

Wanne, T. (2002). PFC3D simulation procedure for compressive strength testing of anisotropic hard rock. 1st. Intl. PFC Symposium, Numerical Modeling in Mocromechanics via Particle Methods, Germany, A.A. Balkema Publishers.

CHAPTER 4: STRESS REDISTRIBUTION DETERMINATION THROUGH COUPLED LABORATORY TESTING AND NUMERICAL MODELING

ABSTRACT:

The ability to understand stress redistribution within a mine allows greater extraction efficiency with reduced safety concerns. Stress redistribution has been examined at the laboratory scale using ultrasonic tomography and numerical modeling using PFC^{3D}. A data acquisition system was built to obtain tomograms as samples are loaded in uniaxial compression. Limestone samples were loaded to failure. The tomograms of the samples correlate to various stress distributions. The tomograms are compared to analytical and PFC^{3D} results.

4.1 INTRODUCTION

Success has been achieved previously in the area of simulating the mechanical behavior of rock failure using two- and three-dimensional continuum modeling techniques. The new trend in this area however, is the use of the two- and three-dimensional discontinuum modeling codes. The advantage of using these micro-mechanical modeling techniques is that no prior assumptions have to be made about the location and type of fracture and failure – cracking takes place spontaneously and can exhibit a variety of mechanisms when certain local stress conditions are exceeded. Interesting insights about the micro-mechanics of deformation and failure under different stress conditions will be obtained if the failure mechanisms produced by the models are quantified and studied (Hazzard and Young 2002).

PFC^{2D} (Itasca Consulting Group) has been used with much success in various fields. Some of the areas in which it has been used include simulating acoustic emissions (Hazzard and Young 2000; Hazzard and Young 2001; Hazzard and Young 2002), failure around circular openings (Fakhimi, Carvalho et al. 2002), unstable fault slips and heavily jointed rock slopes (Wang, Tannant et al. 2003). Laboratory experiments and numerical simulations using PFC^{3D} (Itasca Consulting Group 2003) were performed to study the behavior of jointed blocks of model material under uniaxial loading (Kulatilake, Malama et al. 2001).

Laboratory tomographic systems have been developed in past experiments (Terada and Yanagidani 1986; Couvreur, Vervoort et al. 2001). Basic tomographic imaging acquisition systems are designed to collect ultrasonic data directly from a specimen in a stressed condition to view a cross-sectional image of the relative stress state inside of the specimen. Systems developed to date are not designed to accommodate upgrades for new technologies such as faster acquisition computers and higher resolution A/D converters. Some laboratory experiments that have investigated ultrasonic tomography involve the stress distribution from indentation (Scott, Ma et al. 1994), and stress distribution and acoustic emission location in hydraulically loaded samples (Falls, Young et al. 1992; Villaescusa, Seto et al. 2002). The current study compares experimental results from a data acquisition system designed to obtain tomograms for stress redistribution imaging from different rock types and sample sizes using LabVIEW programming to numerical

models. The fundamental relationship is that as stress is applied, the density of the rock increases, allowing the elastic wave to travel at a higher velocity.

Laboratory Virtual Instrument Engineer's Workbench (LabVIEW) was developed by National Instrument's Corp. for instrument acquisition and control. This graphical programming language develops Virtual Instruments (VIs) for the control of acquisition from an instrument. This program is widely used by test and research engineers for customized instrument acquisition and control.

The numerical modeling in the current study has been done with the help of Particle Flow Code in 3-dimensions (PFC^{3D}). PFC^{3D} is a well-documented and commercially available tool for modeling the behavior of brittle rock including fracture propagation and mechanical stability in the near-field around underground openings (Wanne 2002).

4.2 DISCRETE ELEMENT CODE – PFC^{3D}

PFC^{3D} is a distinct element code that simulates a rock as an assemblage of spheres of specified stiffness bonded together with bonds of specified strength. The distinct-element method (DEM) was introduced by Cundall (1971) for the analysis of rock mechanics problems and then applied to soils by Cundall and Strack (1979). The micro-stiffnesses (normal and shear) and micro-strengths (normal and shear) can be adjusted to produce realistic macro rock behavior. PFC uses an explicit approach to solve the equations of motion (Cundall 1971) meaning that the information propagates through the model and time steps are small. For this reason, the code can be used in dynamic simulations in which seismic waves propagate out from new faults and fractures.

The calculation cycle in PFC^{3D} is a time-stepping algorithm that requires the repeated application of the law of motion to each particle, a force-displacement law to each contact and a constant updating of wall positions. Contacts, which may exist between two balls or walls, are formed and broken automatically during the course of a simulation.

4.3 METHODS

4.3.1 LABORATORY EXPERIMENTS

Experimental tests of the data acquisition system were conducted to calibrate and verify the system for tomographic imaging. The objective of these tests was to observe stress redistribution patterns within rock samples. Ultrasonic velocity calibration and validation tests were conducted on Plexiglas samples (Johnson 2005). Tomograms were calculated from the arrival time data using GeotomCG (Tweeton 2001). This program uses the simultaneous iterative reconstruction technique (SIRT) to construct a velocity tomogram.

Limestone samples were obtained from the Five Oaks Limestone bed in southwest Virginia. The rock was chosen for this study because it is very uniform, and it was anticipated that the behavior between samples would not vary significantly. A summary of the index properties are shown in Table 4.1.

From Table 4.1 the P-Wave velocity is seen to be 6,645 m/s. The average value of transmission frequency through the limestone was found to be 250 kHz. These properties result in an ultrasonic wavelength of 2.66 cm; therefore the smallest structure that was expected to be resolved was 2.66 cm in length. Knowing this restriction for tomographic reconstruction, a limestone block was prepared for tomographic testing. The dimensions of the block, the placement, and size of the load and the sensor locations are shown in Figure 4.1.

The sensors were attached to the limestone using a cyanoacrylate adhesive. An indentation load was used to apply a concentrated stress on the limestone sample. This stress would create a large velocity contrast that should be able to be imaged with the UDAQ system. Ultrasonic data were acquired at the points shown in Table 4.2. The indentation load was applied in an eccentric manner, resulting in the stress being concentrated beneath one half of the 5 cm (2 in) diameter platen.

TABLE 4.1 FIVE OAKS LIMESTONE INDEX PROPERTIES

	Metric Units		**English Units**	
Property	**Avg.**	**St. Dev.**	**Avg.**	**St. Dev.**
P Velocity m/s (ft/sec)	6,645	288	21,802	943
S Velocity m/s (ft/sec)	2,747	131	9,012	430
Porosity (%)	0	0	0	0
Density g/cm3 (lb/in3)	2.696	0.009	168.31	0
Peak Load N (lbs)	324,583	86,310	72,969	19,403
Peak Stress MPa (psi)	164	43	23,802	6,307
Elastic Modulus MPa (psi)	35,119	4,428	5,093,579	642,181

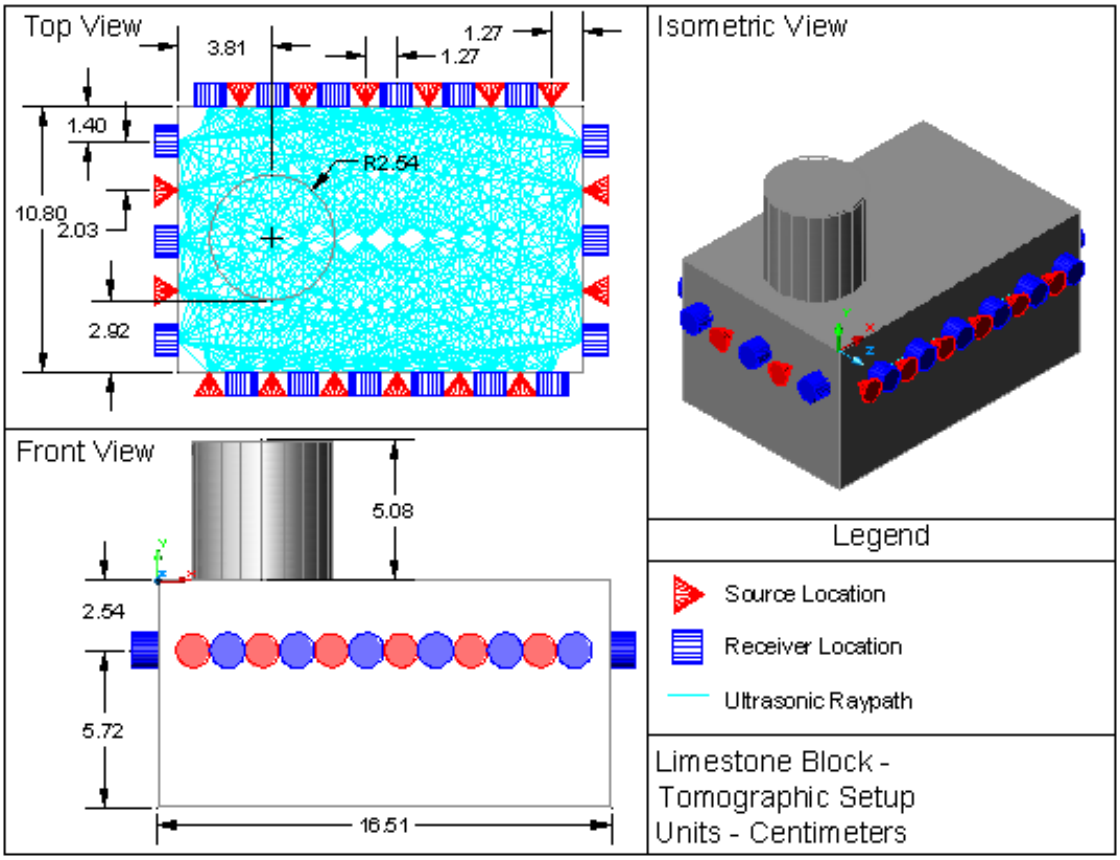

FIGURE 4.1 FIVE OAKS LIMESTONE TOMOGRAPHIC SETUP

TABLE 4.2 LOAD CONDITIONS FOR TOMOGRAPHIC DATA COLLECTION.

Load	MPa	PSI
1	0	0
2	17	2,500
3	34	5,000
4	52	7,500
5	69	10,000
6	86	12,500
7	103	15,000
8	0	0

At each load, 288 ultrasonic waveforms were collected, one for each source and receiver pair. From these waveforms the arrival time was independently picked and checked. To

improve the accuracy of the program two independent picks were done at each load and the arrival times uncommon to both correlations were removed as outliers.

The samples were monitored by an ultrasonic data acquisition system which was controlled by LabVIEW. The data acquisition system developed for the study is shown in Figure 4.2. This figure shows how the ultrasonic data are passed from one device to the next.

An ultrasonic pulse is generated by a Panametrics 5077PR Ultrasonic Square Wave Pulser. The ultrasonic pulser can output an ultrasonic square wave tuned to a particular frequency. For this study a 500 kHz ultrasonic square wave was pulsed at a rate of 100 Hz. The pulse is then passed to an ESG Ultrasonic Switchbox Pulser. This unit is controlled in the LabVIEW environment by the control PC. The pulse is digitally relayed by the PC to one of 16 source transducers on the sample. The ultrasonic waveform is received by National Instrument's PXI-5102 Digital Oscilloscopes. These analog to digital conversion instruments are 2 channel modules that can be interconnected by using a PCI Extension Interface (PXI). The National Instrument's PXI chassis used allows for simultaneous acquisition of ultrasonic data at a rate up to 20 million samples per second on up to 20 analog channels. Acquisition of the ultrasonic data was controlled using LabVIEW.

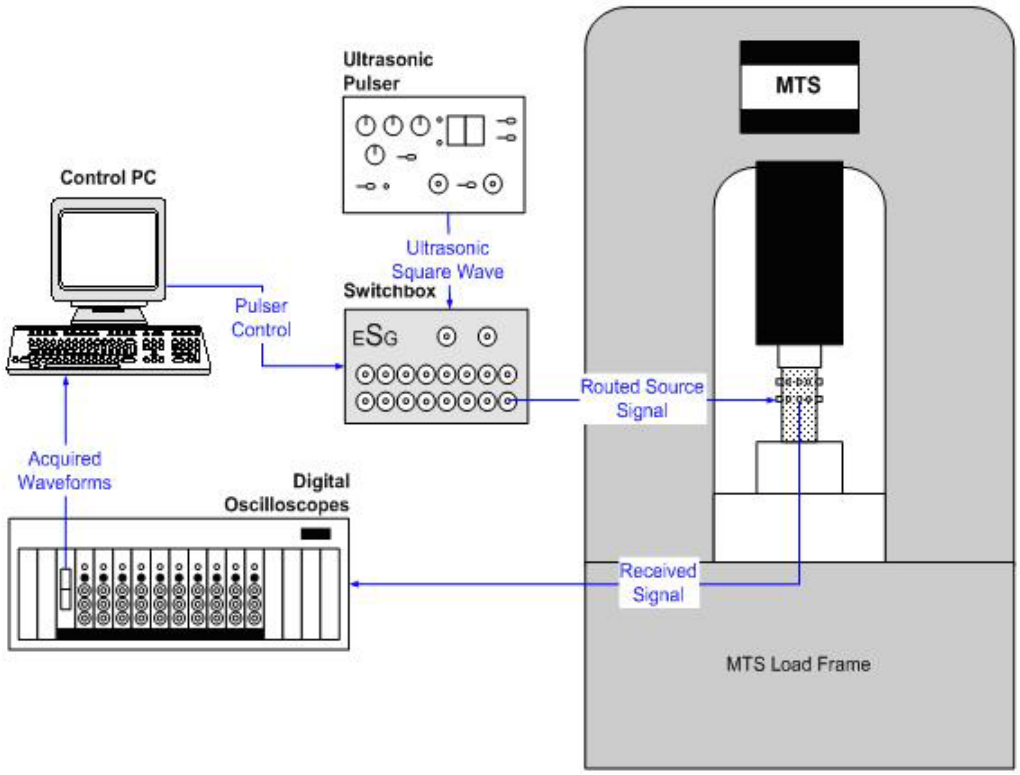

FIGURE 4.2 HARDWARE FLOWCHART (JOHNSON 2005)

4.4 NUMERICAL MODELING

4.4.1 CALIBRATION

In the first half of the study, the macro-properties of this limestone sample in the laboratory were converted to the micro-properties for the PFC^{3D} model. Also, the fracture mode was matched with that in the laboratory. Calibration is the term used to describe the iterative process of determining and modifying the micro-properties for a PFC^{3D} model. In this process, the behavior of the model is compared to those in the laboratory and the micro-properties of the PFC^{3D} model are modified in an iterative way to achieve the correct macro-mechanical properties (Wanne 2002). This process of converting the macro-properties to the micro-properties is a trial and error approach as no theory exists to obtain the correct relationship between the two properties. Figure 4.3 shows the simple flowchart that was developed in order to transform the macro-properties of the rock to the micro-properties of the sample. Cylindrical samples were developed using PFC^{3D} having a height-to-width ratio of 2:1 and the Young's modulus, peak load and the fracture mode was matched with the laboratory results.

The initial particle stiffness and strengths are calculated using equations as shown in the flowchart, obtained from PFC^{3D} manual where,

E = Young's modulus of the rock, calculated from the laboratory tests

σ_t = Tensile strength of the rock sample, calculated from the laboratory tests

K_n / K_s = Normal / shear stiffnesses of the particle

S_n / S_s = Normal / shear bond strength

$k^{(pb)}$ = Parallel bond stiffness

A = Cross-sectional area of the parallel-bond material.

The model was made to run until failure with each set of values. The Young's modulus, the peak load and the mode of failure were compared with those obtained in the laboratory. If the results were within a range of ±10%, they were accepted, else the values were changed and the entire program was made to run again. Once the results were within the range the micro-properties of the model were accepted. Figure 4.4 shows the final model that was used for the validation process.

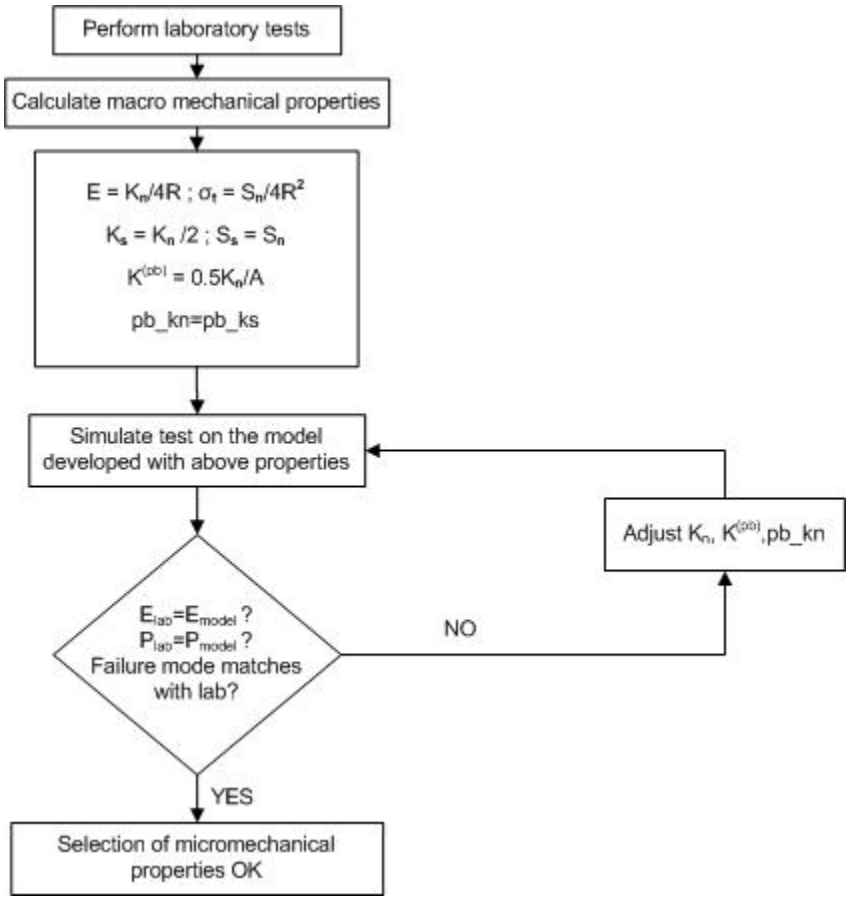

FIGURE 4.3 FLOWCHART FOR CONVERSION OF MACRO- TO MICRO-PROPERTIES.

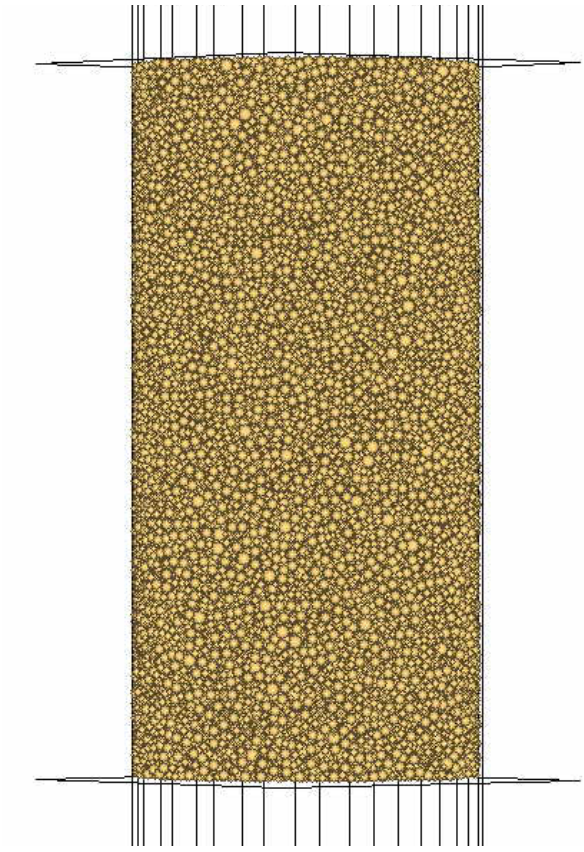

FIGURE 4.4 INITIAL MODEL USED IN PFC^{3D} ALONG WITH THE FLAT PLATENS FOR THE VALIDATION PROCESS.

4.4.2 MODEL DEVELOPMENT & PROCEDURE

A rectangular sample was developed having the same dimensions as the sample prepared in the laboratory. The code does not permit creation of a circular loading wall, so a square loading wall having the dimension equal to the diameter of the circular platen was used to apply load to the block. The particle radii chosen for the study varied from 0.015m to 0.025m.

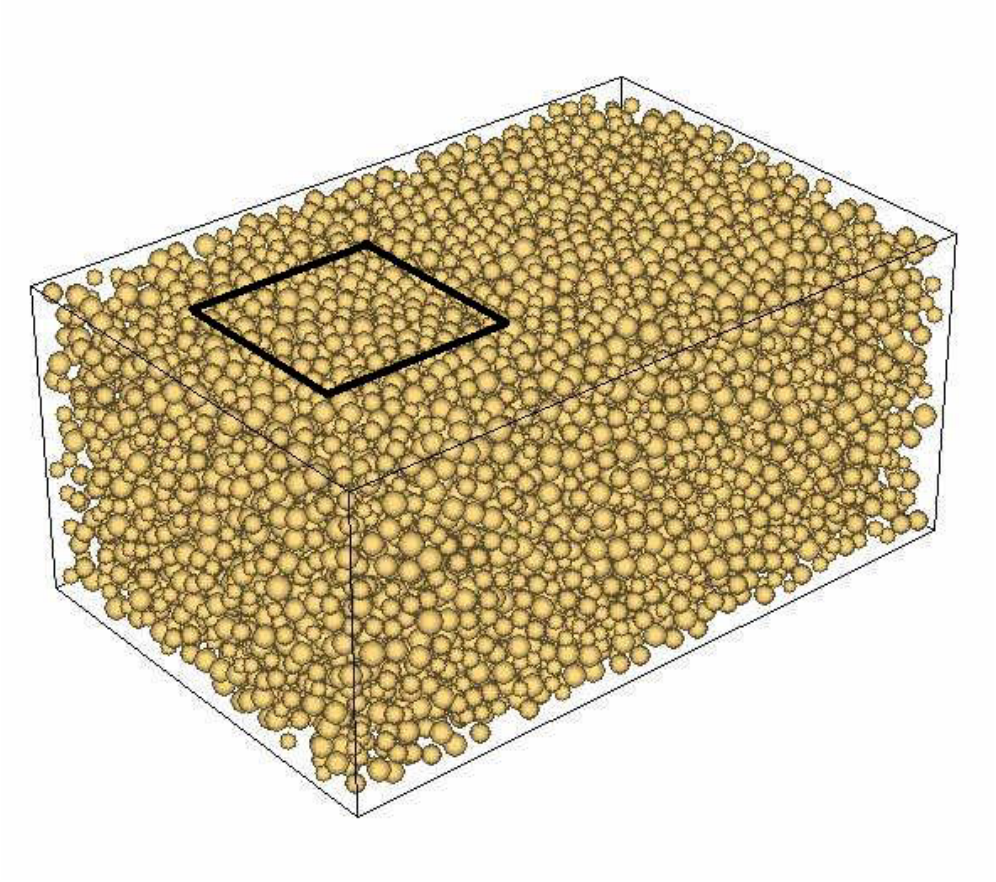

FIGURE 4.5 RECTANGULAR BLOCK MODEL USED IN PFC3D WITH POINT LOAD PLATEN.

Approximately 27,000 particles were formed in the rectangular block. Figure 4.5 shows the initial rectangular block that was developed using the numerical code. Uniform velocity was applied on the small wall at the top. The model was made to run until it failed.

4.5 RESULTS AND DISCUSSIONS

The peak load, Young's modulus and the fracture type were calibrated in the first half of the numerical modeling study. Table 4.3 shows the results from the laboratory and those that were obtained with the PFC^{3D} model. Considering the variation of the values that are obtained in the laboratory during testing, the values obtained from the PFC^{3D} model were accepted for the study and the next part of the study was conducted with these properties.

A grid system was developed throughout the entire rectangular block and the stress values were noted at those grid points. A commercial package, Surfer® was used to plot the stress distribution in the model. Figures 4.6 (A) and (B) show the tomograms at various portions of the peak load along with the results that were obtained from the numerical model at the same load. In the figures below, (i) shows the tomograms depicting the velocity in ft/sec obtained from the laboratory, while (ii) shows the stress in MPa obtained from the numerical modeling.

From the figures below it can be seen that there is a correlation between the results obtained in the laboratory and that from the numerical modeling. The results from the tomogram shows that at the point where the load was applied there is an increase in the velocity while at a similar position an increment in the stress can be observed from the numerical model as the sample is loaded.

TABLE 4.3 COMPARISON OF LABORATORY AND NUMERICAL MODEL

	Laboratory	Standard Deviation	PFC3D Model	Diff. between Lab and Model (%)
Peak Load (N)	3.68E+05	6.65E+04	3.57E+05	-2.99
Compr. Str. (N/m^2)	1.86E+08	34	1.82E+08	-2.15
Young's Modulus (N/m^2)	3.50E+10	1.49E+03	3.90E+10	11.43

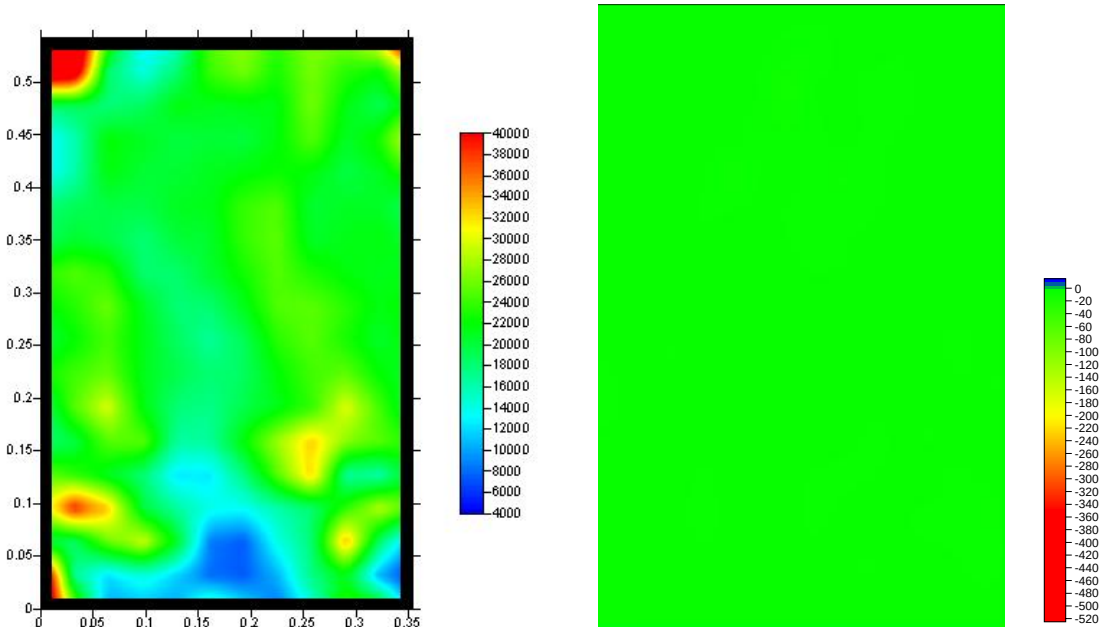

(I) (II)

FIGURE 4.6A I) TOMOGRAM SHOWING VELOCITY (FT/SEC), II) PFC^{3D} MODEL SHOWING STRESS (MPA)

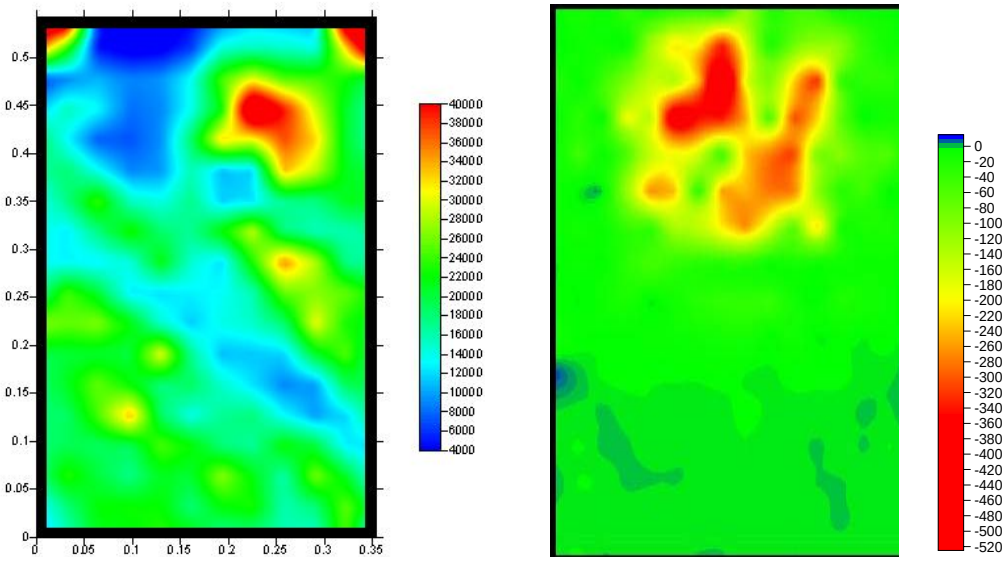

(I) (II)

FIGURE 4.6B I) TOMOGRAM SHOWING VELOCITY (FT/SEC), II) PFC3D MODEL SHOWING STRESS (MPA)

4.6 CONCLUSIONS AND RECOMMENDATIONS

The current study was conducted to correlate the stress redistribution between the results obtained from laboratory tomograms and numerical modeling. The first half of the study was used to calibrate both the laboratory tomographic system as well as the numerical modeling. Both the calibration results showed usefulness.

In the numerical study, the results of the PFC^{3D} model were calibrated to the Five Oaks limestone sample that was tested in the laboratory. One of the biggest advantages of using discontinuum models is that no assumptions have to be made in advance regarding the position and type of failure. On loading the sample, fractures are developed with the breaking of bonds. Thus PFC^{3D} is best suited to model rock samples and conduct tests on them. The goal was to convert the macro-properties to the micro-properties of the PFC^{3D} model and also to simulate the fracture mode to that obtained in the laboratory. The current study matches the Young's modulus, peak load and also the fracture mode obtained in the laboratory to that from the model. The peak load obtained from the PFC^{3D} model was approximately 3% less than the value obtained from the model, while the value of the Young's modulus was approximately 11% more than that obtained from the laboratory. Considering the variation of the values that are obtained in the laboratory during testing, the values obtained from the PFC^{3D} model were accepted.

In the second part of the study, a rectangular block was loaded with an eccentric indentation load and tomograms were obtained at varying portions of the peak load. A similar rectangular block was developed in the PFC^{3D} model and was loaded. It was observed that there is a correlation between the velocity and the stress. It was seen from the PFC^{3D} model that there was a high stress around the point where the load was applied. From the tomograms it was observed that at this point there was a very high velocity due to the presence of the high stress. The results obtained from the laboratory tomograms closely matched the PFC^{3D} model.

The ability to image stress redistribution within laboratory samples coupled with PFC^{3D} modeling may allow for prediction of failure within laboratory samples. Clear imaging of the redistribution of the stress in laboratory samples will allow for accurate stress evaluation. New technologies that will benefit from this area of study are real time tomography, acoustic emission monitoring coupled with acoustic emission tomography, and calibrated PFC^{3D} modeling for crack propagation prediction.

ACKNOWLEDGEMENT

We would like to acknowledge the support provided by the National Science Foundation (CMS-0134034).

REFERENCES

Couvreur, J. F., M. S. Vervoort, et al. (2001). "Successive cracking steps of a limestone highlighted by ultrasonic wave propagation." Geophysical Prospecting **49**: 71 - 78.

Cundall, P. A. (1971). A computer model for simulating progressive large scale movements in blocky rock systems. Symposium of the International Society of Rock Mechanics Nancy, France:

Cundall, P. A. and O. D. L. Strack (1979). "A discrete element model for granular assemblies." Geotechnique **29**(1): 47 - 65.

Fakhimi, A., F. Carvalho, et al. (2002). "Simulation of Failure around a circular opening in rock." Int. J of R Mech. & Min. Sc. **39**(4): 507 - 515.

Falls, S. D., R. P. Young, et al. (1992). "Ultrasonic tomography and acoustic emission in hydraulically fractured Lac du Bonnet grey granite." Journal of Geophysical Research **97**(B5): 6867 - 6884.

Hazzard, J. F. and R. P. Young (2000). "Simulating Acoustic Emissions in Bonded-Particle Models of Rock." Int. J. of R. Mech. & Min. Sc. **37**(5): 867-872.

Hazzard, J. F. and R. P. Young (2001). Seismic validation of micromechanical models. 38th. US Rock Mech. Sym., DC Rocks 2001, Washington DC, A.A.Balkema: 1327 - 1333

Hazzard, J. F. and R. P. Young (2002). 3D numerical modeling of acoustic emission. 5th. Int. Workshop on the Appl. of Geophysics in Rock Engg., Toronto,Canada: 40 - 47

Hazzard, J. F. and R. P. Young (2002). "Moment Tensors and Micromechanical Models." Tectonophysics **356**(1 - 3): 181 - 197.

Itasca Consulting Group, Inc., PFC^{2D}. Minneapolis, MN

Itasca Consulting Group, Inc., PFC^{3D} (2003). Minneapolis, MN.

Johnson, W. B. (2005). Design and testing of a laboratory ultrasonic data acquisition system for tomography. Mining & Minerals Engineering. Blacksburg, Virginia Tech. **M.S.**: 108.

Kulatilake, P. H. S. W., B. Malama, et al. (2001). "Physical and particle flow modeling of jointed rock block behavior under uniaxial loading." Int. J. of R. Mech. & Min. Sc. **38**: 641 - 657.

Scott, T. E., Q. Ma, et al. (1994). Dynamic stress mapping utilizing ultrasonic tomography. Rock Mechanics. Nelson and Laubach, Balkema, Rotterdam**:** 427 - 434.

Terada, M. and T. Yanagidani (1986). Application of Ultrasonic Computer Tomography to Rock Mechanics. Ultrasonic spectroscopy and its applications to material science**:** 205 - 210.

Tweeton, D. (2001). GeoTom CG: Users Manual, GeoTom LLC, Apple Valley, MN.

Villaescusa, E., M. Seto, et al. (2002). "Stress measurements from oriented core." Int. J. of Rock Mech. and Min. Sc. **39**: 603 - 615.

Wang, C., D. D. Tannant, et al. (2003). "Numerical analysis of the stability of heavily jointed rock slopes using PFC2D." Int J of R Mech. & Min. Sc. **40**: 415-424.

Wanne, T. (2002). PFC3D simulation procedure for compressive strength testing of anisotropic hard rock. 1st. Intl. PFC Symposium, Numerical Modeling in Mocromechanics via Particle Methods, Germany, A.A. Balkema Publishers: 241 – 249.

CHAPTER 5: STUDY ON THE EFFECT OF ANISOTROPY IN ROCKS ON STRESS REDISTRIBUTION USING NUMERICAL MODELING

ABSTRACT

The majority of the studies to understand the complex problem of stress redistribution in rocks have considered rock as an isotropic material. However, rock in nature is never isotropic. Rocks need to be considered as an anisotropic material to get more accurate information about stress redistribution. Earlier analytical and numerical modeling studies were conducted to study the effect of peak stress on bedding planes. In addition to this effect, the current study discusses the effect of rock anisotropy on the stress redistribution. The modeling was done using the numerical code, Particle Flow Code in 3-Dimensions (PFC^{3D}). The results matched with both analytic and numerical modeling studies.

5.1 INTRODUCTION

Many successes have been achieved in the area of simulating the mechanical behavior of rock failure using two- and three- dimensional continuum modeling techniques. The new trend in this area is the use of the two- and three-dimensional discontinuum modeling codes. The advantage of using micro-mechanical modeling techniques is that no prior assumptions have to be made about the location and type of fracture and failure – cracking takes place spontaneously and can exhibit a variety of mechanisms when certain local stress conditions are exceeded. Interesting insights about the micro-mechanics of deformation and failure under different stress conditions will be obtained if the failure mechanisms produced by the models are quantified and studied (Hazzard and Young 2002a).

Rock is frequently treated as a linearly elastic, homogeneous and isotropic medium. However, this particular assumption provides only limited insight into the true character of the stresses and deformations within a rock mass. By assuming anisotropic rocks to be isotropic significant errors can be introduced in stress and deformation analyses (Barla 1974). Barla (1974) conducted extensive laboratory experiments on anisotropic behavior of rocks. Amadei (1996) and Tonon and Amadei (2003) also conducted laboratory and field experiments on anisotropic rock behavior.

Su (2004) studied the effect of a single fault on in situ stresses by the distinct element method. The study concluded that in situ stresses are reoriented and their magnitudes vary near faults. However, in these simulations, elastic and isotropic properties are assumed for the intact rocks and the Mohr-Coulomb model of strength is assumed for the fractures.

Discontinuum models like PFC^{2D} developed by Itasca Consulting Group Inc. have been used with much success in various fields. A two dimensional bonded-particle model was used to simulate shear-type micro-seismic events induced by tunnel excavation in granite by Hazzard, Collins et al. (2002). A plane of weakness is included in the model and is subjected to increasing shear load while the normal load across the plane is held constant. The results are compared with actual results obtained from seismic monitoring around an underground excavation. According to the authors, the combination of monitoring the same rock mass using both micro-seismic and ultrasonic techniques affords the unique

ability to investigate fracturing over different magnitude scales. Hazzard and Young (2002b) presents a numerical modeling approach using PFC^{2D} that simulates cracking and failure in rock and the associated seismicity. A technique is also described for quantifying the seismic source mechanisms of the modeled events. The procedure describes how moment tensors and moment magnitudes can be calculated for these simulated seismic events. A new geomechanical modeling technique was developed using PFC^{2D} by Hazzard and Young (2001) in which the models can generate seismicity from induced cracks and fractures. Hazzard and Young (2000) also simulated acoustic emissions in Lac du Bonnet granite using PFC^{2D}.

A plane strain (biaxial) test was performed by Fakhimi, Carvalho et al. (2002) on a rectangular prism of Berea sandstone with a circular opening to simulate a loading-type failure around an underground excavation in brittle rock. To model the observed damage zone around the opening, PFC^{2D} was used. The results from the modeling were in good agreement with the experimental test. It was concluded that by simulating the rock as an assemblage of cylindrical particles, surface spalling and crack propagation can be easily modeled. Wang, Tannant et al. (2003) studied the stability of heavily jointed rock slopes using PFC^{2D}. The modeling methods and procedures presented in this study demonstrate a new approach to the simulation of a rock mass and the stability analysis of excavations in a rock mass. With this new approach, study of the stability of excavations can be carried out in such a way that the development and movement of the rock mass and failure surface can be visualized in two dimensions. Park et al. (Park et al. 2003)

simulated the mechanical behavior of discontinuous rock masses using UDEC also developed by Itasca Consulting Group Inc. and PFC^{2D}. The paper reviews the methodology developed in Sweden for the Rock Mechanical Descriptive Model. The results from the UDEC Rock Mechanical Descriptive Model are compared to results from the discrete element software PFC^{2D}. The post-peak response of the PFC model was not determined by a user-specified model, while the UDEC results were determined by the constitutive model applied to the joints.

All the studies mentioned above were done using the two dimensional micro-mechanical models. The models were able to develop fracture and failure of its own while there was no need to specify any constitutive models for them. However due to the two dimensional nature of these models, only a section of the model could be analyzed. Analysis of the model in its entirety can be made using the three dimensional version of this code. The Particle Flow Code in 3-dimensions (PFC^{3D}) is a well-documented and commercially available tool for modeling the behavior of brittle rock including fracture propagation and mechanical stability in the near-field around underground openings (Wanne 2003). Hazzard and Young (2002c) extended their earlier study on acoustic emission using PFC^{3D}. Kulatilake, Malama et al. (2001) investigated the effect of joint geometry parameters on the uniaxial compressive strength of jointed blocks and the results of the laboratory experiments and numerical simulations were compared. It was concluded from the study that there is a great dependence of the block strength of a jointed rock on the

joint geometry configuration. The joint geometry configuration was also found to control the mode of failure of a jointed block of rock under uniaxial loading.

Wanne (2003) studied the effect of rock anisotropy on strength and deformation properties by simulating a standard unconfined compression test with PFC^{3D}. The results obtained from the simulations were similar to the peak strength and Young's modulus from the laboratory.

The current study uses PFC^{3D} to calculate the stress distribution in the rock sample due to the effect of the anisotropy. The study proposes to give a better idea of the stress redistribution due to discontinuities in rocks, which are very commonly found in nature. The results obtained from the model will be compared to analytic and physical modeling results such as those from Amadei (1996), Barla (1974), and Wanne (2003). With the help of this study, stress related problems arising due to anisotropy in rocks can be located in advance and safety concerns can be reduced.

5.2 MICRO-MECHANICAL MODELING

5.2.1 PFC^{3D}

PFC^{3D} is a distinct element code that simulates a rock as an assemblage of spheres of specified stiffness bonded together with bonds of specified strength. The distinct-element method (DEM) was introduced by Cundall (1971) for the analysis of rock mechanics problems and then applied to soils by Cundall and Strack (1979). The micro-stiffnesses (normal and shear) and micro-strengths (normal and shear) can be adjusted to produce realistic macro rock behavior. PFC uses an explicit approach to solve the equations of motion (Cundall 1971) meaning that the information propagates through the model and time steps are small. For this reason, the code can be used in dynamic simulations in which seismic waves propagate out from new faults and fractures.

The calculation cycle in PFC^{3D} is a time-stepping algorithm that requires the repeated application of the law of motion to each particle, a force-displacement law to each contact and a constant updating of wall positions. Contacts, which may exist between two balls or walls, are formed and broken automatically during the course of a simulation.

5.2.2 MODEL GENERATION AND CALIBRATION

Limestone samples were obtained from the Five Oaks limestone bed in southwestern Virginia. In the first half of the study, the macro-properties of this limestone sample in the laboratory were converted to the micro-properties for the model. Also, the fracture

mode was matched with that in the laboratory. Calibration is the term used to describe the iterative process of determining and modifying the micro-properties for a PFC^{3D} model. In this process, the behavior of the model is compared to those in the laboratory and the micro-properties of the model are modified in an iterative way to achieve the correct macro-mechanical properties (Wanne 2003). This process of converting the macro-properties to the micro-properties is a trial and error approach as no theory exists to obtain the correct relationship between the two properties. Figure 5.1 shows the simple flowchart that was developed in order to transform the macro-properties of the rock to the micro-properties of the sample. Cylindrical samples were developed using PFC^{3D} having a height-to-width ratio of 2:1 and the Young's modulus, peak load and the fracture mode was matched with the laboratory results.

The initial particle stiffness and strengths are calculated using equations as shown in the flowchart in Figure 5.1, obtained from PFC^{3D} manual, where,

E = Young's modulus of the rock, calculated from the laboratory tests

σ_t = Tensile strength of the rock sample, calculated from the laboratory tests

K_n / K_s = Normal / shear stiffnesses of the particle

S_n / S_s = Normal / shear bond strength

$k^{(pb)}$ = Parallel bond stiffness

A = Cross-sectional area of the parallel-bond material.

The model was made to run until failure with each set of values. The Young's modulus, the peak load and the mode of failure were compared with those obtained in the laboratory. If the results were within a range of ±10%, they were accepted, else the values were changed and the entire program was made to run again. Once the results were within the range the micro-properties of the model were accepted.

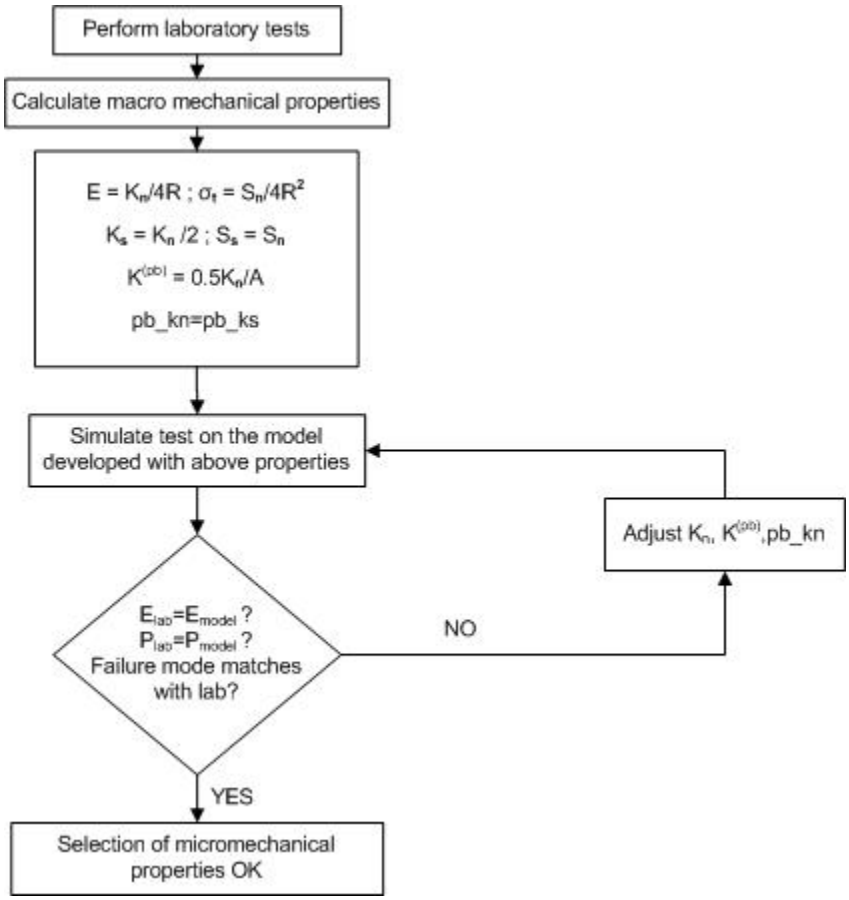

FIGURE 5.1 FLOWCHART FOR CONVERSION OF MACRO- TO MICRO-PROPERTIES.

5.2.3 DEVELOPMENT OF JOINTS IN THE MODEL

The second step in the study was to include bedding planes in the model. After the model reached equilibrium, three joint sets were induced into the model. The study was conducted for joint sets at angles of 0° to 90° with an increment of 15°. The model was loaded at the top and bottom and was made to run to failure. Figure 5.2 shows a joint set that was developed at an angle of 60°. The bedding planes were developed at a spacing of 1.25 cm from each other. Only three bedding planes were developed in all the models.

Joint planes are created in PFC^{3D} by setting the contact bond strengths across these planes to be zero. The joint planes that result in a PFC^{3D} model are irregular due to the spherical nature of the particles that constitute the model (Kulatilake et al. 2001).

Kulatilake et al. (2001) conducted some studies and based on their study, the normal and shear stiffness values for the particles along the joint planes were set to one-tenth of the values assigned to the particle contacts in the intact portion of the assembly. Based on their experiments, the normal and shear bond strength values for these contacts were set to 100 N. The friction value for these joint sets was set to 0.10.

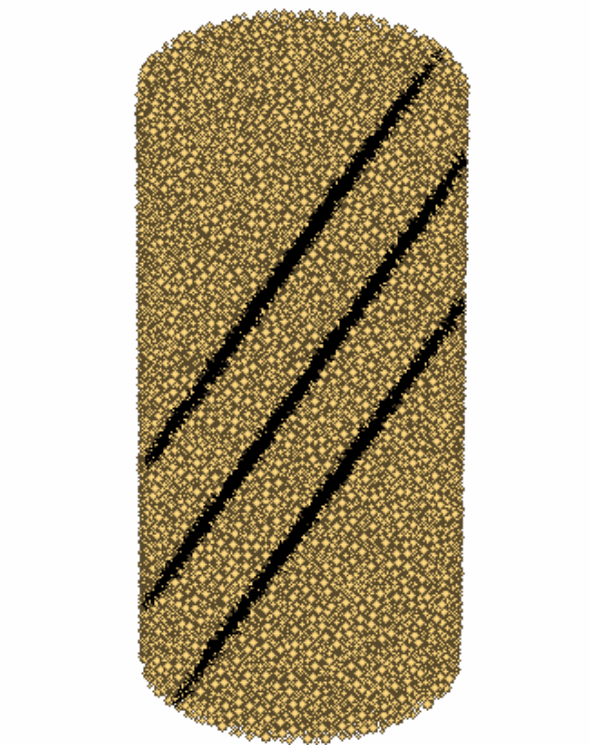

FIGURE 5.2 MODEL WITH JOINT SET WITH A DIP ANGLE OF 60°.

5.3 RESULTS AND DISCUSSIONS

The peak load, Young's modulus and the fracture type were calibrated in the first half of the study. Table 5.1 shows the results from the laboratory and those that were obtained with the micro-properties of the model. Considering the variation of the values that are obtained in the laboratory during testing, the values obtained from the model were accepted for the study and the next part of the study was conducted with these properties.

TABLE 5.1 COMPARISON OF LABORATORY AND NUMERICAL MODEL

	Laboratory	Standard Deviation	PFC3D Model	Diff. between Lab and Model (%)
Peak Load (N)	3.68E+05	6.65E+04	3.57E+05	-2.99
Compr. Str. (N/m^2)	1.86E+08	34	1.82E+08	-2.15
Young's Modulus (N/m^2)	3.50E+10	1.49E+03	3.90E+10	11.43

For the second part of the study, the peak load and Young's modulus were plotted for the varying joint set angles. Figure 5.3 shows a plot of the variation of the peak stress along with the earlier results that were obtained from analytical and numerical modeling studies. Figure 5.4 shows the fracture developed along with the position of the joint sets at a dip angle of 60° just after the model reached the peak load.

The orange and black cracks denote the normal and shear failures respectively. The program was developed by Hazzard (1998) in which the cracks are formed when the load applied exceeds the strength of the bonds. It can be observed that the cracks are formed

only along one of the bedding planes. Similar plots were obtained for the other bedding planes. From Figure 5.3, it can be observed that the peak stress distribution initially decreases with the increase in the dip angle and then increases after the dip angle increases from 60°. This is in direct agreement with the results obtained from earlier studies as can be seen from the Figure. The plot for the peak stress showed a similar trend even for a different friction value for the bedding planes.

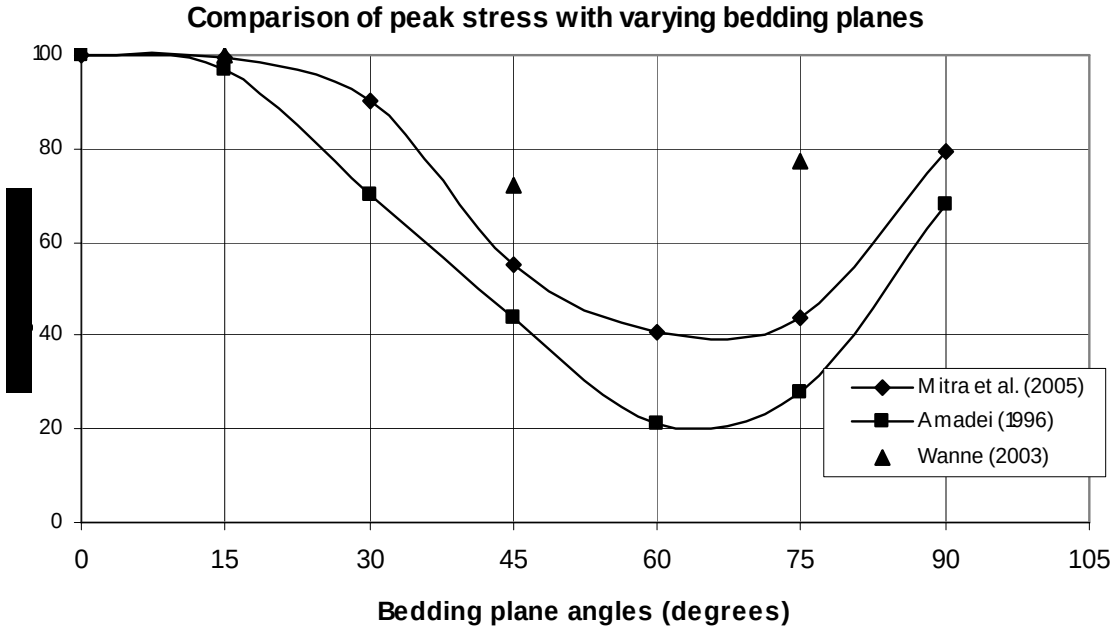

FIGURE 5.3 VARIATION OF THE PEAK STRESS WITH JOINT SETS AT VARIOUS DIP ANGLES. COMPARISON SHOWS VALIDITY OF CURRENT STUDY WITH EARLIER ANALYTICAL AND NUMERICAL MODELING RESULTS.

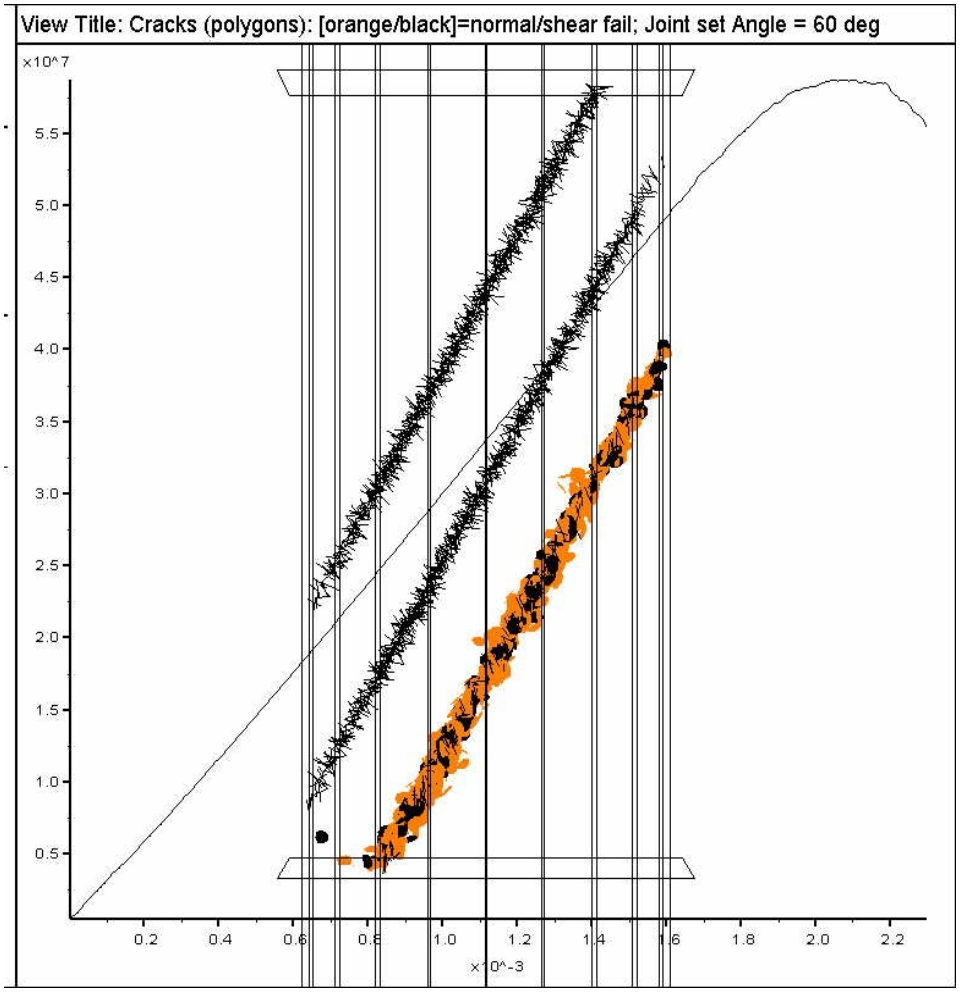

FIGURE 5.4 MODEL AFTER FAILURE WITH CRACKS IN THE MODEL WITH JOINT SET AT A DIP ANGLE OF 60°

Vertical stress was computed at 95% of the peak stress values. A grid system was developed throughout the entire model and the stress values were noted at those grid points. A commercial package, Slicer Dicer® was used to plot the stress distribution in the model. Figure 5.5 shows the stress redistribution in the model at 95% of the peak stress. From the figure below it can be seen that the maximum stress redistribution at 95% peak stress takes place along the bedding plane along which the fracture occurred. Thus the presence of bedding planes can be detected from these stress redistribution plots in two-dimensions.

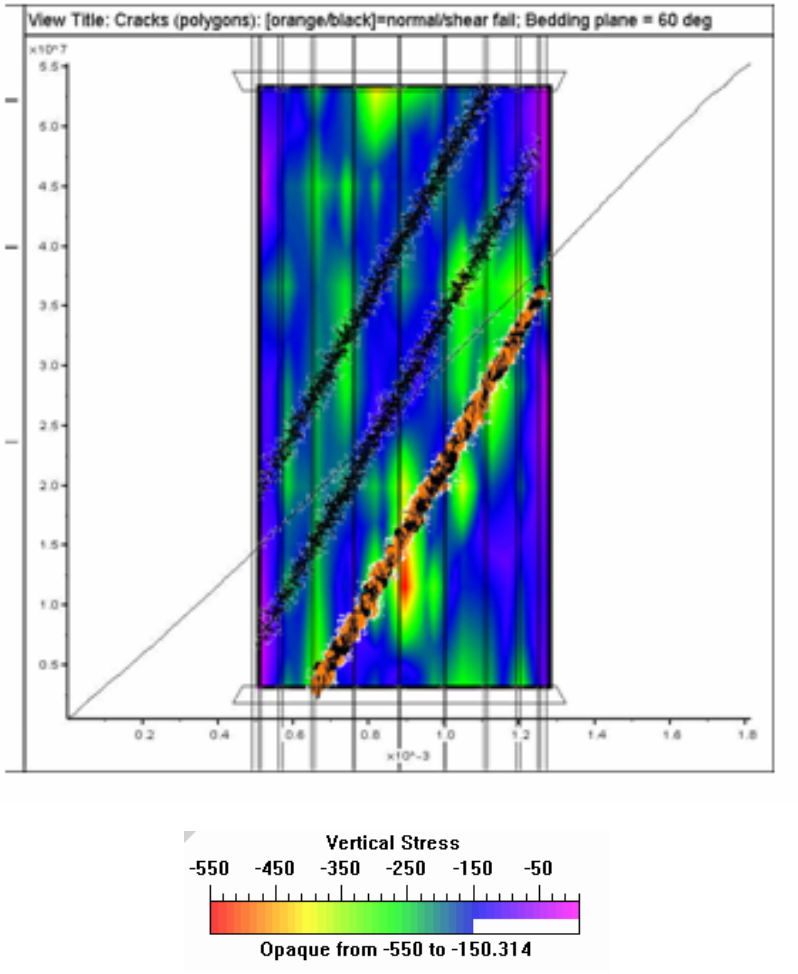

FIGURE 5.5 STRESS REDISTRIBUTION PLOTS AT 95% OF PEAK STRESS ALONG THE VERTICAL PLANE FOR BEDDING PLANES AT 60°

5.4 CONCLUSIONS AND RECOMMENDATIONS

The initial study calibrated the numerical model to the Five Oaks limestone sample that was tested in the laboratory. It was aimed to convert the macro-properties to the micro-properties of the model and also to simulate the fracture mode to that obtained in the laboratory. The results of the Young's modulus, peak load and also the failure mode obtained in the model were compared to that in the laboratory. A flowchart was developed on the basis of an earlier study in order to simulate these properties. However, the earlier studies made a comparison of the Young's modulus and the uniaxial compressive strength of the rock to that in the model. The authors felt that it is also necessary to match the fracture mode too. Thus the current study matches the Young's modulus, peak load and also the fracture mode obtained in the laboratory to that from the model. The peak load obtained from the model was approximately 3% less than the value obtained from the model, while the value of the Young's modulus was approximately 11% more than that obtained from the laboratory. Considering the variation of the values that are obtained in the laboratory during testing, the values obtained from the model were accepted.

The second part of the study was conducted to observe the variation in the stress distribution due to the presence of anisotropy in a rock. Three bedding planes were developed in each of the models at angles from 0° to 90° at a spacing of 1.25cm. The model was made to run to failure and the peak load from each of these models was noted.

It was observed that the peak load decreased as the angle of the bedding planes increased until the angle approached 60° after which it increased. The results for the peak load were found to match with the earlier work that has been done in this area. The failure was observed to take place along one of the bedding planes for all the models. It was also observed that stress redistribution takes place in the models due to the presence of these bedding planes. Vertical stress readings were noted at various portions of the stress-strain curve and stress redistribution was observed due to the presence of these bedding planes. At 95% of the peak stress a high stress concentration was observed along the failure plane.

This type of numerical modeling has already been used with much success as fractures do not have to be included during the modeling process. Faults and fractures develop of it own with the application of load. Further from this study it can be seen that high stress zones can be detected and hence anomalies in a rock can be predicted in advance. Thus stress related problems arising due to anisotropy in rocks can be better understood using this study and hence safety concerns can be reduced.

ACKNOWLEDGEMENT

We would like to acknowledge the support provided by the National Science Foundation (CMS-0134034).

REFERENCE

Amadei, B. 1996. Importance of Anisotropy when estimating and measuring In Situ Stresses in Rock. *International Journal of Rock Mechanics, Mineral Science & Geomechanics Abstract*, 33, 3. 293-325.

Barla, G. 1974. Rock Anisotropy: Theory & Laboratory Testing. In *Courses & Lectures (International Center for Mechanical Sciences)*; ISSN: 0254-1971, 165. 131-169.

Cundall, P.A. 1971. A computer model for simulating progressive large scale movements in blocky rock systems. In *Proceedings of the Symposium of the International Society of Rock Mechanics.* Nancy, Francs, 1971. 1. Paper No. II-8.

Cundall, P.A. & O.D.L. Strack. 1979. A discrete numerical model for granular assemblies. *Geotechnique.* 29, 1, 47-65.

Fakhimi, A., F, Carvalho, T. Ishida & J.F. Labuz, 2002. Simulation of failure around a circular opening in rock. *International Journal of Rock Mechanics and Mining Sciences* (1997), Jun 2002, 39, 4. 507 – 515.

Hazzard, J.F., November 1998. Numerical modeling of acoustic emissions and dynamic rock. **Ph.D**, Department of Earth Sciences, Keele University.

Hazzard, J.F. & R.P. Young, 2000. Simulating acoustic emissions in bonded-particle models of rock. *International Journal of Rock Mechanics and Mining Sciences* (1997), Jul 2000, 37, 5. 867 – 872.

Hazzard, J.F. & R.P. Young, 2001. Seismic validation of micromechanical models. In *Proceedings of the 38th. U.S. Rock Mechanics Symposium, DC Rocks 2001, Washington D.C., 7-10 July, 2001*, eds. Elsworth, Tinucci & Heasley. Rotterdam: Balkema.

Hazzard, J.F. & R.P. Young, 2002a. 3D numerical modeling of Acoustic Emissions. In *Proceedings of the Fifth International Workshop on the Application of Geophysics in Rock Engineering, Toronto, Canada, 7 July 2002*, eds. C.S. Desai et al, 40 - 47. Rotterdam: Balkema.

Hazzard, J.F. & R.P. Young, 2002b. Moment tensors and micromechanical models. *Tectonophysics*, 7 Oct 2002, 356, 1-3. 181 – 197.

Hazzard,J.F. & R.P.Young. 2002c. 3D numerical modeling of Acoustic Emission. In *Proceedings 5th. International Workshop on the Application of Geophysics in Rock Engineering*. Toronto,Canada. July 7, 2002. 40 – 47.

Hazzard, J.F., D.S. Collins, W.S. Pettit & R.P. Young. 2002. Simulation of Unstable fault slip in granite using a bonded-particle model. *Pure & Applied Geophysics*. 159. 221-245.

Itasca Consulting Group, Inc., UDEC, Minneapolis, Minnesota, MN.

Itasca Consulting Group, Inc., PFC^{2D}, Minneapolis, Minnesota, MN.

Itasca Consulting Group, Inc., PFC^{3D}, Minneapolis, Minnesota, MN.

Kulatilake, P.H.S.W., B.Malama & J. Wang. 2001. Physical and particle flow modeling of jointed rock block behavior under uniaxial loading. *International Journal of Rock Mechanics and Mining Sciences.* 38. 641 - 657.

Park, E.S, C.D. Martin & R. Christiansson. 2004. Simulation of the Mechanical Behavior of Discontinuous Rock Masses Using a Bonded-particle Model. In *Proceedings Gulf Rocks 2004, ARMA/NARMS*. 04-483. July 5-10, 2004.

Su, S. 2004. Effect of fractures on in situ rock stresses studied by the distinct element method. *Int. Journal of Rock Mechanics & Mineral Science.* Jan 2004. 41. 159-164.

Tonon, F. & B. Amadei. 2003. Stresses in anisotropic rock masses: an engineering perspective building on geological knowledge. *International Journal of Rock Mechanics and Mining Sciences* (2003), 40. 1099 – 1120.

Wang, C., D.D. Tannant & P.A. Lily, 2003. Numerical analysis of the stability of heavily jointed rock slopes using PFC2D. *International Journal of Rock Mechanics and Mining Sciences* (1997), 2002, 40. 415 – 424.

Wanne, T., 2003. PFC^{3D} simulation procedure for compressive strength testing of anisotropic hard rock. In *Proceedings of the First International PFC Symposium, Germany, Numerical Modeling in Micromechanics via Particle Methods, 6-8 November, 2002*, ed. Heinz Konietzky. Rotterdam: Balkema.

CHAPTER 6: INVESTIGATION OF THE STRESS IMAGING IN ROCK SAMPLES USING NUMERICAL MODELING AND LABORATORY TESTING

ABSTRACT

The ability to understand stress redistribution within a mine will allow for greater extraction efficiency with reduced safety concerns. Stress redistribution has been examined at the laboratory scale using ultrasonic tomography and numerical modeling using PFC^{3D}.

In the first part of the study an equation is developed to convert the macro-properties of the rock to the micro-properties of the particles in the model. In the second half of the study, an attempt is made to investigate the stress distribution in rock samples in three-dimensions, as they are uniaxially loaded to failure using both numerical modeling and laboratory tomograms. This study will help to predict failure in laboratory samples and when applied to mines this will help to prevent rockbursts and roof falls.

6.1 INTRODUCTION

Underground mining has one of the highest fatal injury rates among any of the industries in the United States, which is more than five times compared to the national average of the other industries (NIOSH). According to statistics obtained between 2001 to July 2005, approximately 33% of the fatalities have been due to geologic failure of roof/back or face/rib/highwall (MSHA). Many of these incidents can take place due to a redistribution of the stress resulting from mine workings. Catastrophic rock failure often results in loss of life and property along with increased public awareness. The ability to understand this stress redistribution within a mine will allow for greater extraction

efficiency with reduced safety concerns. In a discussion organized by the National Science Foundation, it was unanimously decided that with respect to catastrophic rock failure some sort of predictive tools to mitigate loss of life and property should be developed (Glaser and Doolin 1999). The current study is a step towards that development. An investigation of the stress distribution in rock samples is conducted using laboratory tomography and a discrete element model.

6.1.1 FAILURE OF ROCKS

When load is applied to a rock mass, initially the microcracks normal to the direction of the load are closed. With further application of the load, cracks start to develop at an angle to the application of the load. Finally these microfractures coalesce into the failure plane. It has been found in earlier studies that damage accumulated in a homogeneous rock is randomly located until the applied stress reaches 90 – 95% of the rock's peak strength. Above this stress, the event locations exhibit clustering on the eventual failure plane (Scholz 1968; Scholz 1968; Hazzard 1998). It has been assumed that the initial events are independent, but the events occurring after 90% of the peak strength are not. The orientation of the failure plane is a function of several parameters, including size and shape of the sample, loading conditions, material properties, anisotropy, and jointing within the rock mass (Westman 2004).

Several failure criteria have been developed for predicting failure as a function of applied stress. The simplest and most important criterion was introduced by Coulomb (1773).

According to his studies, the shear stress causing failure across a plane is resisted by the cohesion of the material and the normal stress across the plane. Mohr (1900) proposed that when shear failure takes place across a plane, the normal stress σ and shear stress τ across this plane are related by a functional relation characteristic of the material,

$$\tau = f(\sigma) \tag{6.1}$$

The Griffith criterion is based on the hypothesis enunciated by Griffith in 1921 that fracture is caused by stress-concentrations at the tips of minute *Griffith cracks* which are supposed to pervade the material, and that fracture is initiated when the maximum stress near the tip of the most favorable oriented crack reaches a value which is characteristic of the material. Various other criteria have also been developed based on empirical data over the years.

6.1.2 STRESS DETERMINATION IN ROCKS

Determination of the strength of the rock is the biggest concern in any engineering discipline using it for structural or supporting purposes (Karfakis 2003). The mechanical properties of a rock depend upon its physical properties and the presence of discontinuities (Jaeger and Cook 1979).

The current study was conducted with the uniaxial compression test. It is oldest and simplest test and continues to be one of the most convenient and useful ways to determine the properties of the rock (Jaeger and Cook 1979). It may be regarded as the largest stress that a rock specimen can carry when a unidirectional stress is applied to the

ends of a specimen. In other words, the unconfined compressive strength represents the maximum load supported by the specimen during the test divided by the cross-sectional area of the specimen. Although the utility of the compressive strength value is limited, the unconfined compressive strength allows comparisons to be made between rocks and provides some indications of rock behavior under more complex stress systems (Tang, Liu et al. 2000). In the uniaxial compression test, right circular cylindrical rocks are compressed parallel to their longitudinal axis. The failure mode is dependent on the strength of the platen. The uniaxial compressive strength test is the basic test in numerous design methods (Pells 1993).

It is necessary to have an idea of the initial stress in a rock mass. If the initial stresses are high, the shape of the opening have to selected in such a way as to minimize the stress concentration. Further the layout of the opening can be arranged accordingly (Goodman 1980). Stresses in rocks have been studied since decades. One of the earlier methods to determine the stress state in a body due to application of load has been the photoelastic method. Since then, innumerable studies have been conducted to monitor the stress distribution using both analytical and numerical models. The current study will monitor the stress in rock samples as it is loaded to failure and attempt to predict the failure plane.

6.1.3 TOMOGRAPHY

Tomography is derived from the Greek word *tomos*, meaning section. It is a nondestructive testing method to view the interior of a body without penetrating its

surface by physical means. It is based on the mathematical procedure called tomographic reconstruction. Tomography has been defined by Lo and Inderwiesen (1994) as an "imaging technique which generates a cross-sectional picture (a tomogram) of an object by utilizing the object's response to the nondestructive, probing energy of an external source". This technology was first described by Radon (1917), who said that the interior of the body can be imaged by analyzing energy which passed from one boundary to another. It has been widely used in the medical field, where x-ray is used to create the images. Dines and Lytle (1979) used the idea of tomography in geophysical applications. When load is applied to a rock, the microcracks are initially closed. This makes the elastic waves to travel at a higher velocity through the rock.

Ultrasonic waves are used for laboratory tomographic studies while seismic waves are employed in the field studies. Westman (2004) discusses the various factors affecting the quality of the tomograms. The difference between the seismic and the ultrasonic tomographic imaging is in the frequency ranges used. Seismic tomography utilizes low frequency waves to measure anomalies like fracture or high stressed zones within the earth. The low frequencies correspond to long wavelengths capable of traveling long distances. In ultrasonic tomography, the waves have smaller wavelengths which can resolve small structures; however these waves attenuate quickly and can therefore only be transmitted over short distances. Ultrasonic tomography can be used to measure both the velocity change as well as the attenuation through the sample.

Rocks behave elastically and when load is applied to a rock, the velocity of the waves through the rock will increase proportionately due to the closing of the microfractures. This effect is known as the acousto-elastic effect. Tomograms taken at various stages of loading will show this change in velocity which is directly proportional to the stress change.

Tomography has been applied in various fields including volcanic imaging, earthquake tomography, geologic hazard detection and stress identification. Computerized tomography was adapted and applied to geophysical exploration using data collected by cross-borehole electromagnetic probing (Dines and Lytle 1979). Various studies have been conducted on both seismic and ultrasonic tomography, since then (Gustavsson, Ivansson et al. 1986; Leung, Downey et al. 1988; Goulty, Thatcher et al. 1990). Tomography has also been used in mines to monitor roof or pillar failure, identify regions of relatively higher stress, and strata identification (Mason 1981; Peterson, Paulsson et al. 1985; Westman, Haramy et al. 1996). The capabilities of ultrasonic tomography on identifying inhomogeneity and fractures inside the rock were investigated by Li, Zhang et al (2005). Scott, Ma et al. (1993) conducted indentation loading tests on a Berea sandstone sample. Tomograms constructed of the cross-section of the sample showed that the density underneath the load increases with the application of the load.

Most of these laboratory studies have been done using two-dimensional tomography. The current study will develop tomograms in three-dimensions. This study will attempt to

predict the failure plane in rock samples as it will be loaded to failure in uniaxial compressive tests. This study can be extended to the mine site and further studies can be conducted to monitor the increase in the stress field using coupled numerical modeling and tomographic imaging.

6.1.4 NUMERICAL MODELING IN ROCK MECHANICS

Success has been achieved in the area of simulating the mechanical behavior of rock using two- and three-dimensional continuum modeling techniques. The success of the continuum approach is because the microstructure has a length scale much smaller than that of the objects that are normally of interest (e.g. dams, bridge decks). But it is often rewarding to model such 'continua' as discontinua, because new knowledge can be gained about their macroscopic behavior when their microscopic mechanisms are understood (Cundall and Hart 1993). The new trend in this area is the use of the two- and three-dimensional discontinuum modeling codes. The advantage of using these micro-mechanical modeling techniques is that no assumptions have to be made about the location and type of fracture and failure – cracking takes place spontaneously and can exhibit a variety of mechanisms when certain local stress conditions are exceeded. Interesting insights about the micro-mechanics of deformation and failure under different stress conditions will be obtained if the failure mechanisms produced by the models are quantified and studied (Hazzard and Young 2002).

Discontinuum models like PFC^{2D} (Itasca Consulting Group) have been used with much success in various fields. Numerous studies have been conducted using this modeling code to simulate cracking and failure under various loading conditions (Hazzard and Young 2000; Hazzard and Young 2001; Fakhimi, Carvalho et al. 2002; Hazzard, Collins et al. 2002; Hazzard and Young 2002; Wang, Tannant et al. 2003; Park, Martin et al. 2004).

All the studies mentioned above were done using the two dimensional micro-mechanical models. The models were able to develop fracture and failure on their own and there was no need to specify any constitutive models for them. However due to the two dimensional nature of these models, only a section of the model could be analyzed. Analysis of the model in its entirety can be made using the three dimensional version of this code. The Particle Flow Code in 3-dimensions (PFC^{3D}) (Itasca Consulting Group 2003) is a well-documented and commercially available tool for modeling the behavior of brittle rock including fracture propagation and mechanical stability in the near-field around underground openings (Wanne 2002). Hazzard and Young (2002) extended their earlier study on acoustic emission using PFC^{3D}. Kulatilake, Malama et al (2001) investigated the effect of joint geometry parameters on the uniaxial compressive strength of jointed blocks and the results of the laboratory experiments and numerical simulations were compared. Wanne (2002) studied the effect of anisotropy of the rock on strength and deformation properties by simulating a standard unconfined compression test with PFC^{3D}.

The program has been very successful in predicting fracture without the use of any interfaces. Fractures develop as the stress exceeds the strength of the bonds. However, attempts have not been made to study the stress redistribution at the micro scale using this modeling method. One of the objectives of this study is to observe the stress distribution for the models along with the fracture development as they are loaded to failure. Observing this change in stress will help to detect the fracture in advance and thereby prevent problems in the mine arising due to this high stress.

6.2 MICRO-MECHANICAL MODEL

PFC^{3D} simulates a rock as an assemblage of spheres of specified stiffness bonded together with bonds of specified strength using the distinct element method. Cundall (1971) introduced the distinct-element method (DEM) for analyzing rock mechanics problems and later Cundall and Strack (1979) applied it to soils. The interaction of the particles in the distinct element method is viewed as a transient problem with equilibrium state developing whenever the internal forces balance each other (Cundall and Strack 1979).

The calculation cycle in PFC^{3D} is a time stepping algorithm that requires the repeated application of the law of motion to each particle, a force-displacement law to each contact and a constant updating of wall positions. Contacts, which may exist between two balls or walls, are formed and broken automatically during the course of a simulation (Itasca Consulting Group 2003). The micro-stiffnesses (normal and shear) and micro-strengths (normal and shear) can be adjusted in the model to produce realistic macro rock behavior.

The particles in a PFC^{3D} model can be bonded together either with a contact bond, parallel bond or both. Two particles with a contact bond behave as though they are welded together at the contact point; no slip is possible while the bond remains. However, contact bonds provide no resistance to rolling. A parallel bond, on the other hand,

provides a connection between two particles that resists both forces and moments applied to particles after the bond has been installed. It can be envisioned as a cylinder of elastic glue that connects the two particles.

Calibration is the term used to describe the iterative process of determining and modifying the micro-properties for a PFC^{3D} model. In this process, the responses of the model are compared to that in the laboratory and the micro-properties of the model are modified in an iterative way to achieve good agreement (Wanne 2002). An inverse modeling method is used to determine the correct micro-mechanical properties of the numerical models from the macro mechanical properties of the rock obtained during laboratory testing. This is a trial-and-error approach as no theory exists in order to obtain the correct relationship between the two properties. Figure 6.2 shows the simple flowchart that is used in order to transform the macro-properties of the rock to the micro-properties of the sample. However, many iterations were required in order to find the correct micro-mechanical properties. Thus the first part of the study develops an equation to find the relation between the macro- and micro-mechanical properties. Since the current study dealt with rocks which have cementation in it, parallel bonds were used for the study and the equation developed was one involving parallel bonds.

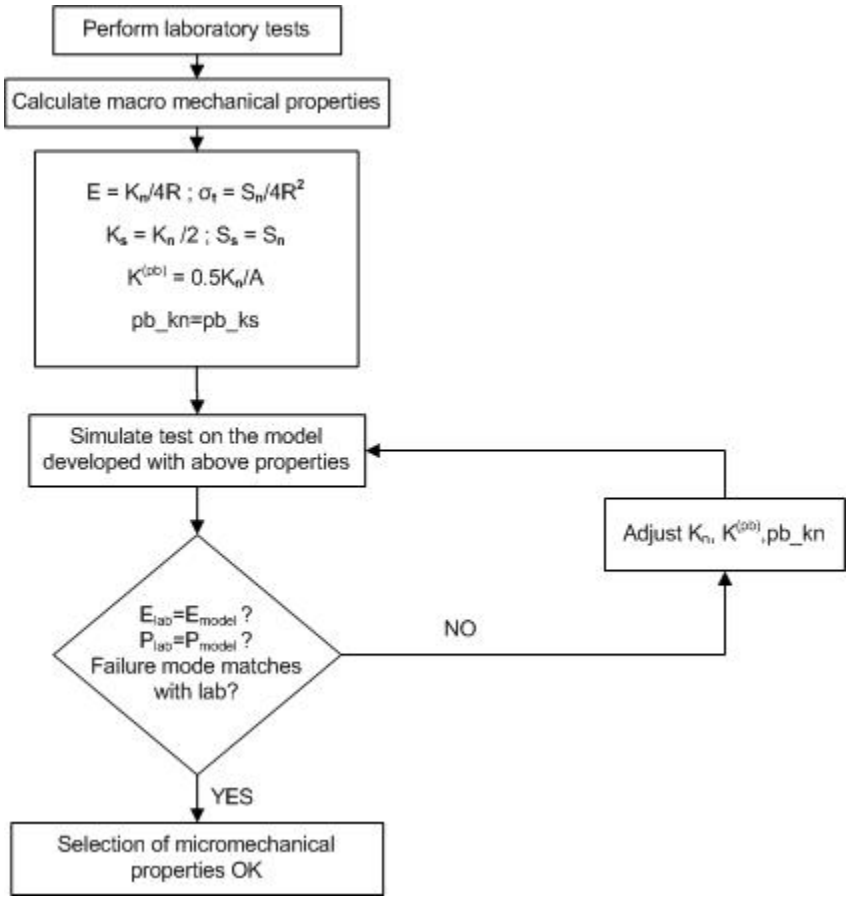

FIGURE 6.1 FLOWCHART FOR CONVERSION OF MACRO- TO MICRO-PROPERTIES.

In the second half of the numerical modeling portion of the study, cylindrical models were developed in PFC^{3D} having a height-to-width ratio of 2:1 with the micro-properties obtained from the first half of the study. Uniaxial compressive strength tests were simulated on these models. The stresses were monitored on these models as they were loaded to failure.

6.3 METHODS

6.3.1 NUMERICAL METHODS

6.3.1.1 DEVELOPMENT OF MACRO-TO-MICRO EQUATION

Cylindrical samples having a height-to-width ratio of 2:1were developed using PFC^{3D}. The particle radii varied from 1.50 to 2.00 mm (0.059 – 0.079 inches) which resulted in the formation of approximately 6000 particles in the model. Table 6.1 shows the various particle micro-properties that were used for the models. A total of 375 programs were run using the various combinations of the properties as shown in the table below. The Young's Modulus and the compressive strength were calculated from these programs.

TABLE 6.1 MICRO-PROPERTIES USED IN THE MODELS.

K_n	$K^{(pb)}$	***Friction Coeffn.***	***P_bond N_str = S_str***
5.00E+07	1.04E+13	0.3	1.00E+08
7.50E+07	2.54E+13	0.6	2.50E+08
1.00E+08	5.04E+13	0.9	5.00E+08
2.50E+08	7.54E+13		7.50E+08
5.00E+08	1.04E+14		1.00E+09

The density for the particles in the model was calculated on the basis of an earlier study by Hazzard (1998). A porosity of 35% was chosen for the model. Attempts were made to reduce the porosity below the chosen value. However it was observed that there are limits to which the porosity can be lowered. It is not possible to pack particles to an arbitrarily low porosity value (Itasca Consulting Group 2003).

Equations 6.1 – 6.5 below were obtained from the PFC^{3D} manual (Itasca Consulting Group 2003).

$$\overline{E} = \frac{K_n}{4R} \tag{6.1}$$

$$\sigma_t = \frac{S_n}{4R^2} \tag{6.2}$$

$$K_s = \frac{K_n}{2} \tag{6.3}$$

$$S_s = S_n \tag{6.4}$$

$$k^{(pb)} = \frac{0.5\,K_n}{A} \tag{6.5}$$

where, $\overline{E}$ = apparent Young's modulus of the rock of a cubic array of spheres, assuming that the principal axes coincide with the axes of symmetry of the particle array.

σ_t = tensile strength of the of the cubic array, as discussed in $\overline{E}$.

K_n / K_s = Normal / shear stiffnesses of the particle

S_n / S_s = Normal / shear bond strength

$k^{(pb)}$ = Parallel bond stiffness

A = Cross-sectional area of the parallel-bond material, discussed below.

Parallel bonds were used in the model so as to get a better compaction in the model, with a porosity of 35%. However, there is no method to calculate the strength and stiffnesses

of the parallel bonds. The cross-sectional area of the parallel bond material is dependent on the parallel bond radius, as shown below.

$$A = \pi(pb\_rad \times ave\_rad)^2 \tag{6.6}$$

where, pb_rad = parallel bond radius

ave_rad = average radius of the particles.

6.3.1.2 STRESS MONITORING IN PFC

Numerous studies have been conducted earlier using this modeling method. However, monitoring the stress at the micro-scale using this model has not been attempted earlier. The current study attempts to determine the stress redistribution in the model as it is loaded to failure. Initial attempts were made to monitor the stress for each particle and plot the stress redistribution at certain load intervals. However the results were not successful. The author feels that this was due to the high porosity used for the model. Another attempt was made to use measurement spheres around each particle and then monitor the stress in each of these measurement spheres. Various parameters within a PFC^{3D} model can be measured over a given spherical volume. The location and size of these measurement spheres are specified by the user. Measurement spheres can be defined to measure porosity, stress, strain rate, coordination number and sliding fraction. This also proved to be unsuccessful because of the same reason as above.

Thus it was decided to monitor the strength of the bonds. In this code, the cracks are formed when either the normal or shear stress in these parallel bonds exceed their

respective strength. Once it exceeds the strength, the bonds are broken and the data is removed from the memory. Thus if both these stresses can be monitored together then the growth of a crack can be predicted. In the current study, the parallel bond stresses are monitored at certain interval of the load and the stress redistribution for the model is plotted at that load.

6.3.2 LABORATORY EXPERIMENTS

Cylindrical samples having height-to-width of 2:1 were tested uniaxially in the laboratory and their Young's modulus and peak strength were monitored. Each of the samples was surrounded by sensors to acquire the tomograms as these rocks were loaded to failure. Ramp loading was used for these tests and at certain load intervals, the data for the tomograms was acquired. Samples of diameter 0.0508 m (2 in.) and 0.0762 m (3 in.) were chosen for the study. A total of 15 sources and 18 receivers were used for the study as can be seen in Figure 6.3. Tomograms were calculated from the arrival time data using GeotomCG (Tweeton 2001). This program uses the simultaneous iterative reconstruction technique (SIRT) to construct a velocity tomogram.

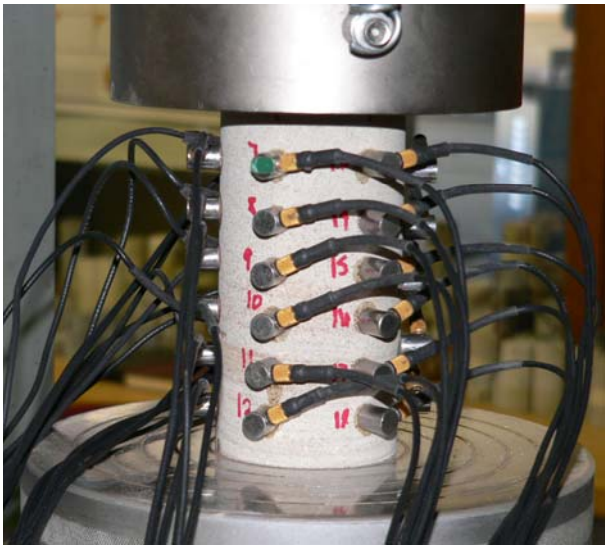

FIGURE 6.2 SAMPLE WITH SENSORS READY FOR TEST

A data acquisition system developed by Johnson (Johnson 2005) was used to acquire the data. The entire programming for the system was done in LabVIEW. Figure 6.4 shows the hardware flowchart for the system.

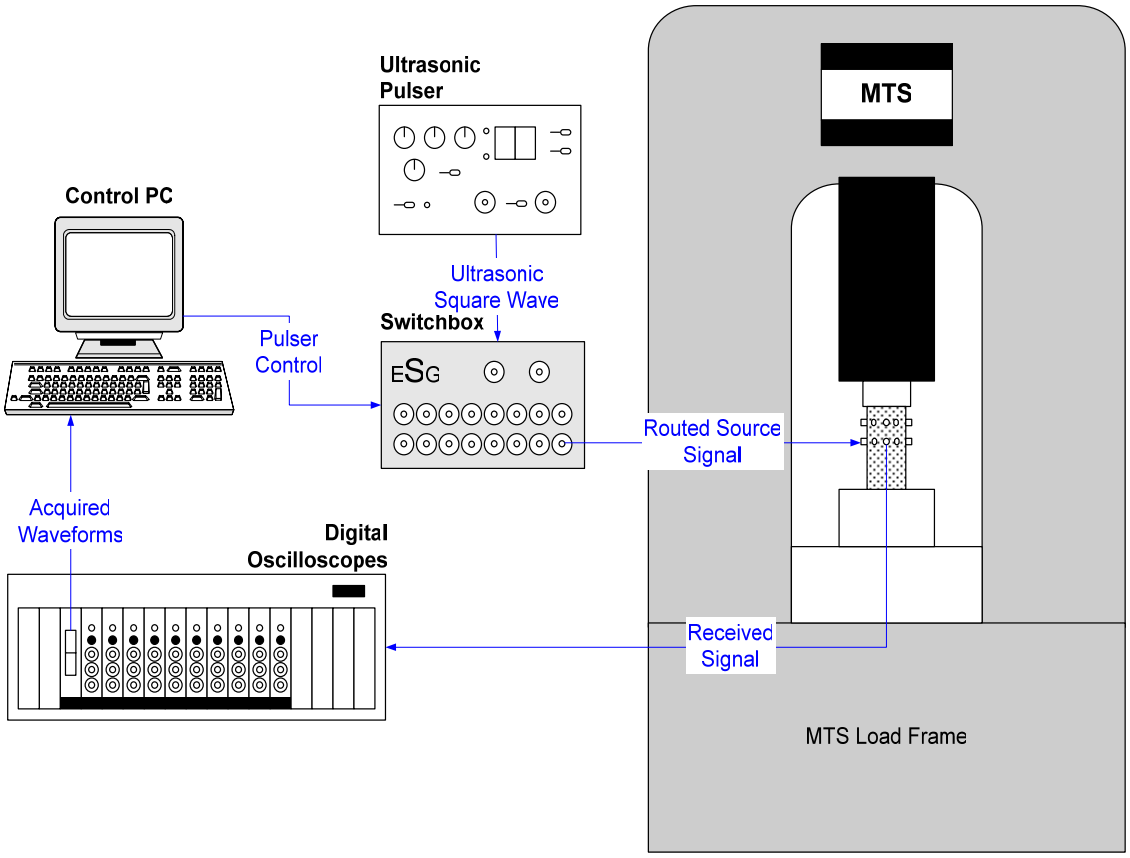

FIGURE 6.3 HARDWARE FLOWCHART (JOHNSON 2005)

An ultrasonic pulse is generated by a Panametrics 5077PR Ultrasonic Square Wave Pulser. The pulser can output an ultrasonic square wave tuned to a particular frequency. For this study a 500 kHz ultrasonic square wave was pulsed at a rate of 100 Hz. The pulse is then passed to an ESG Ultrasonic Switchbox Pulser. This unit is controlled in the LabVIEW environment by the control PC. The pulse is digitally relayed by the PC to one of 16 source transducers on the sample. The ultrasonic waveform is received by National Instrument's PXI-5102 Digital Oscilloscopes. These analog to digital conversion instruments are 2 channel modules that can be interconnected by using a PCI Extension

Interface (PXI). The National Instrument's PXI chassis used allows for simultaneous acquisition of ultrasonic data at a rate up to 20 million samples per second on up to 20 analog channels. Acquisition of the ultrasonic data was controlled using LabVIEW.

6.4 RESULTS AND DISCUSSION

6.4.1 NUMERICAL MODELING

The first step in this modeling was to develop the equation so as to convert the macro-properties of the sample to the micro-properties of the particles. The Young's modulus and the uniaxial compressive strength were calculated from all the programs that were simulated combining the values as shown in Table 6.1. A total of 375 programs were made to run till failure. The results were then analyzed with the help of the commercial statistical package SAS. The Young's modulus and the compressive strength were expressed as a function of the normal stiffness and coefficient of friction of the particles and the strength and stiffness of the parallel bonds. Equations 6.7 and 6.8 show the relationship that was developed from the study.

$$E = -1.03971 + 0.10765 k_n + 0.91709 k^{(pb)} + 1.87547\, fric + 0.17694\, p\_bond\_str \quad (6.7)$$

$$C_0 = 2.17026 - 1.31334 k^{(pb)} + 5.22120\, fric + 4.71001\, p\_bond\_str \quad (6.8)$$

where, E = Young's modulus (Pa, x10^9)

C_0 = Uniaxial compressive strength (Pa, x10^6)

k_n = Normal stiffness of the particles (N/m, x10^7)

$k^{(pb)}$ = Parallel bond stiffness (Pa/m, x10^{13})

fric = coefficient of friction

p_bond_str = Parallel bond strength (Pa, x10^8).

After developing the equations, it was observed that there are four variables but only two equations. In order to calculate the values of the micro-parameters from the Young's modulus and the compressive strength of the rock it was decided that the user will provide the friction value to the equation. Also, the relation between the parallel bond stiffness and the normal stiffness of the particle obtained from the PFC^{3D} manual will be used so as to reduce the equation to two variables. Since this relation was dependent on the radius of the parallel bond, it was also used as an input from the user. The parallel bond radius affects the compaction of the rock. So a more compact rock will have a higher parallel bond radius. Thus, once the coefficient of friction, minimum and maximum particle radii, parallel bond radius, Young's modulus and compressive strength of the rock was specified, the equation provided the micro-mechanical properties.

The results of the tests have been summarized in Table 6.2 along with the deviations from the original values. Considering the variation of the values that are obtained in the laboratory during testing, the values obtained using the equation can be accepted. Further, these results were obtained in a couple of iterations and hence time was saved in comparing the macro- to the micro-properties.

After the success of the equation, attention was focused on obtaining the stress distribution from the models. As mentioned earlier, the normal and shear stresses of the parallel bonds were monitored in order to predict the formation of the cracks. The values were noted at certain load intervals. Whenever a crack was formed that bond was

provided with a high value so that the anomaly can be observed in the stress distribution plots. RockWorks 2004 was used for visualization of the stress distribution in the models. Figures 6.5 – 6.9 show the results for the crack development, normal and shear stress distribution for a limestone sample that was modeled using PFC^{3D}. Monitoring both the normal and shear stress together will help to predict the formation of the failure plane. However, it can be seen from both the crack formation as well as the stress distribution plots that just prior to failure the cracks align themselves along a plane and develop the failure zone as observed from earlier studies. Also from Figure 6.10, it can be observed that the number of cracks begin to increase at approximately 90 - 95% of peak load. Also it was observed that there were more tensile cracks formed as expected from the model.

TABLE 6.2 VALUES OBTAINED FROM THE LABORATORY TESTS AND NUMERICAL MODELING

	Lab Results		PFC^{3D} Model			
			Values obtained		Deviation	
Rock Type	Young's Mod.	Comp. Str.	Young's Mod.	Comp. Str.	Young's Mod.	Comp. Str.
	E, GPa	C_o, MPa	E, GPa	C_o, MPa	E, %	C_o, %
Kimballton Limestone	23.11	87.56	24.14	91.97	-4.47	-5.04
Kimballton Limestone	37.66	212.17	35.62	210.1	5.42	0.98
Kimballton Limestone	37.61	216.88	37.04	207.14	1.52	4.49
Kimballton Limestone	35.12	137.98	36.55	137.15	-4.08	1
Kimballton Limestone	29.29	108.93	29.85	117	-1.90	-7.41
Kimballton Limestone	37.47	204.33	35	188.68	6.60	7.66
Kimballton Limestone	33.42	192.70	32.93	187.06	1.45	2.93
Kimballton Limestone	36.72	207.87	37.5	236.7	-2.12	-13.87
Berea Sandstone	15.56	92.80	15.65	99.72	-0.61	-7.46
Berea Sandstone	11.67	98.76	12.3	108.93	-5.43	-10.30
Berea Sandstone	28.13	262.48	28.45	288.36	-1.16	-9.86
Berea Sandstone	2.20	10.19	2.86	9.3	-30.00	8.75
Berea Sandstone	2.53	12.85	4.19	13.62	-65.39	-6.01
Berea Sandstone	7.07	29.48	6.94	27.89	1.83	5.41
Berea Sandstone	2.62	8.80	4.19	7.67	-60.21	12.84
Berea Sandstone	2.60	13.35	3.67	12.41	-41.15	7.07
Berea Sandstone	5.07	19.79	6.34	19.75	-25.09	0.23
Berea Sandstone	7.27	31.69	7.36	30.93	-1.20	2.40
Limestone	30.50	242.62	29.47	264.68	3.39	-9.09
Limestone	23.99	105.35	25.08	114.71	-4.54	-8.88
Berea Sandstone	5.00	28.93	5.38	28.09	-7.6	2.90
Berea Sandstone	9.26	38.65	8.00	32.64	13.62	15.54
Berea Sandstone	9.93	46.38	10	44.68	-0.69	3.67
Berea Sandstone	10.77	55.12	11.62	57.31	-7.93	-3.97
Shale	12.18	79.10	12.93	85.41	-6.17	-7.98
Quartz Arenite	23.83	105.09	21.38	101.94	10.27	2.99
Quartz Arenite	26.77	110.85	23.42	102.96	12.52	7.11

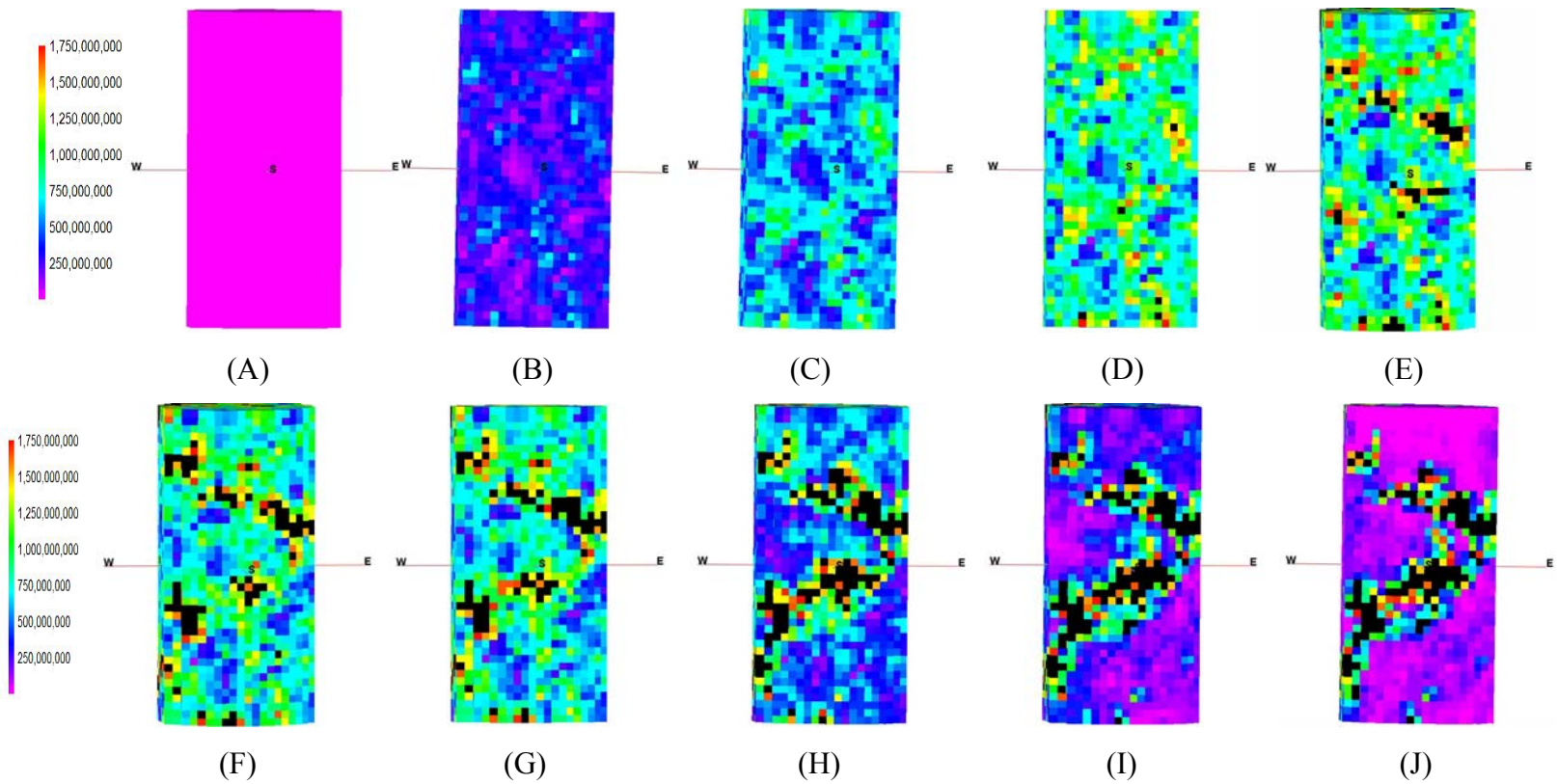

FIGURE 6.4 SHEAR STRESS DISTRIBUTION FOR THE MODEL EXTERIOR AT (A) 7%; (B) 28%; (C) 62%; (D) 95%; (E) 100%; (F) 91.5%; (G) 83%; (H) 57%; (I) 35%; AND (J) 8.7% OF PEAK LOAD

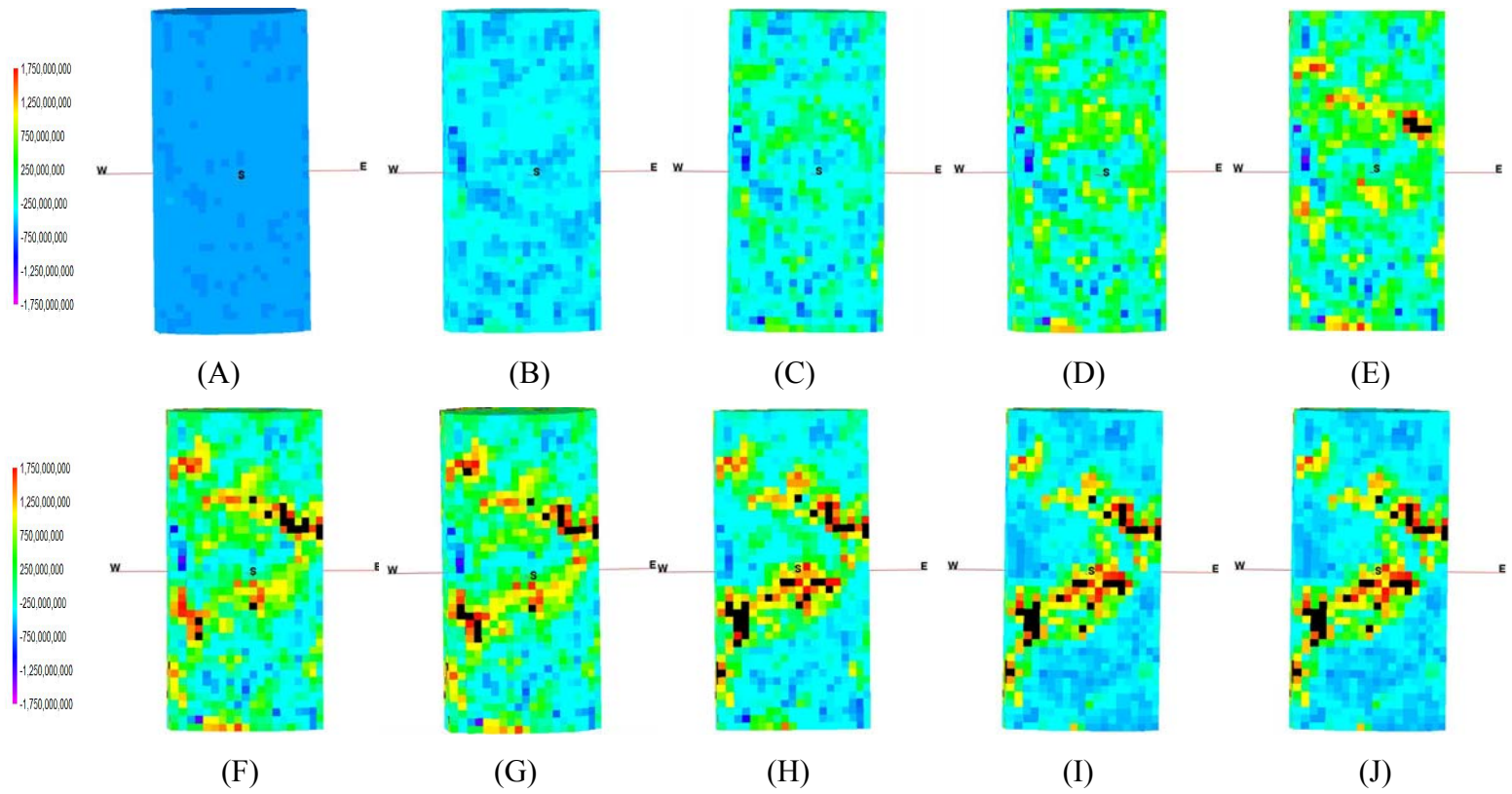

FIGURE 6.5 NORMAL STRESS DISTRIBUTION FOR THE MODEL EXTERIOR AT (A) 7%; (B) 28%; (C) 62%; (D) 95%; (E) 100%; (F) 91.5%; (G) 83%; (H) 57%; (I) 35%; AND (J) 8.7% OF PEAK LOAD

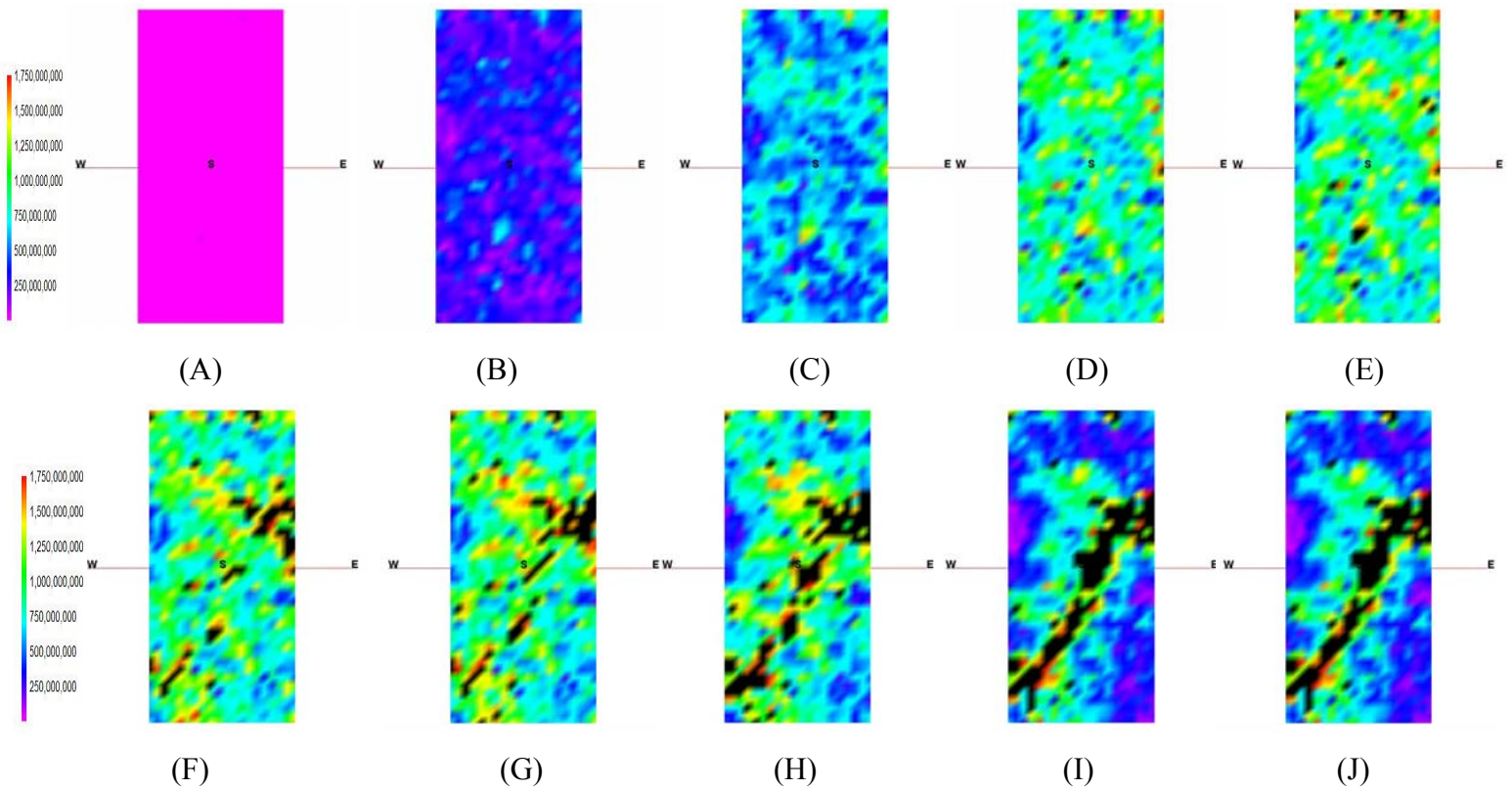

FIGURE 6.6 SHEAR STRESS DISTRIBUTION AT THE CROSS-SECTION Y=0 FOR THE MODEL AT (A) 7%; (B) 28%; (C) 62%; (D) 95%; (E) 100%; (F) 91.5%; (G) 83%; (H) 57%; (I) 35%; AND (J) 8.7% OF PEAK LOAD

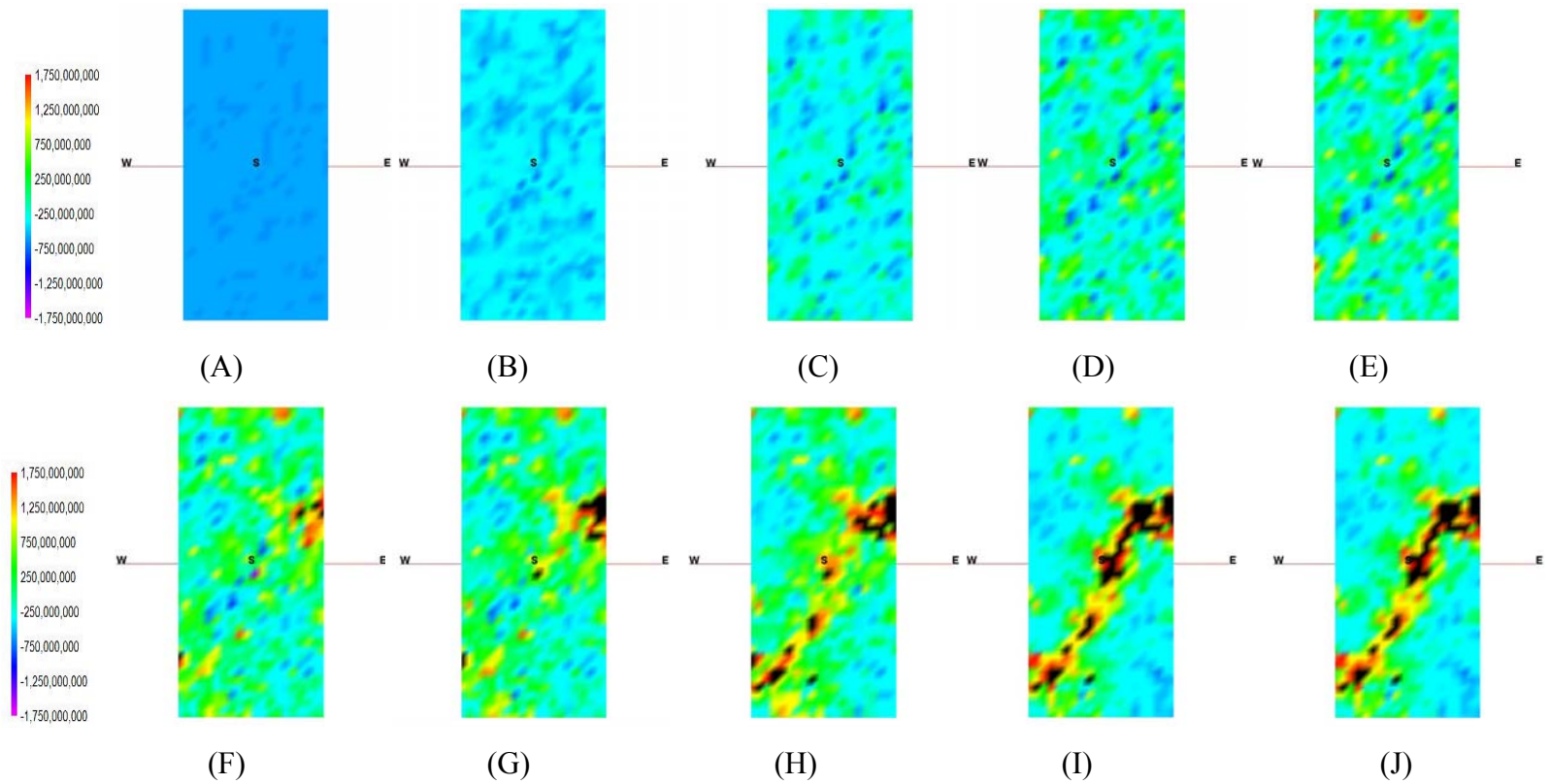

FIGURE 6.7 NORMAL STRESS DISTRIBUTION AT THE CROSS-SECTION Y=0 FOR THE MODEL AT (A) 7%; (B) 28%; (C) 62%; (D) 95%; (E) 100%; (F) 91.5%; (G) 83%; (H) 57%; (I) 35%; AND (J) 8.7% OF PEAK LOAD

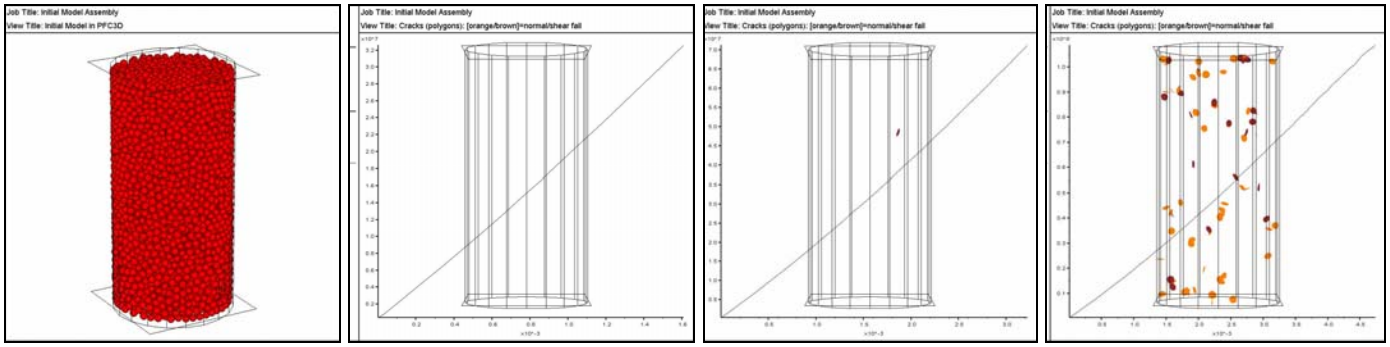

(A) (B) (C) (D)

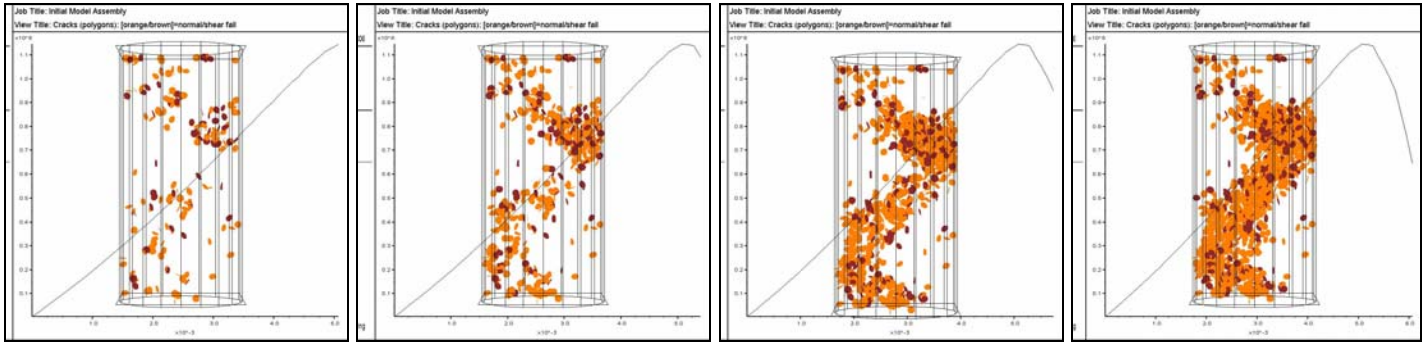

(E) (F) (G) (H)

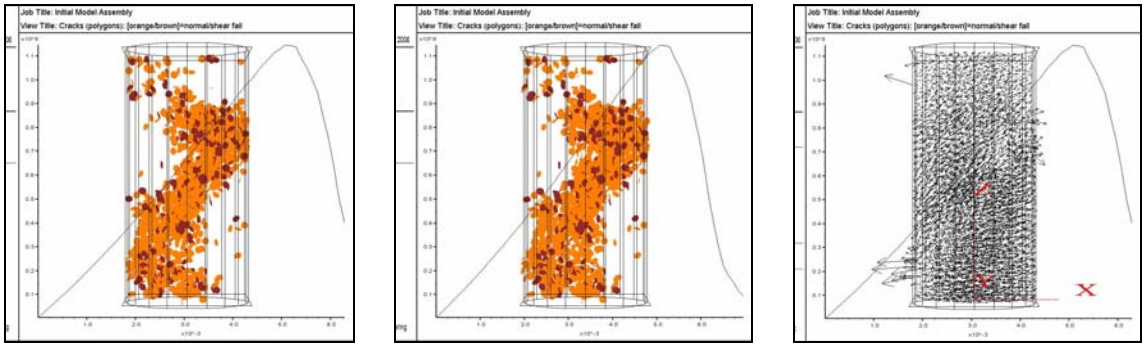

(I) (J) (K)

FIGURE 6.8 (A) INITIAL MODEL IN PFC3D; DEVELOPMENT OF CRACKS AT (B) 28%; (C) 62%; (D) 95%; (E) 100%; (F) 91.5%; (G) 83%; (H) 57%; (I) 35%; AND (J) 8.7% OF PEAK LOAD; (K) VELOCITY DISTRIBUTION OF THE PARTICLES AT 35% OF PEAK LOAD

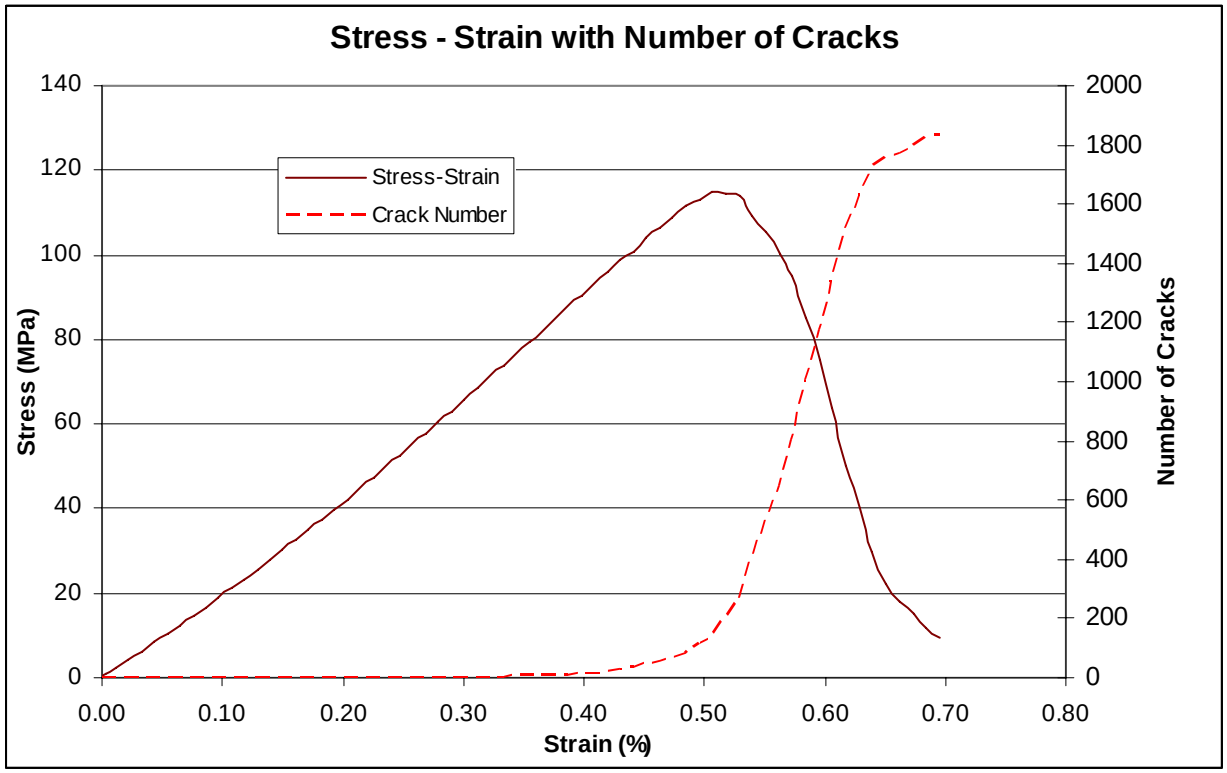

FIGURE 6.9 STRESS - STRAIN WITH NUMBER OF CRACKS FOR LIMESTONE SAMPLE MODELED IN PFC3D

6.5 LABORATORY RESULTS AND DISCUSSION

Uniaxial compressive strength tests were conducted on cylindrical rock samples having a height-to-width ratio of 2:1. The sample was loaded in ramps and at certain load intervals, the data were acquired. The acquired data were analyzed using both IXSeg2SegY [Interpex ((http://www.interpex.com/ixseg2segy/ixseg2segy.htm))] and an in-house software code IPicker (Delinger 2006). The tomograms were calculated from the arrival time data using GeotomCG (Tweeton 2001).

As load is applied to the rock, the microcracks perpendicular to the applied load initially close. Thus the velocity of the wave traveling through the rock increases with the application of the load. With further loading, new cracks are formed and near the peak load they coalesce to form the failure plane at a certain angle to the applied load. The tomograms taken at regular intervals were expected to show this stress increase with the application of the load. A uniaxial test was conducted on a cylindrical sample of 0.0508 x 0.1016 m (2 x 4 in.). The tomograms obtained from the test are shown in the plots in Figure 6.11. Figure 6.12 shows the relation between the stress and the velocity for the sample. Figure 6.13 shows the sandstone sample after it has failed.

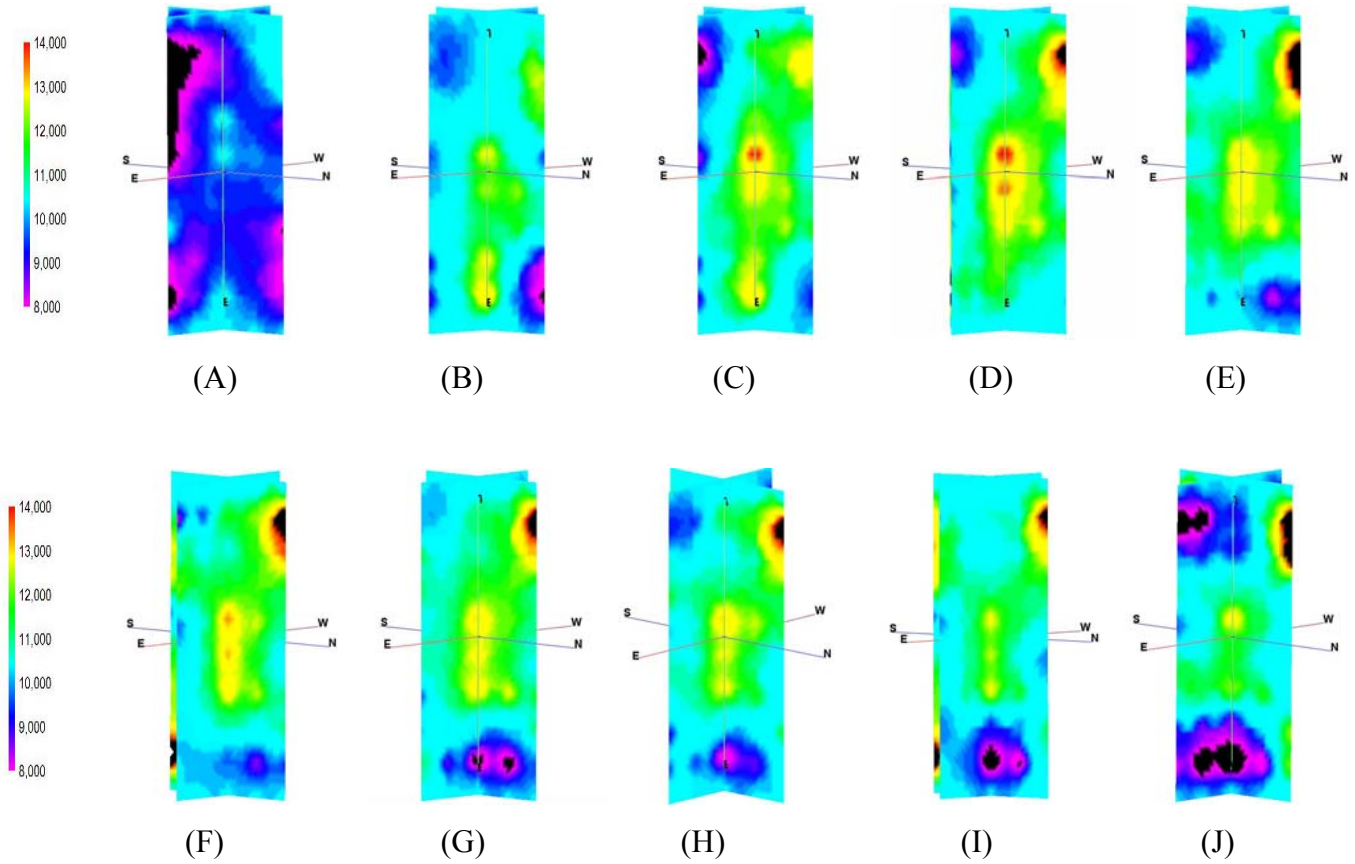

FIGURE 6.10 VELOCITY TOMOGRAMS OF BEREA SANDSTONE UNDER UNIAXIAL COMPRESSION STRENGTH TEST AT (A) 0%; (B) 15%; (C) 30%; (D) 45%; (E) 60%; (F) 75%; (G) 81%; (H) 87%; (I) 94% OF PEAK LOAD; AND (J) JUST PRIOR TO FAILURE.

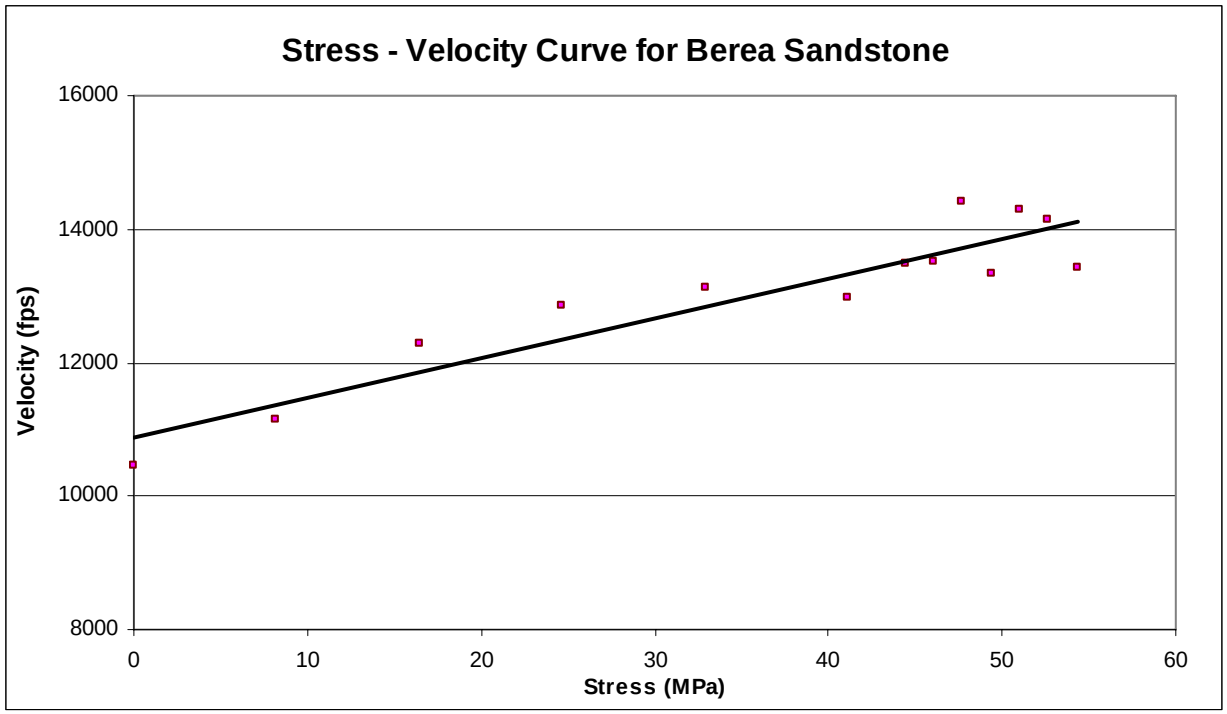

FIGURE 6.11 RELATION BETWEEN STRESS AND VELOCITY WITH THE APPLICATION OF LOAD IN BEREA SANDSTONE.

FIGURE 6.12 BEREA SANDSTONE AFTER FAILURE

From the plots in Figure 6.11 it can be observed that there is a high stress concentration initially at the center of the sample with increasing load. This is in compliance with the observations made in coal mine pillars. (Wagner 1974; Mark and Iannacchione 1992). The velocity also increases with the increase of the load as can be observed from the stress-velocity curve. However, as expected the stress concentration leading to the failure of the rock was not evident from these results. The growth of high stress leading the failure of the rock sample could not be observed from the study.

The difference velocity tomograms in Figure 6.14 were obtained by subtracting the tomogram obtained at 6% peak load from the data at the other loads. It can be observed from these tomograms that with the application of the load, there is a growth of velocity inside the sample till about 80% of the peak load. However, the high stress leading to the failure plane could not also be observed later from these tomograms. Further there is a presence of an anomaly at the bottom of the sample which can be due to some errors in the data obtained from the receivers.

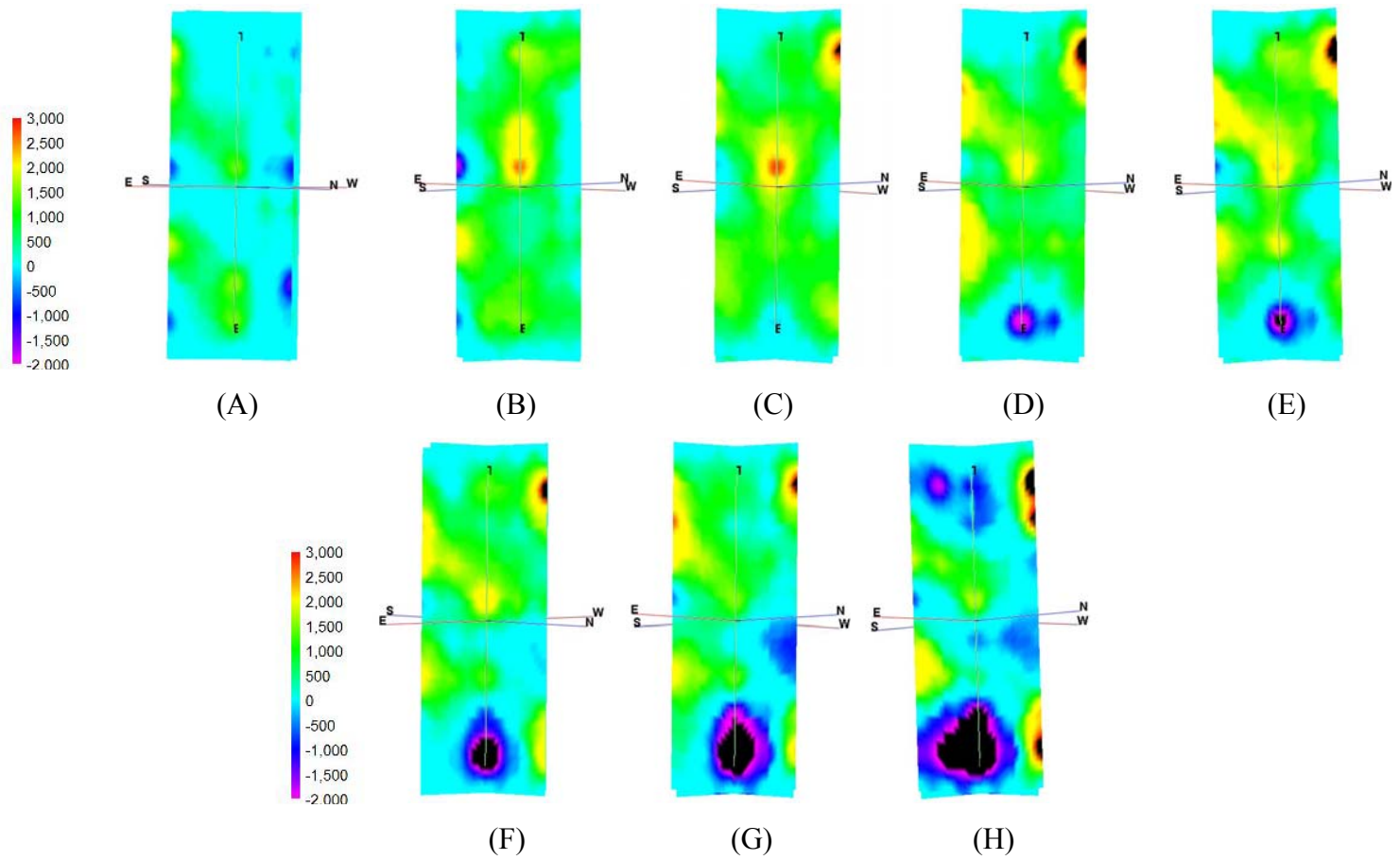

FIGURE 6.13 DIFFERENCE VELOCITY TOMOGRAMS WITH RESPECT TO THE MODEL AT 6% PEAK LOAD AT (A) 15%; (B) 30%; (C) 45%; (D) 60%; (E) 75%; (F) 87%; (G) 94% OF PEAK LOAD; AND (H) JUST PRIOR TO FAILURE

6.6 CONCLUSIONS AND RECOMMENDATIONS

The current study used numerical modeling and laboratory tomograms to investigate the stress redistribution in rock samples as they were loaded to failure. An attempt was made to understand the stress growth in rock samples as they were loaded to failure in uniaxial compression strength tests and thereby predict failure in advance.

The discrete element code PFC^{3D} was used for the numerical part of the study. The biggest advantage of using this model was that fracture develops of its own without the need of any assumption regarding the location and type of failure. The first step in this modeling process involves converting the macro-properties of the rock to the micro-properties of the particles used in the model. Currently there is no theory available for this conversion. A trial-and-error process exists which requires many iterations to find the correct micro-properties for the study. In the current study, an equation was developed that converts the macro-properties of the rock to the micro-properties based on the user input. After successful validation of the equation, attention was focused on determining the stress redistribution in the models as they were loaded to failure. Numerous studies have been conducted using other methods of modeling. The current study attempts to observe the stress distribution in rock samples using the discrete element model. It was observed that the majority of the cracks form after the load was approximately 95% of the peak load and only after that could the failure plane be determined. Regions of high stress were observed from both the normal and shear stress distribution before the

development of the failure plane. One of these high stress planes later dominated to become the failure plane for the model.

In the other half of the study, uniaxial compressive tests were conducted on rock samples and velocity tomograms were observed during the loading process at certain intervals. With the application of the stress, the velocity of an elastic wave through the rock increases. Thus using the velocity tomograms, it was expected to observe this increase in stress and predict the failure plane.

From the tomograms it was observed that there is an increase in the stress at the center of the rock as had been observed in coal mine pillars. The increase in the stress leading to formation of the failure plane could not be observed from them. Difference velocity tomograms were constructed by the difference between the data at 6% peak load and that at a particular load. This also showed the presence of a high velocity with the application of the load but the presence of a failure plane could not be observed in advance from these tomograms too. It is known from earlier studies that the cracks in the rocks coalesce into a failure plane only above 95% of the peak stress. The current study was done by acquiring the data at regular intervals. Thus the author feels that more data should be acquired near the peak stress. Further, the position of the sensors attached to the rock should be accurately noted for plotting the tomograms.

In the end, it can be observed that the actual mechanism leading to the failure of the rocks still needs clarification. Stress redistribution leading to failure can only be determined near the peak load. The current study tried to conduct studies on numerous rock types. The failure mode is different in different rock types. Thus the author feels that in order to understand the mechanism correctly, tests should be conducted initially only on one type of rock. The failure pattern will be consistent in it and this should help in investigating more into the behavior of the rock. After success of this study, it should be extended to other rock types.

Success in the laboratory scale can be extended to the field studies. Tomograms coupled with numerical modeling will assist in the prediction of the stress condition ahead of the face or in mine pillars that will prevent catastrophic failure from stress increase leading to loss of property and life. Some of the other technologies that will benefit from this study are real time tomography and acoustic emission monitoring coupled with acoustic emission tomography.

ACKNOWLEDGEMENT

We would like to acknowledge the support provided by the National Science Foundation (CMS-0134034).

REFERENCES

Coulomb, C. A. (1773). "Sur une application des règles de Maximis et Minimis a quelques problèmes de stratique relatifis à l'Architecture " Acad. Roy. des Sciences Memoires de math. et de physique par divers savans **7**: 343 - 382.

Cundall, P. A. (1971). A computer model for simulating progressive large scale movements in blocky rock systems. Symposium of the International Society of Rock Mechanics Nancy, France.

Cundall, P. A. and R. D. Hart (1993). Comprehensive Rock Engineering, Vol. 2: Analysis and Design Methods

Cundall, P. A. and O. D. L. Strack (1979). "A discrete element model for granular assemblies." Geotechnique **29**(1): 47 - 65.

Delinger, M. (2006). IPicker.

Dines, K. A. and R. J. Lyttle (1979). "Computerized geophysical tomography." Proceedings of the IEEE **67**(7): 1065-1073.

Fakhimi, A., F. Carvalho, et al. (2002). "Simulation of Failure around a circular opening in rock." Int. J of R Mech. & Min. Sc. **39**(4): 507 - 515.

Glaser, S. D. and D. N. Doolin (1999). New directions in Rock Mechanics - A Forum sponsored by the American Rock Mechanics Association, A Report to the National Science Foundation**:** 38.

Goodman, R. E. (1980). Introduction to Rock Mechanics, John Wiley and Sons.

Goulty, N. R., J. S. Thatcher, et al. (1990). "Experimental investigation of crosshole seismic techniques for shallow coal exploration." Q. J. Eng. Geol. **23**: 217 - 228.

Gustavsson, M., S. Ivansson, et al. (1986). "Seismic borehole tomography - measurement system and field studies." Proc. IEEE **74**(2): 339 - 346.

Hazzard, J. F. (1998). Numerical modeling of acoustic emissions and dynamic rock behavior. Dept. of Earth Sciences, Keele University. **Ph.D. :** 231.

Hazzard, J. F., D. S. Collins, et al. (2002). "Simulation of unstable fault slip in granite using a bonded-particle model." Pure & Applied Geophysics **159**: 221 - 245.

Hazzard, J. F. and R. P. Young (2000). "Simulating Acoustic Emissions in Bonded-Particle Models of Rock." Int. J. of R. Mech. & Min. Sc. **37**(5): 867-872.

Hazzard, J. F. and R. P. Young (2001). Seismic validation of micromechanical models. 38th. US Rock Mech. Sym., DC Rocks 2001, Washington DC, A.A.Balkema.

Hazzard, J. F. and R. P. Young (2002). 3D numerical modeling of acoustic emission. 5th. Int. Workshop on the Appl. Of Geophysics in Rock Engg., Toronto,Canada.

Hazzard, J. F. and R. P. Young (2002). "Moment Tensors and Micromechanical Models." Tectonophysics **356**(1 - 3): 181 - 197.

Itasca Consulting Group, Inc., PFC2D PFC^{2D}. Minneapolis, MN.

Itasca Consulting Group, Inc., PFC3D (2003). PFC^{3D}. Minneapolis, MN,.

IXSeg2SegY - http://www.interpex.com/ixseg2segy/ixseg2segy.htm)

Jaeger, J. C. and N. G. W. Cook (1979). Fundamentals of Rock Mechanics, Chapman and Hall.

Johnson, W. B. (2005). Design and testing of a laboratory ultrasonic data acquisition system for tomography. Mining & Minerals Engineering. Blacksburg, Virginia Tech. **M.S. :** 108.

Karfakis, M. G. (2003). Rock Mechanics Notes.

Kulatilake, P. H. S. W., B. Malama, et al. (2001). "Physical and particle flow modeling of jointed rock block behavior under uniaxial loading." Int. J. of R. Mech. & Min. Sc. **38**: 641 - 657.

Leung, L., M. Downey, et al. (1988). Cross-hole seismic tomography for mineral exploration and mine planning. Expanded Abstracts, 58th. SEG Annual Meeting, Anaheim, CA.

Li, H., T. G. Zhang, et al. (2005). Laboratory experiment and computer simulation of ultrasonic wave propagation in fractured and imhomogeneous rock. Alaska Rocks 2005 - Rock Mechanics for Energy, Mineral and Infrastructure Development in the Northern Regions. S. H. G. Chen, W. Zhou, J. Tinucci. Anchorage, AL**:** Preprint # ARMA/USRMS 05-861.

Lo, T. and P. L. Inderwiesen (1994). Fundamentals of Seismic Tomography. L. R. Lines. **6:** 178.

Mark, C. and A. T. Iannacchione (1992). Coal pillar mechanics: Theoritical models and field measurements compared, US Bureau of Mines, Pittsburgh, PA, USBM IC 9315.

Mason, I. M. (1981). "Algebraic reconstruction of a two-dimensional velocity inhomogeneity in the High Hazles seam of Thoresby Colliery." Geophysics **46**(3): 298 - 308.

Mohr, O. (1900). "Welche Umstände bedingen die Elastizitätsgrenze und den Bruch eines Materials?" Z. Ver. dt. Ing. **44**: 1524 - 1530; 1572 - 1577.

MSHA Mine Safety and Health Administration, US Department of Labor ,http://www.msha.gov.

NIOSH National Institute of Occupational Safety and Health, http://www.cdc.gov/niosh.

Park, E., C. D. Martin, et al. (2004). Simulation of the mechanical behavior of discontionous rock masses using a bonded-particle model. Gulf Rocks 2004 - 6th. North American North American Rock Mechanics Association. Houston ,Texas. Preprint No. ARMA/NARMS 04/480.

Pells, P. J. N. (1993). Uniaxial strength testing. Comprehensive Rock Engineering - Principles, Practice & Projects. J. A. Hudson, Pergamon Press. **3:** 67 - 85.

Peterson, J. E., B. N. P. Paulsson, et al. (1985). "Application of algebraic reconstruction techniques to crosshole seismic data." Geophysics **50**(10): 1566 - 1580.

Radon, J. (1917). "Uber die bestimmung von functionen durch ihre integralwere lange gewisser mannigfaltigkeiten." Ber. Verh. Saechs. Akad. Wiss. **69**: 262 - 267.

Scholz, C. H. (1968). "Experimental study of the fracturing process in brittle rock." J. Geophy. Res. **73**(4): 1447 - 1454.

Scholz, C. H. (1968). "Microfracturing and the inelastic deformation of rock in compression." J. Geophy. Res. **73**(4): 1417 - 1432.

Scott, T. E., Q. Ma, et al. (1993). "Tomographic acoustic velocity changes induced during indentation of Berea sandstone." EOS, Trans. Amer. Geophys. Union **74**(43): 408.

Tang, C. A., H. Liu, et al. (2000). "Numerical studies of the influence of microstructure on rock failure in uniaxial compression - Part I: effect of heterogeneity." Int. J. of Rock Mech. and Min. Sc. **37**: 555 - 569.

Tweeton, D. (2001). GeoTom CG: Users Manual, GeoTom LLC, Apple Valley, MN.

Wagner, H. (1974). Determination of the complete load-deformation characteristics of coal pillars. 3rd. Int. Cong. Rock Mechanics, Denver, CO: 1076 - 1081.

Wang, C., D. D. Tannant, et al. (2003). "Numerical analysis of the stability of heavily jointed rock slopes using PFC2D." Int J of R Mech. & Min. Sc. **40**: 415-424.

Wanne, T. (2002). PFC3D simulation procedure for compressive strength testing of anisotropic hard rock. 1st. Intl. PFC Symposium, Numerical Modeling in Mocromechanics via Particle Methods, Germany, A.A. Balkema Publishers.

Westman, E. C. (2004). "Use of tomography for inference of stress redistribution in rock." IEEE Transactions on Industry Applications **40**(5): 1413 - 1417.

Westman, E. C., K. Y. Haramy, et al. (1996). Seismic tomography for longwall stress analysis. 2nd. North American Rock Mechanics Symposium: NARMS '96, Montreal, Quebec, Canada, A.A.Balkema, Rotterdam, Brookfield.

CHAPTER 7: CONCLUSIONS AND RECOMMENDATIONS

7.1 SUMMARY AND CONCLUSIONS

A study was conducted to image the stress redistribution in rock samples as they were uniaxially loaded to failure, using numerical modeling and laboratory tomography. A commercially available program, PFC^{3D} was used for the study. It is a discrete element code that models the rock as an assemblage of spheres with defined micro-properties. The biggest advantage of this program is that the failure takes place of its own without the need to specify the presence of any interfaces. There is no need to reformulate the grid when a fracture is formed, as in some other programs.

Laboratory tomograms were used to monitor the stress redistribution in rock samples as they were loaded to failure. Ultrasonic sensors were attached around the rock and tomograms were obtained at certain load intervals. As load is applied to a rock, the microfractures perpendicular to the load initially close. With further application of the load, new cracks are formed and later these cracks coalesce to form the failure plane. Thus as the stress increases in the rock, the velocity of an elastic wave traveling through the rock also increases.

Based on the numerical simulations and laboratory tests, the following conclusions are drawn:

1. The size of the particles plays an important role in the modeling results. A change in the particle radii produces a change in both the Young's modulus and the peak load obtained from the model. The fracture plane was also more prominent with smaller sized particles. Further, due to the spherical nature of the particles, joints formed from smaller sized particles were less rugged. On the other hand, the computing time increased with a decrease in the particle size. Hence, the correct particle size should be carefully chosen based on the purpose of the study along with the computer available for running the code.
2. The fracture pattern observed from the model closely resembled that obtained in the laboratory. Tensile cracking was dominant in the models. The cracks formed in the model coalesce into a failure plane above 90 – 95% of the peak load. This was in compliance with earlier studies.
3. A crack is formed in PFC^{3D} whenever either the normal or the shear stresses of the bonds break. Thus monitoring these stresses provides a better way to image the growth of high stresses in the model.
4. A growth of a high stress region in PFC^{3D} models was also observed after 90 – 95% of the peak load.
5. The variation of the peak load with the bedding angle using PFC^{3D} matched with earlier studies. A region of high stress was observed from these models at around 95% of the peak stress at the same place where the fracture subsequently occurred.

6. The laboratory properties of the rock sample need to be converted to the properties of the particles used in the model. A trial-and-error process had been used earlier which requires numerous iterations to get the correct properties. An equation developed in the current study helps in obtaining the correct micro-properties in fewer iterations than the earlier procedure.
7. An indentation load was applied on a rectangular block, both on a numerical model and on a laboratory sample. As expected, regions of high stress and velocity were observed below the load from both the model and the tomograms, respectively. A correlation between the stress and velocity, in two dimensions, could be observed from these results.
8. The three-dimensional tomograms obtained from the uniaxial tests on rock samples showed a high velocity at the center of the sample, as had been observed in coal pillars. However, they were not able to predict the failure plane as was expected from the study. Similar observations were made from the difference velocity tomograms. However, they were also not able to predict the failure plane in advance.

7.2 RECOMMENDATIONS

The author recommends the following work to be done in future:

1. The tomograms obtained from this study indicate that more experiments need to be conducted to better understand the failure mechanism in rock samples. Initially the tests should be conducted on just one rock type. Once the failure plane can be observed from these tests, other rocks should also be tested to see if similar observations can be made.
2. Attention should be taken while attaching the sensors to the rock. It is very important to note their exact location on the sample.
3. It has been observed that the cracks coalesce into the failure plane above 90 – 95% of the peak load. Thus data should be collected at frequent intervals during this period of the load to image the growth of high stress and predict the failure plane in advance. A stress-strain curve plotted during the test will help in this process.
4. Acoustic emission monitoring coupled with laboratory tomography will help to monitor the cracks along with the stress redistribution and may provide for better understanding of the mechanism behind rock failure in unconfined compression.
5. Success from the earlier recommendations can be extended to field studies by monitoring the mine pillars and observing the stress state in them as mining progresses.

6. Coupled numerical codes (eg. FLAC^{3D} and PFC^{3D}) should be used for failure prediction with numerical modeling on a larger scale.
7. Some of the other technologies that will benefit from this study are real time tomography and acoustic emission monitoring coupled with acoustic emission tomography.

APPENDIX A: EFFECT OF RANDOM PARTICLE GENERATOR

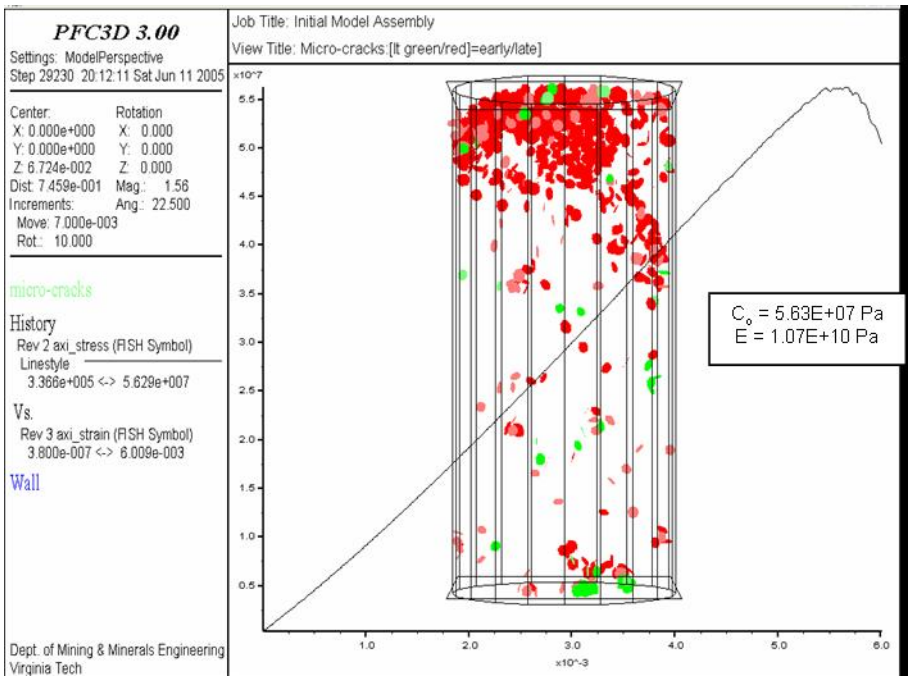

(A)

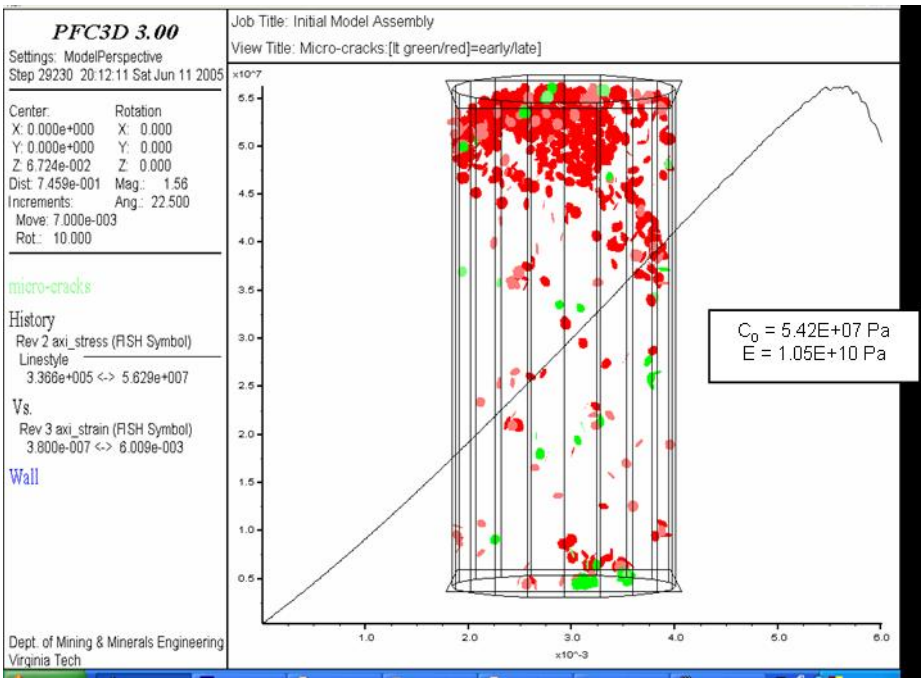
PFC3D 3.00
Settings: ModelPerspective
Step 29230 20:12:11 Sat Jun 11 2005
Center: Rotation
X: 0.000e+000 X: 0.000
Y: 0.000e+000 Y: 0.000
Z: 6.724e-002 Z: 0.000
Dist: 7.459e-001 Mag.: 1.56
Increments: Ang.: 22.500
Move: 7.000e-003
Rot.: 10.000
micro-cracks
History
Rev 2 axi_stress (FISH Symbol)
Linestyle
3.366e+005 <-> 5.629e+007
Vs.
Rev 3 axi_strain (FISH Symbol)
3.800e-007 <-> 6.009e-003
Wall
Dept. of Mining & Minerals Engineering
Virginia Tech
Job Title: Initial Model Assembly
View Title: Micro-cracks:[lt green/red]=early/late]
x10^7
x10^-3
C0 = 5.42E+07 Pa
E = 1.05E+10 Pa

(B)

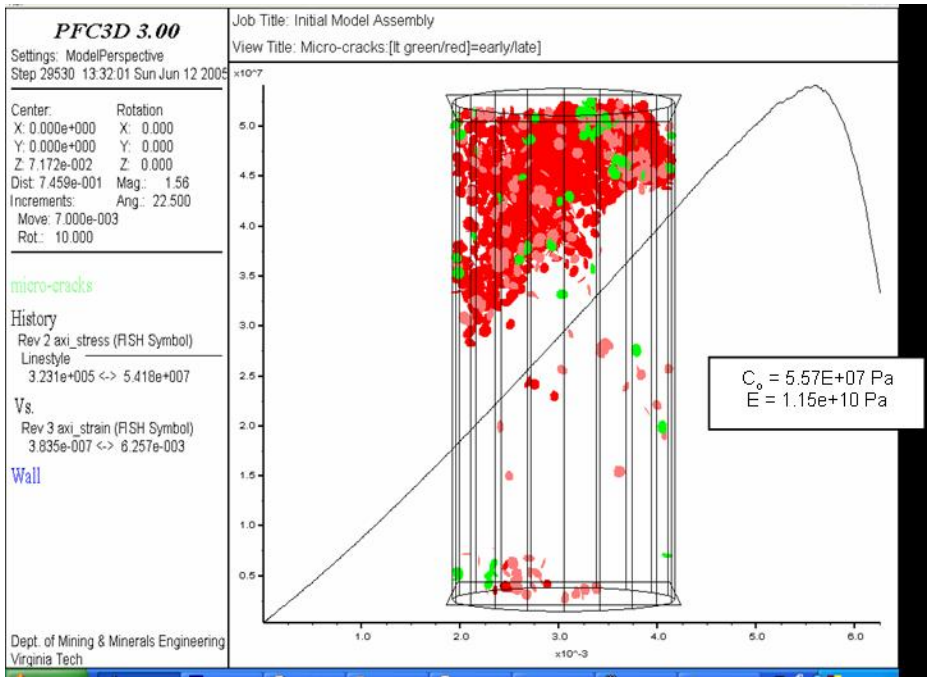
PFC3D 3.00
Settings: ModelPerspective
Step 29530 13:32:01 Sun Jun 12 2005
Center: Rotation
X: 0.000e+000 X: 0.000
Y: 0.000e+000 Y: 0.000
Z: 7.172e-002 Z: 0.000
Dist: 7.459e-001 Mag.: 1.56
Increments: Ang.: 22.500
Move: 7.000e-003
Rot.: 10.000
micro-cracks
History
Rev 2 axi_stress (FISH Symbol)
Linestyle
3.231e+005 <-> 5.418e+007
Vs.
Rev 3 axi_strain (FISH Symbol)
3.835e-007 <-> 6.257e-003
Wall
Dept. of Mining & Minerals Engineering
Virginia Tech
Job Title: Initial Model Assembly
View Title: Micro-cracks:[lt green/red]=early/late]
x10^7
x10^-3
C0 = 5.57E+07 Pa
E = 1.15e+10 Pa

(C)

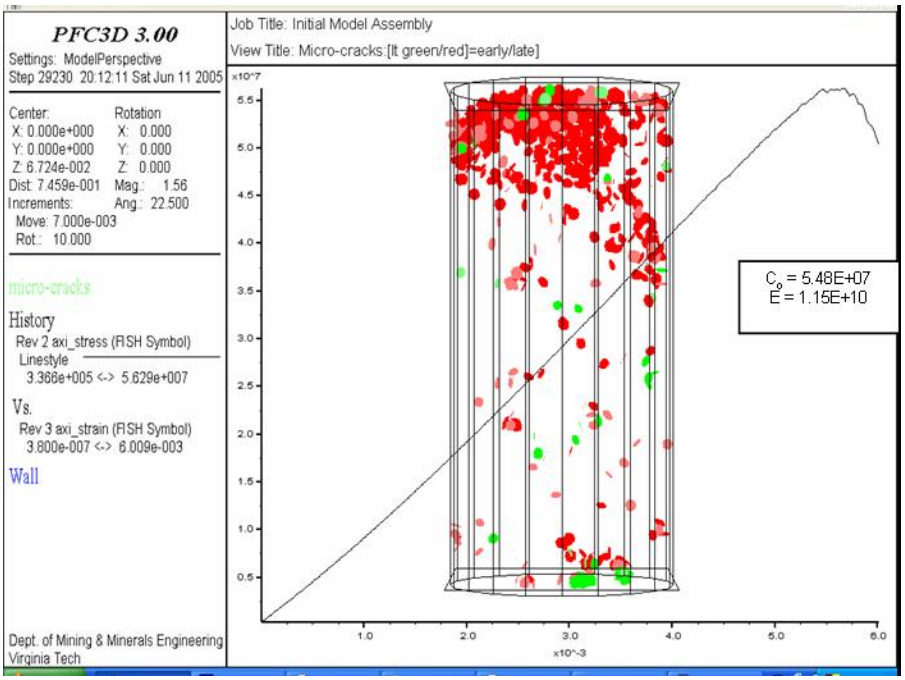
PFC3D 3.00
Settings: ModelPerspective
Step 29230 20:12:11 Sat Jun 11 2005
Center: Rotation
X: 0.000e+000 X: 0.000
Y: 0.000e+000 Y: 0.000
Z: 6.724e-002 Z: 0.000
Dist: 7.459e-001 Mag.: 1.56
Increments: Ang.: 22.500
Move: 7.000e-003
Rot.: 10.000
micro-cracks
History
Rev 2 axi_stress (FISH Symbol)
Linestyle
3.366e+005 <-> 5.629e+007
Vs.
Rev 3 axi_strain (FISH Symbol)
3.800e-007 <-> 6.009e-003
Wall
Dept. of Mining & Minerals Engineering
Virginia Tech
Job Title: Initial Model Assembly
View Title: Micro-cracks:[lt green/red]=early/late]
x10^7
x10^-3
C0 = 5.48E+07
E = 1.15E+10

(D)

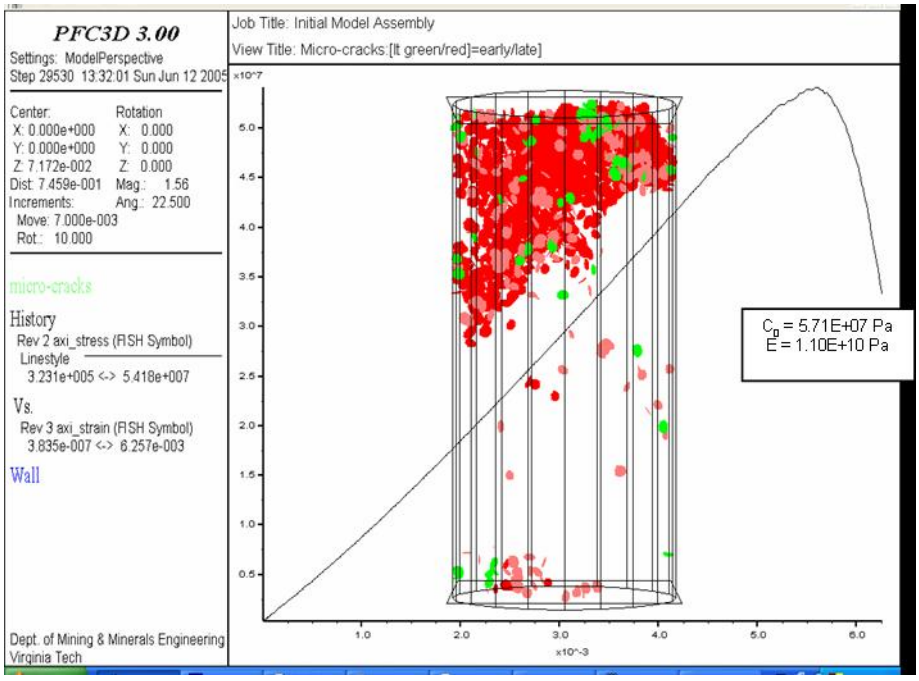
PFC3D 3.00
Settings: ModelPerspective
Step 29530 13:32:01 Sun Jun 12 2005
Center: Rotation
X: 0.000e+000 X: 0.000
Y: 0.000e+000 Y: 0.000
Z: 7.172e-002 Z: 0.000
Dist: 7.459e-001 Mag.: 1.56
Increments: Ang.: 22.500
Move: 7.000e-003
Rot.: 10.000
micro-cracks
History
Rev 2 axi_stress (FISH Symbol)
Linestyle
3.231e+005 <-> 5.418e+007
Vs.
Rev 3 axi_strain (FISH Symbol)
3.835e-007 <-> 6.257e-003
Wall
Dept. of Mining & Minerals Engineering
Virginia Tech
Job Title: Initial Model Assembly
View Title: Micro-cracks:[lt green/red]=early/late]
x10^7
x10^-3
C0 = 5.71E+07 Pa
E = 1.10E+10 Pa

(E)

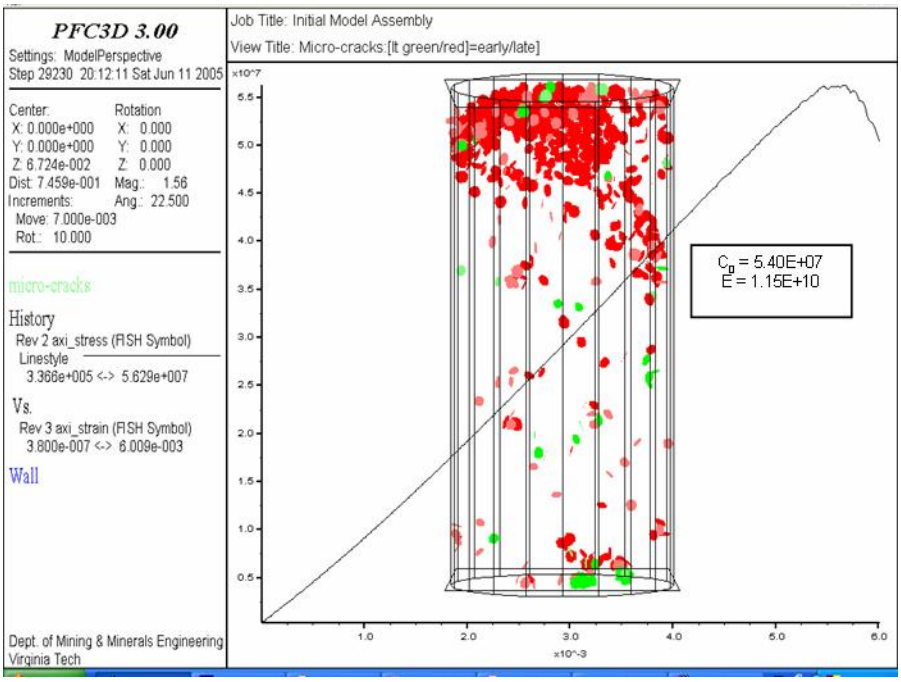
PFC3D 3.00
Settings: ModelPerspective
Step 29230 20:12:11 Sat Jun 11 2005
Center: Rotation
X: 0.000e+000 X: 0.000
Y: 0.000e+000 Y: 0.000
Z: 6.724e-002 Z: 0.000
Dist: 7.459e-001 Mag.: 1.56
Increments: Ang.: 22.500
Move: 7.000e-003
Rot.: 10.000
micro-cracks
History
Rev 2 axi_stress (FISH Symbol)
Linestyle
3.366e+005 <-> 5.629e+007
Vs.
Rev 3 axi_strain (FISH Symbol)
3.800e-007 <-> 6.009e-003
Wall
Dept. of Mining & Minerals Engineering
Virginia Tech
Job Title: Initial Model Assembly
View Title: Micro-cracks:[lt green/red]=early/late]
x10^7
C0 = 5.40E+07
E = 1.15E+10
x10^-3

(F)

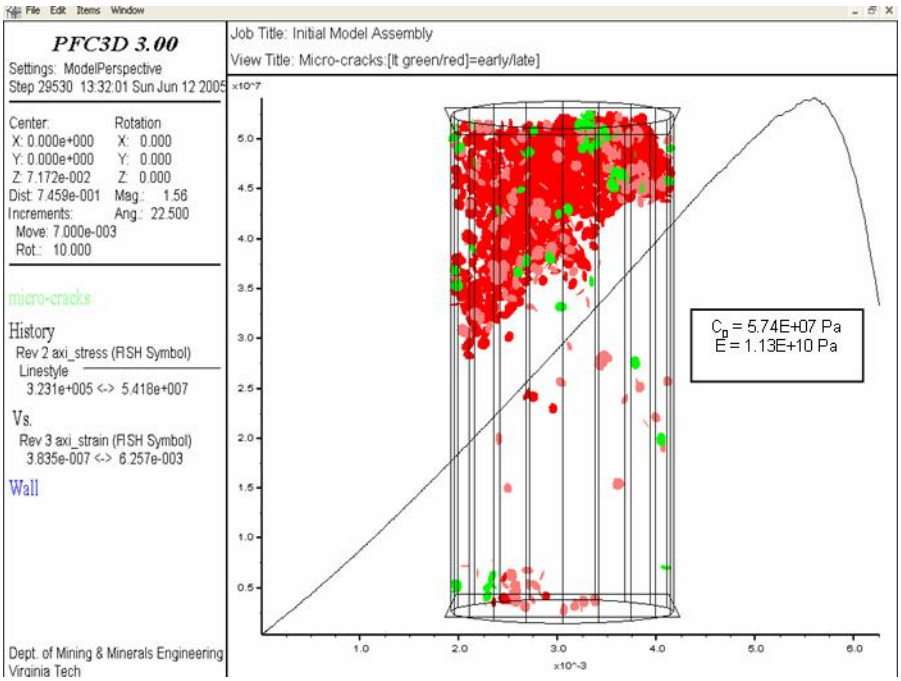
File Edit Items Window
PFC3D 3.00
Settings: ModelPerspective
Step 29530 13:32:01 Sun Jun 12 2005
Center: Rotation
X: 0.000e+000 X: 0.000
Y: 0.000e+000 Y: 0.000
Z: 7.172e-002 Z: 0.000
Dist: 7.459e-001 Mag.: 1.56
Increments: Ang.: 22.500
Move: 7.000e-003
Rot.: 10.000
micro-cracks
History
Rev 2 axi_stress (FISH Symbol)
Linestyle
3.231e+005 <-> 5.418e+007
Vs.
Rev 3 axi_strain (FISH Symbol)
3.835e-007 <-> 6.257e-003
Wall
Dept. of Mining & Minerals Engineering
Virginia Tech
Job Title: Initial Model Assembly
View Title: Micro-cracks:[lt green/red]=early/late]
x10^7
C0 = 5.74E+07 Pa
E = 1.13E+10 Pa
x10^-3

(G)

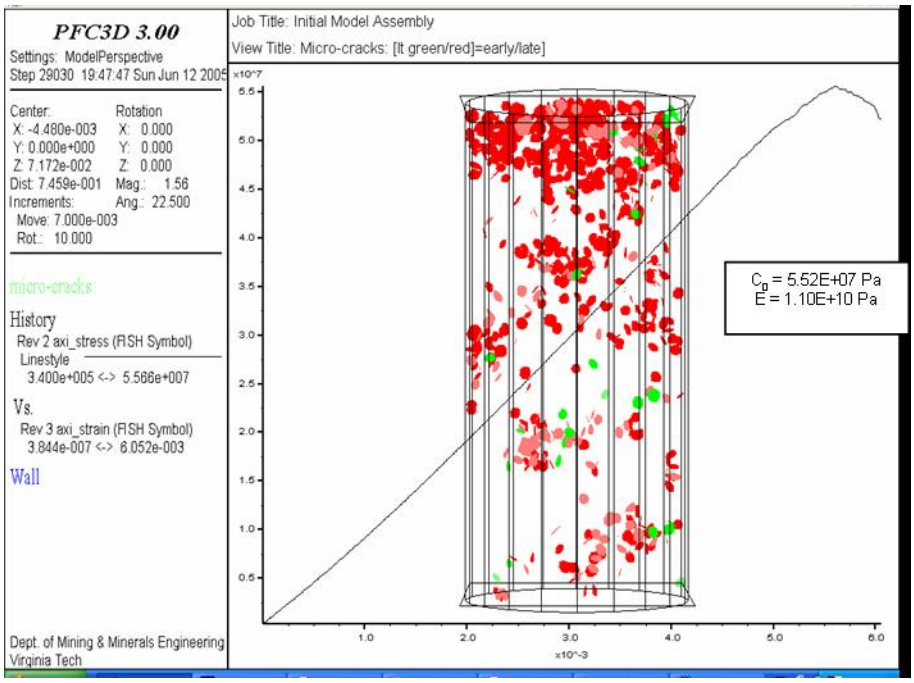

(H)

FIGURE A1 EFFECT OF RANDOM PARTICLE GENERATOR ON THE FRACTURE PATTERN. VARYING COLORED CRACKS INDICATE CRACK FORMATION AT VARYING TIMES.

APPENDIX B: STRESS REDISTRIBUTION USING MEASUREMENT SPHERES AND PARTICLES

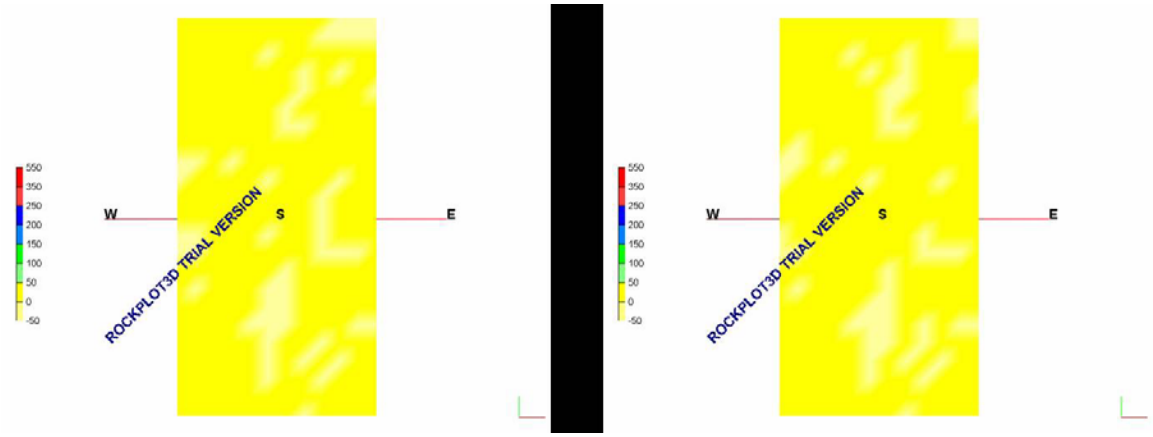

FIGURE A2 STRESS DISTRIBUTION OF THE MODEL AT ZERO LOAD FROM (LEFT) MEASUREMENT SPHERES; (RIGHT) PARTICLES

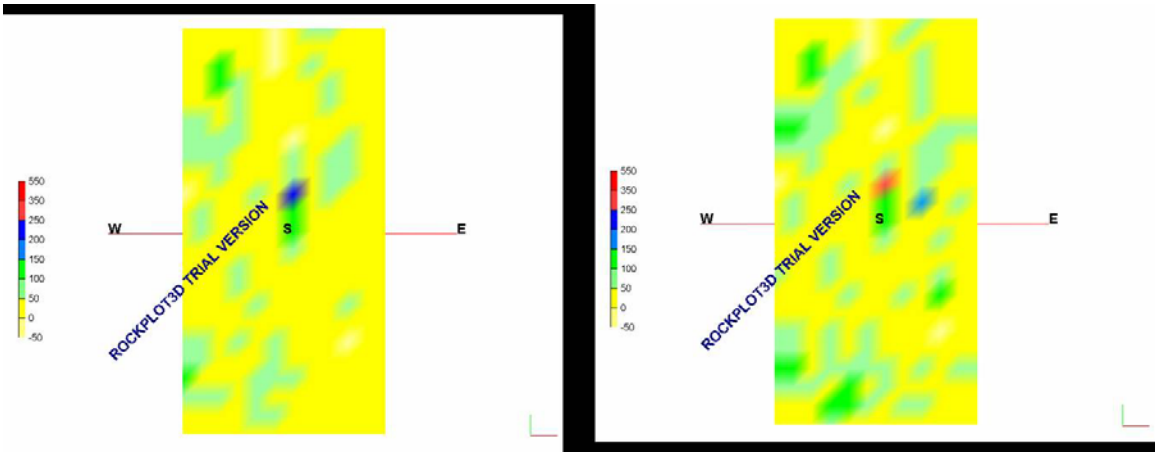

FIGURE A3 STRESS DISTRIBUTION OF THE MODEL AT 50% OF PEAK LOAD FROM (LEFT) MEASUREMENT SPHERES; (RIGHT) PARTICLES

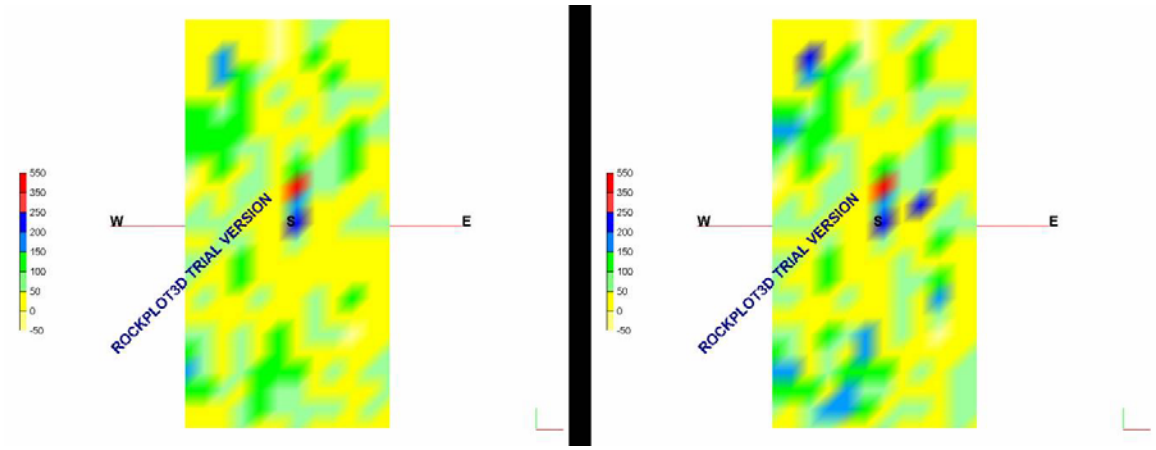

FIGURE A4 STRESS DISTRIBUTION OF THE MODEL AT 75% OF PEAK LOAD FROM (LEFT) MEASUREMENT SPHERES; (RIGHT) PARTICLES

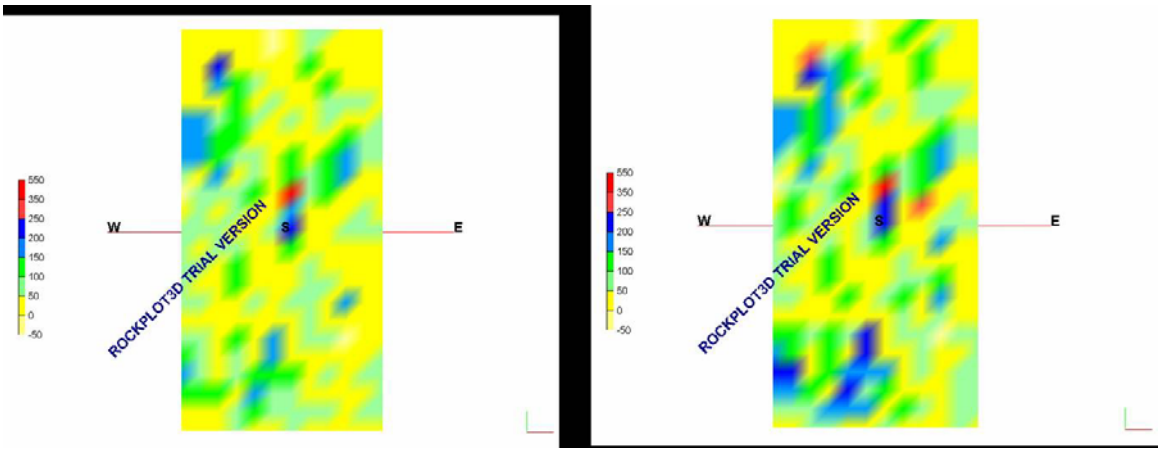

FIGURE A5 STRESS DISTRIBUTION OF THE MODEL AT 90% OF PEAK LOAD FROM (LEFT) MEASUREMENT SPHERES; (RIGHT) PARTICLES

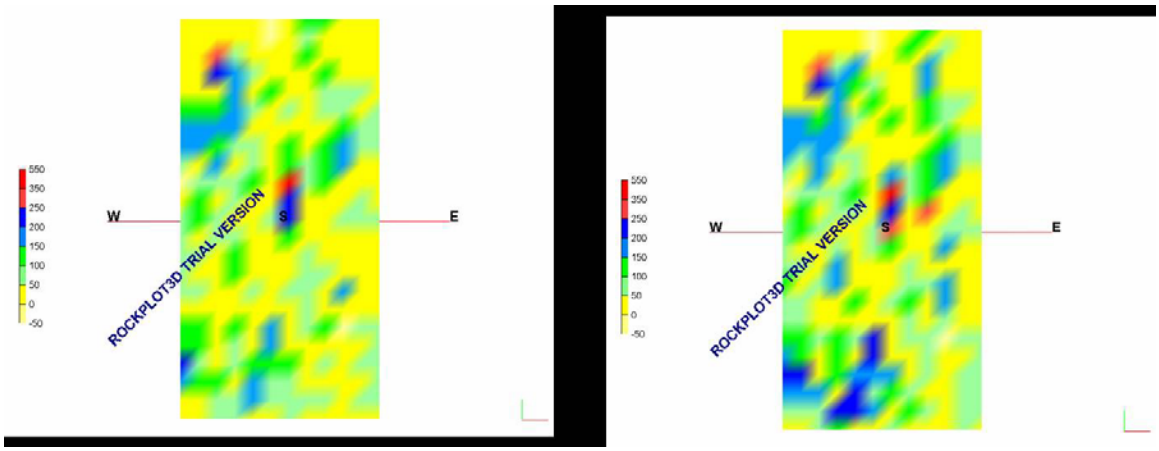

FIGURE A6 STRESS DISTRIBUTION OF THE MODEL AT 95% OF PEAK LOAD FROM (LEFT) MEASUREMENT SPHERES; (RIGHT) PARTICLES

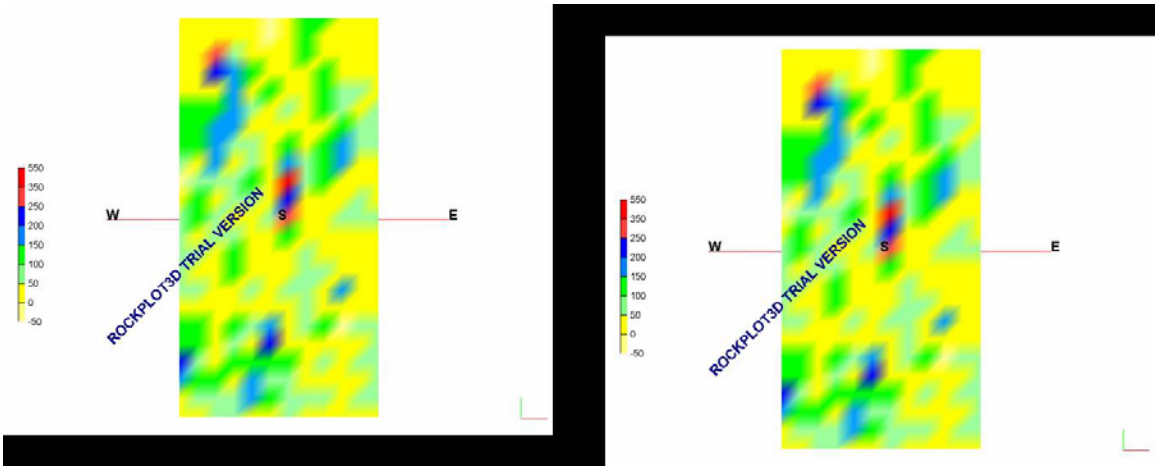

FIGURE A7 STRESS DISTRIBUTION OF THE MODEL AT PEAK LOAD FROM (LEFT) MEASUREMENT SPHERES; (RIGHT) PARTICLES

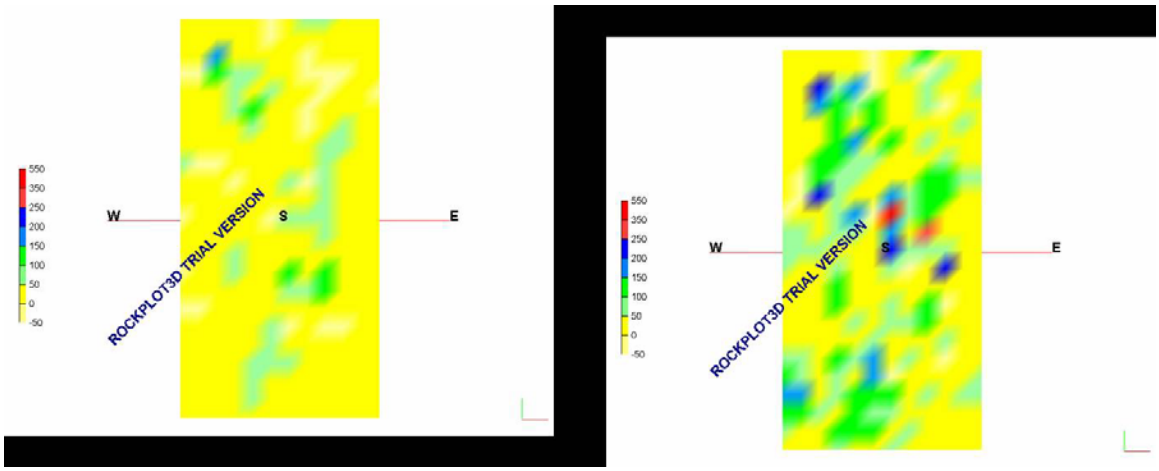

FIGURE A8 STRESS DISTRIBUTION OF THE MODEL AT FAILURE FROM (LEFT) MEASUREMENT SPHERES; (RIGHT) PARTICLES

RUDRAJIT MITRA

EDUCATION

Doctor of Philosophy, Mining Engineering, Expected May 2006

Virginia Polytechnic Institute and State University (Virginia Tech), Blacksburg, VA

Master of Science, Mining Engineering, June 2003

The Pennsylvania State University (Penn State), University Park, PA

Bachelor of Engineering, Mining Engineering, May 2001

B. E. College, Shibpur, India

AFFILIATIONS

Society of Mining, Metallurgy and Exploration Inc., (SME), 2001 – present

American Rock Mechanics Association (ARMA), 2004 – present

EXPERIENCE

Research

Graduate Research Assistant, Department of Mining & Minerals Engineering, Virginia Tech, Blacksburg, VA, July 2003 – present

Graduate Assistant, Department of Mining Engineering, Penn State, University Park, PA, August 2001 – June 2003

Teaching

Instructor, Ventilation Engineering, Department of Mining & Minerals Engineering, Virginia Tech, Blacksburg, VA, January 2006 – May 2006

Teaching Assistant, Department of Mining & Minerals Engineering, Virginia Tech, Blacksburg, VA, August 2005 – December 2005

Teaching Assistant, Department of Mining & Minerals Engineering, Virginia Tech, Blacksburg, VA, January 2005 – May 2005

Teaching Assistant, Department of Mining & Minerals Engineering, Virginia Tech, Blacksburg, VA, August 2004 – December 2004

Teaching Assistant, Department of Mining Engineering, Penn State, University Park, PA, January 2003 – May 2003

Teaching Assistant, Department of Mining Engineering, Penn State, University Park, PA, January 2002 – May 2002

AWARD

Recipient of Pratt Graduate Fellowship from August 2005 – December 2005.

PUBLICATIONS

Mitra, R. and E.C. Westman, 2006. "Investigation of the Stress Imaging in Rock Samples using Numerical Modeling and Laboratory Tomography." – To be submitted to International Journal of Rock Mechanics and Mining Sciences for review.

Mitra, R. and E.C. Westman, 2005. "Stress redistribution determination through coupled laboratory testing and numerical modeling" – Submitted to Transactions of SME for review.

Mitra, R. and E. C. Westman. 2005. "Micro-mechanical modeling of Five Oaks Limestone compared to uniaxial compressive test." – Submitted to Géotechnique for review.

Mitra, R., M. M. Murphy and E. C. Westman. 2005. "Study on the effect of anisotropy in rocks on stress redistribution using numerical modeling." - Submitted to Rock Mechanics and Rock Engineering for review.

Mitra, R., W. B. Johnson and E. C. Westman. 2005. "Stress redistribution imaging through coupled laboratory testing and numerical modeling." 2005 SME Annual Meeting and Exhibit, Salt Lake City, UT, Feb 28 – Mar 2, 2005. Preprint No. 05-107.

Mitra, R., E. C. Westman and M. J. Mrugala. 2004. “Use of Numerical Modeling for Longwall Roof Performance Analysis.” Gulf Rocks 2004: Rock Mechanics across Borders & Disciplines. Proceedings of the 6th NARMS Conference, Houston, TX. June 2004. D. P. Yale, S. M. Willson, and A. S. Abou-Sayed, Eds. Paper No. ARMA/NARMS 04-483.

Mrugala, M.J. and R. Mitra. 2003. “Performance of coal mine pillars under varying roof and floor conditions.” 2003 SME Annual Meeting and Exhibit, Cincinnati, OH. Feb 24 – 26, 2003. Preprint No. 03-036.